

Design and Synthesis of a Macrocyclic Phospholipid

by

Gavin Maxwell Mitchell

B.Sc. University of Northern British Columbia, 2011

A Thesis Submitted in Partial Fulfillment

of the Requirements for the Degree of

MASTER OF SCIENCE

in the Department of Chemistry

© Gavin Maxwell Mitchell, 2014
University of Victoria

All rights reserved. This thesis may not be reproduced in whole or in part, by photocopy or other means, without the permission of the author.

Supervisory Committee

Design and Synthesis of a Macrocyclic Phospholipid

by

Gavin Maxwell Mitchell

B.Sc. University of Northern British Columbia, 2011

Supervisory Committee

Dr. Thomas Fyles, Department of Chemistry
Supervisor

Dr. Lisa Rosenberg, Department of Chemistry
Departmental Member

Abstract

Supervisory Committee

Dr. Thomas Fyles, Department of Chemistry
Supervisor

Dr. Lisa Rosenberg, Department of Chemistry
Departmental Member

The membrane-spanning phospholipids of the domain Archaea are postulated to provide membrane stability; this thesis reports the design and synthesis of a synthetic membrane-spanning macrocyclic lipid to test this hypothesis. Protected glutaric anhydride reacted with 10-undecyn-1-ol to produce a glutarate monoester. Copper-mediated azide-alkyne coupling (CuAAC) using 1,5-diazido-3-oxapentane(bis-azide) afforded a dicarboxylic acid with a hydrophobic chain of sufficient length to span a 35 Å bilayer membrane. The carboxylic acids were each esterified with an equivalent of 10-undecyn-1-ol. After optimization an 87% yield was obtained in the closure of the 72-membered macrocycle with the bis-azide using CuAAC. Deprotection and coupling with p-nitrophenyl phosphorodichloridate completed the synthesis. Two other phospholipids, a linear bolaamphiphile derived from the precursor to the second click reaction, and a linear amphiphile created from a glutarate bis-dodecyl ester, were also synthesized to provide controls for probing the orientation of the macrocyclic phospholipid in the bilayer membrane of vesicles. The amphiphile, linear bolaamphiphile, and macrocyclic bolaamphiphile were synthesized in 4, 5, and 6 steps with yields of 19, 4, and 5% respectively.

The hydrophilic head group of the macrocyclic phospholipid was designed to release p-nitrophenolate in basic conditions from the p-nitrophenylphosphate head group to produce an absorbance at 400 nm. This assay was expected to elucidate the membrane-spanning orientation of the phospholipid in the bilayer membrane of vesicles. The final target compound failed to release p-nitrophenolate under basic conditions and underwent phosphate elimination to produce an α , β -unsaturated ester instead. Although the macrocyclic lipid produced associates with membranes and may be membrane-spanning, this lipid design was unable to reveal its membrane orientation.

Table of Contents

Supervisory Committee.....	ii
Abstract.....	iii
Table of Contents.....	iv
List of Tables.....	v
List of Figures.....	vi
List of Schemes.....	viii
List of Abbreviations.....	x
List of Numbered Compounds.....	xi
Acknowledgements.....	xvii
Chapter 1: Introduction.....	1
1.1: Lipids.....	1
1.2: Synthetic Bolaamphiphiles.....	6
1.3: Design and Project Overview.....	7
Chapter 2: Synthesis of Amphiphiles.....	13
2.1: Synthesis.....	13
2.2: Synthesis of Glutarate Monoester with 10-undecyn-1-ol.....	14
2.3: Dimerization of Glutarate Monoster via CuAAC.....	15
2.4: Esterification of Dimerized Glutarate.....	16
2.5: Macrocyclization of Bis-alkyne.....	17
2.6: Deprotection of Macrocyclic Bolaamphiphile.....	19
2.7: Macrocyclic Bolaamphiphile Head Group Addition.....	20
2.8: Deprotection of Linear Bolaamphiphile.....	24
2.9: Linear Bolaaphiphile Head Group Addition.....	25
2.10: Synthesis of Glutarate Monoester with 1-dodecanol.....	27
2.11: Synthesis of Glutarate Diester.....	27
2.12: Deprotection of linear Amphiphile.....	28
2.13: Linear Amphiphile Head Group Addition.....	29
Chapter 3: Membrane-spanning Assay and Conclusions.....	31
3.1: Moss Assay.....	31
3.2: Membrane-spanning Assay.....	32
3.3: Conclusions and Future Work.....	40
Bibliography.....	42
Appendix 1: Experimental Details.....	44
Appendix 2: Supporting Information; Synthesis.....	57

List of Tables

Table A1: Effective diameter of vesicles containing all three synthesized phospholipids.....	55
Table A2: Absorbance data from the membrane-spanning assay showing no change in absorbance over 100 minutes.....	56

List of Figures

Figure 1.1: Common phospholipids. A: A phosphatidyl choline with regions distinguished by polarity. B: A Phosphatidic Acid.....	1
Figure 1.2: A: Packing parameter calculation for lipids. B: A vesicle bilayer formed when the packing parameter is $0.7 < S < 1$	2
Figure 1.3: The differences between conventional lipids and archaea lipids. A: Differences in attachment and carbon chains. B: Stereochemical difference.....	6
Figure 1.4: The versatility of the midpolar linking unit.....	10
Figure 1.5: The macrocyclic bolaamphiphile target compound and amphiphiles for control against target compound. A: Conventional style lipid with a single 4-nitrophenylphosphate head group. B: Acyclic bolaamphiphile with two 4-nitrophenylphosphate head groups. C: Macrocyclic bolaamphiphile.....	12
Figure 2.1: Accurate mass indicating the presence of the macrocyclic bolaamphiphile. Purple dots indicate masses obtained from M-2H, 2M-4H, and 3M-6H ions. Green dots indicate masses obtained from just 2M-2H ions and yellow dots indicate masses obtained from just 3M-6H ions. The charge(z) finding algorithm of the Orbitrap incorrectly interprets the aggregates as an isotope pattern and therefore associates the wrong charge with the mass peaks.	22
Figure 3.1: The idea behind the absorbance assay developed by Moss. A: A cross section of a lipid bilayer from a vesicle with p-nitrophenylphosphate lipids associated at an initial pH of 5.5. B: A cross section of a lipid bilayer from a vesicle showing how a change in pH cleaves p-nitrophenolate ions from a phospholipid head group.....	32
Figure 3.2: An idealized absorbance versus time graph displaying the difference between U-shaped and membrane-spanning absorbance readings.	33
Figure 3.3: ESI-MS in negative mode. A: A mass spectrum confirming 1-24 was associated with the bilayer membrane of vesicles. B: A mass spectrum confirming 1-23 was associated with the bilayer membrane of vesicles.....	35
Figure 3.4: ESI-MS (-) mode spectra of vesicles, after treatment with a base. A: Vesicles initially containing 1-24; the ion at 806.27 m/z is known to be a contaminant from a previous sample from another user. B: Vesicles initially containing 1-23.	36-37
Figure 3.5: The observed NMR from the reaction that replicated conditions seen by vesicles in the membrane-spanning assay. The NMR is overlaid with a ^1H -NMR from prediction software and the chemical structure that was predicted.....	39
Figure 3.6: Illustrating the difference between naturally occurring midpolar linkers and the one chosen for the syntheses seen here.....	40

Figure A1: Figure A1: Absorbance as a function of time at 400 nm during the membrane-spanning assay. Vesicles prepared with 1-22 at a pH 6.4 following a base pulse to pH 11.8. Absorbance reading every 30 seconds for 100 minutes.....55

List of Schemes

Scheme 1.1: The coupling of two eleven carbon units to create a twenty-two carbon hydrophobic chain.....	8
Scheme 1.2: A hydrophobic linker approximately 35 Å in length.....	9
Scheme 1.3: Demonstrative reaction scheme that uses “click” chemistry as a way to create a hydrophobic core in a relatively fast reaction.....	10
Scheme 2.1: Overview of synthetic route taken to the macrocyclic bolaamphiphile.....	13
Scheme 2.2: 3-(tert-butyl dimethylsilyloxy) glutaric anhydride reacting with 10-undecyn-1-ol to form the glutarate monoester 2-1.	14
Scheme 2.3: The CuAAC dimerization of the glutarate monoester 2-1 with the bis-azide 1-18.....	15
Scheme 2.4: The esterification of the diacid 2-2 with 10-undecyn-1-ol to form the bis-alkyne 2-3.....	17
Scheme 2.5: The macrocyclization of the bis-alkyne 2-3 with the bis-azide 1-18.....	18
Scheme 2.6: The removal of the protecting groups on 2-4, forming the diol 2-6.....	19
Scheme 2.7: Head group addition to the diol 2-6, forming the macrocyclic bolaamphiphile 1-22.....	20
Scheme 2.8: Synthesis of the macrocyclic bolaamphiphile. Synthetic details in Appendix 1, NMR in Appendix 2.....	23
Scheme 2.9: The protecting group removal of TBDMS- to form the linear diol 2-7.....	24
Scheme 2.10: The head group addition to the linear diol to form the linear bolaamphiphile 1-24.....	25
Scheme 2.11: Synthesis of the linear bolaamphiphile. Synthetic detail in Appendix 1, NMR in Appendix 2.....	26
Scheme 2.12: 3-(tert-butyl dimethylsilyloxy) glutaric anhydride reacting with 1-dodecanol to form the glutarate monoester 2-9.....	27
Scheme 2.13: The esterification of glutarate monoester with 1-dodecanol to form the glutarate diester 2-10.....	28
Scheme 2.14: The protecting group removal of TBDMS- to form a glutarate diester with an alcohol.....	29
Scheme 2.15: The head group addition of 2-5 to the glutarate diester 2-11.....	29
Scheme 2.16: Synthesis of amphiphilic lipid. Synthetic detail in Appendix 1, NMR in Appendix 2.....	30
Scheme 3.1: The reaction of a nitrophenylphosphate lipid with a base to a phosphatidic acid and nitrophenolate chromophore.....	31

Scheme 3.2: Elimination of the p-nitrophenylphosphate head group from 1-23, by a hydroxide ion, later undergoing the loss of a proton due to basic conditions which establishes the correct mass as detected by ESI-MS.38

List of Abbreviations

AcOH: acetic acid

DCM: dichloromethane

DiPEA: N,N-diisopropyl ethylamine

DIC: N,N-diisopropyl carbodiimide

DMAP: 4-dimethylaminopyridine

DMF: N,N-dimethylformamide

DMSO: dimethyl sulfoxide

EDTA: ethylenediaminetetraacetic acid

EtOAc: ethyl acetate

Et₂O: ethyl ether

Equiv.: equivalents

HOBt: hydroxybenzotriazole

MeOH: methanol

NMR: nuclear magnetic resonance

¹H-NMR: proton nuclear magnetic resonance

¹³C-NMR: carbon-13 nuclear magnetic resonance

R.T.: room temperature

RBF: round bottom flask

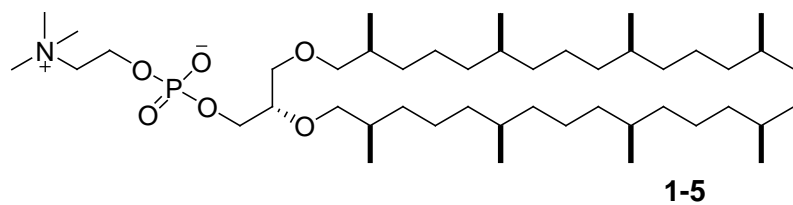
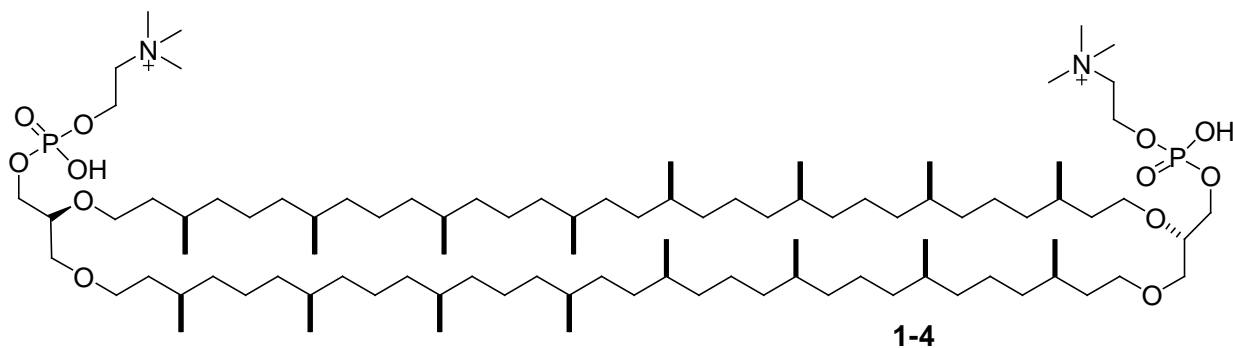
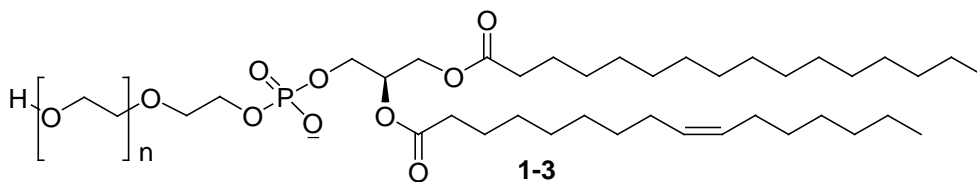
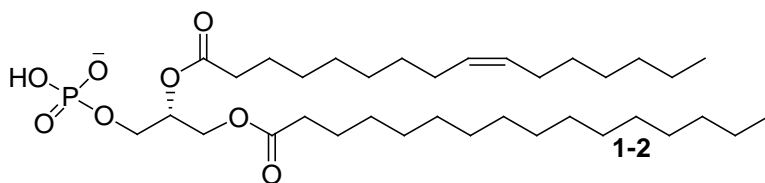
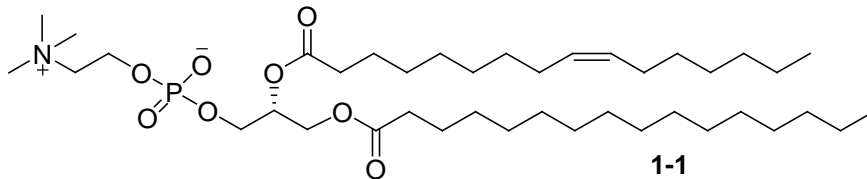
TBAF: *tetra-n*-butylammonium fluoride

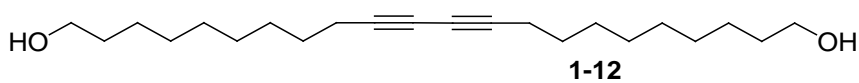
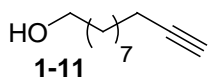
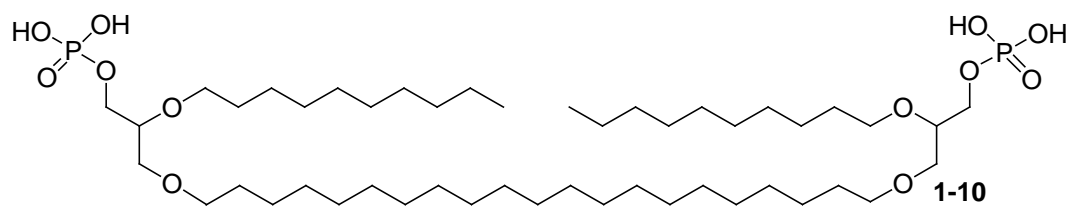
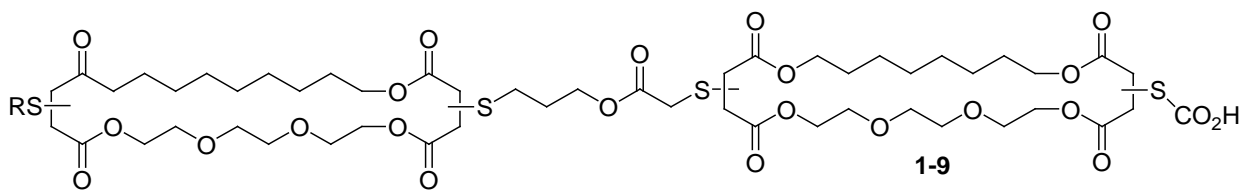
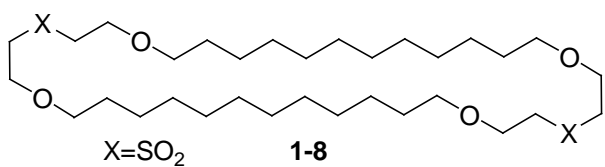
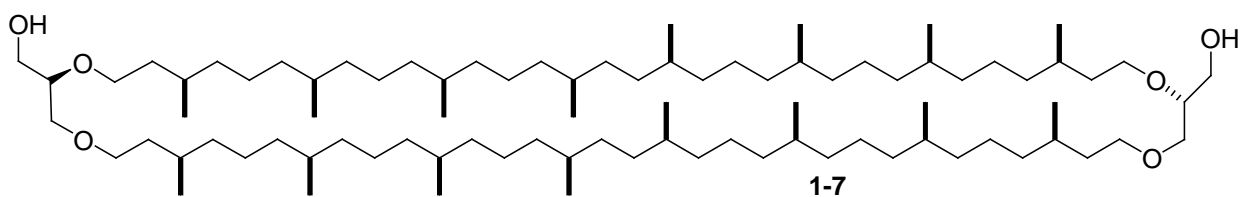
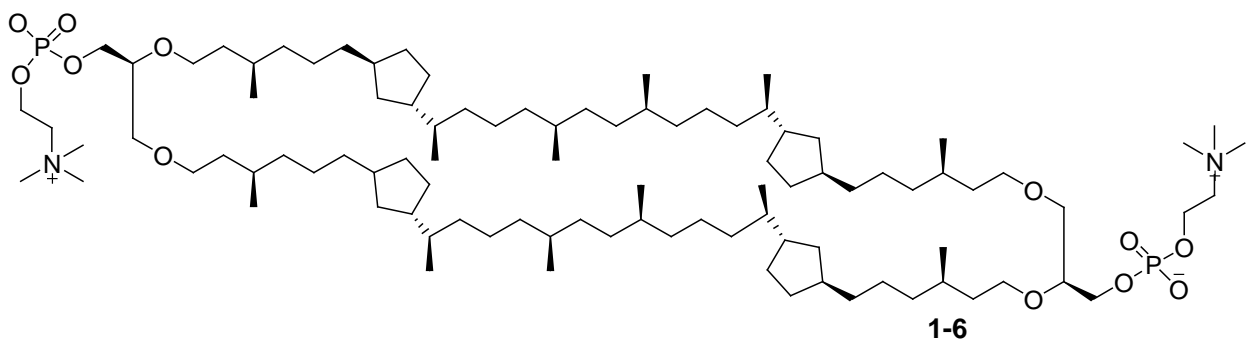
TBDMS: *tert*-butyl dimethylsilane

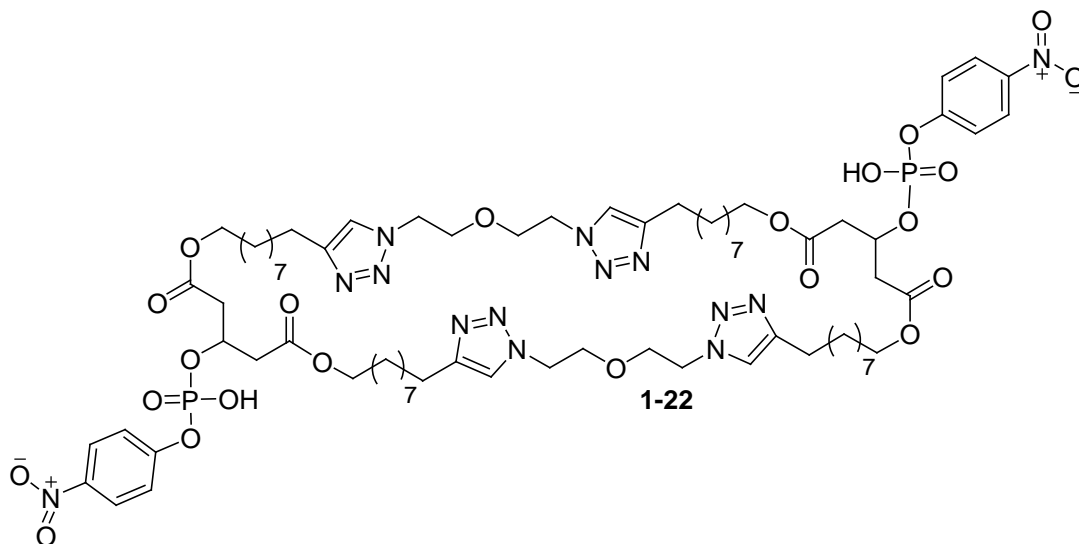
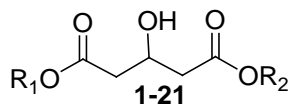
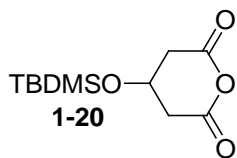
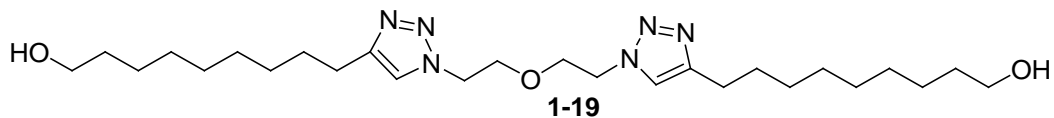
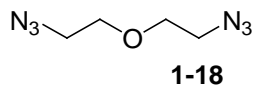
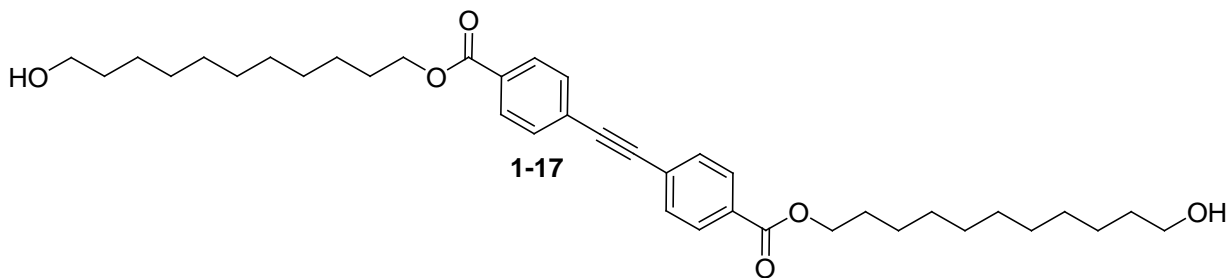
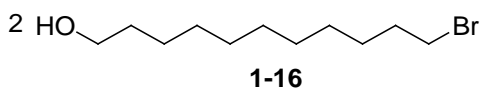
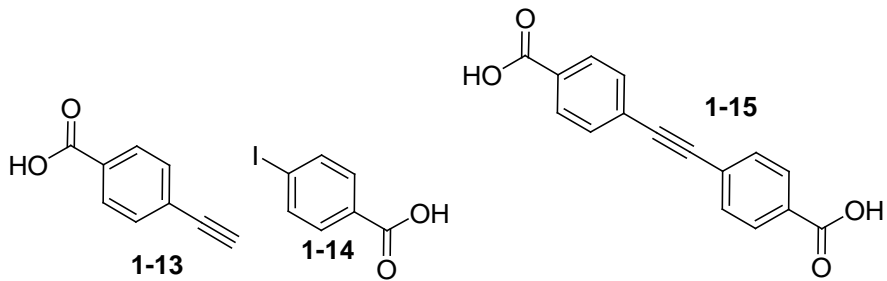
THF: tetrahydrofuran

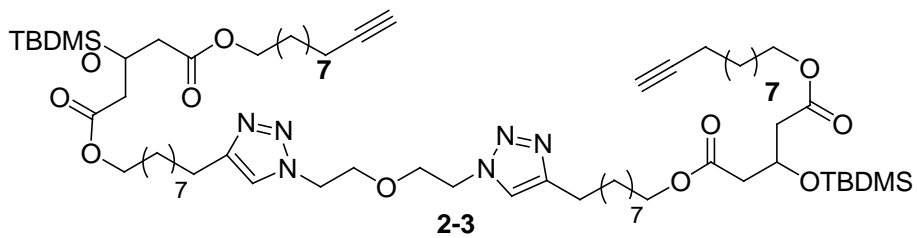
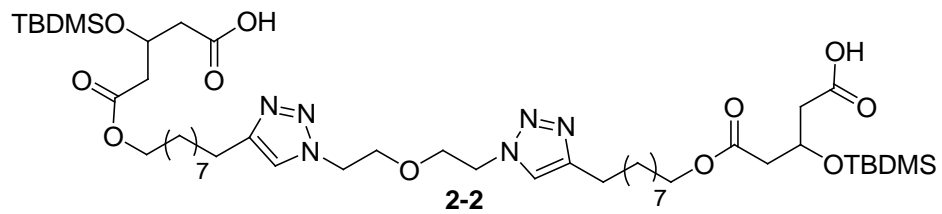
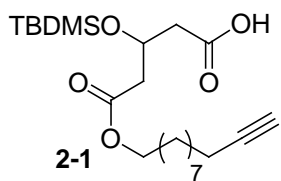
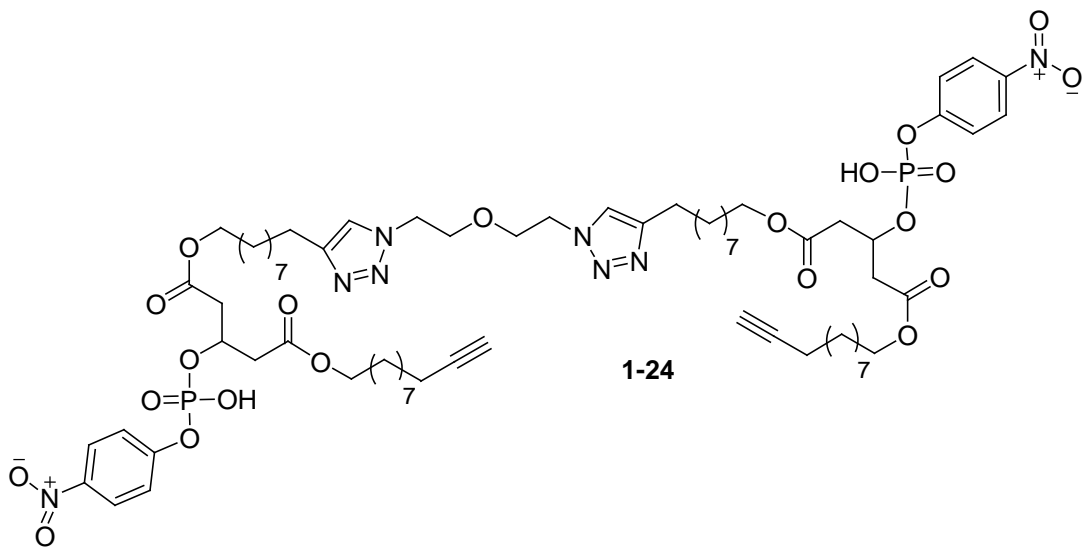
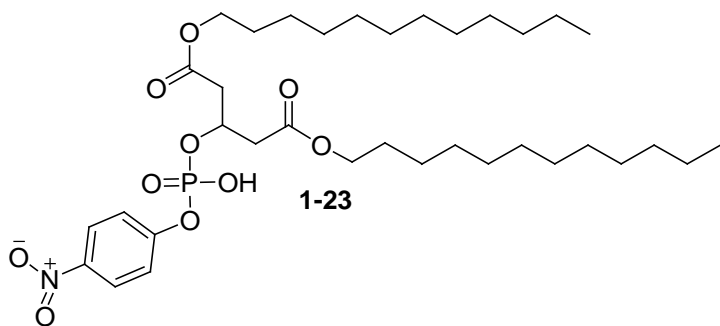
TLC: thin layer chromatography

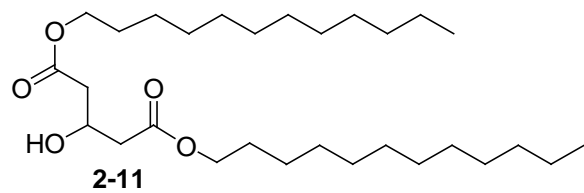
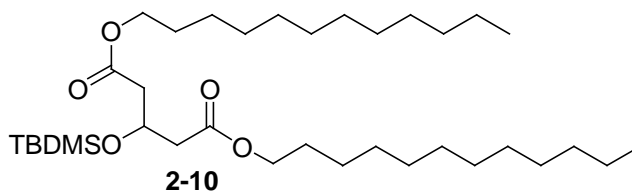
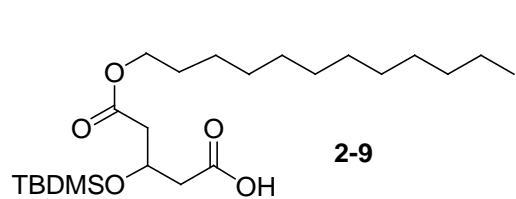
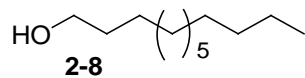
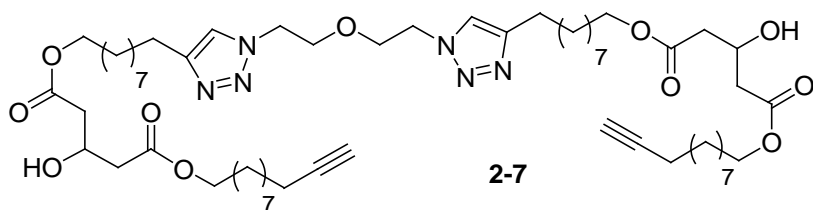
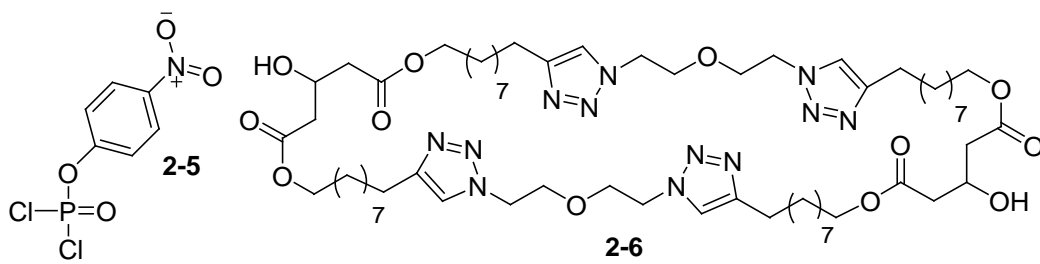
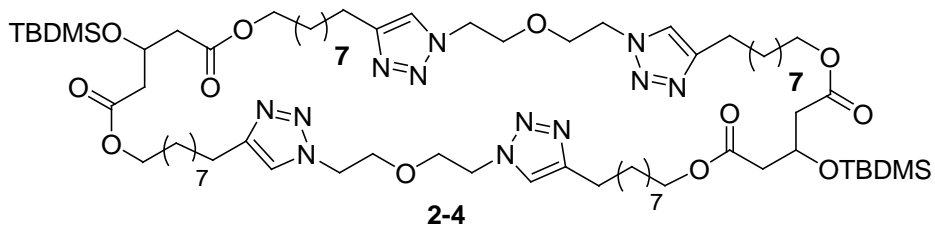
List of Numbered Compounds

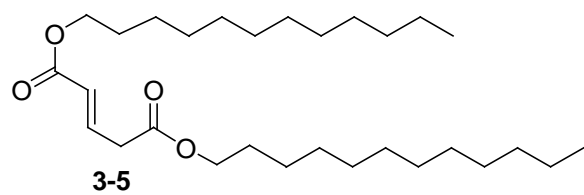
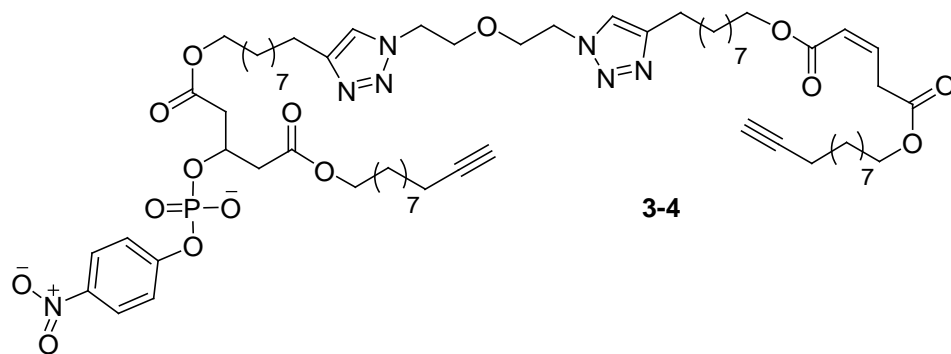
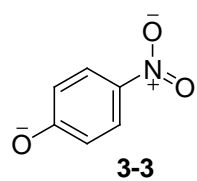
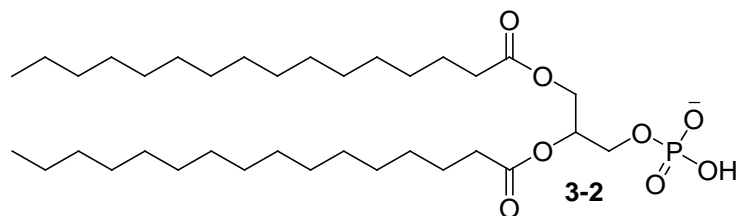
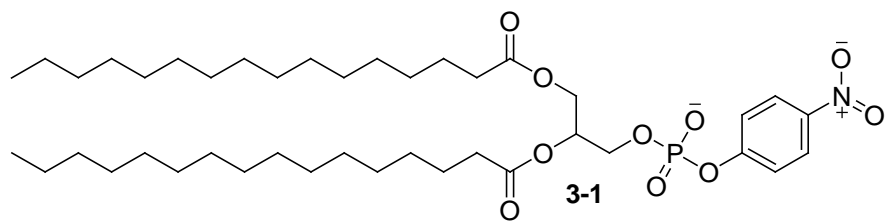












Acknowledgements

It's the hardest section to write but the easiest to feel. Sentence structure can finally be thrown to the wind and everybody gets to peak at who is beneath it all. Unfortunately, words of acknowledgement could not speak to the way I feel about those of you that surround my life. I must instead leave all of you with a piece of myself, with hope that it can provide more than sentences could desire.

Wind

Beautiful day; or night,

Cracked, paned glass, cures

What plagues all souls,

With the Sweet Caress

of infinite hands

Chapter 1: Introduction

1.1: Lipids

Lipids make up the cell membrane of all forms of life and 50% of the cell membrane of an animal¹. Conventional phospholipids, that can be found in animals, contain both, a hydrophobic region, and hydrophilic phosphate head group¹⁻². Most commonly the hydrophobic portion of the lipid is comprised of two long alkyl chains known as tails. The tails of each lipid can vary from being fully saturated to containing many degrees of unsaturation. A glycerol unit links both alkyl chains via ester bonds to the hydrophilic head group. Functionalization of the head group often occurs in natural lipids. These functional groups are ionic, which increases the hydrophilicity of the head group. Common head groups include choline, or simply the anionic phosphatidic acid seen in Figure 1.1. However in biological systems there are an extensive range of head groups that exist from oligosaccharides to sulfates³.

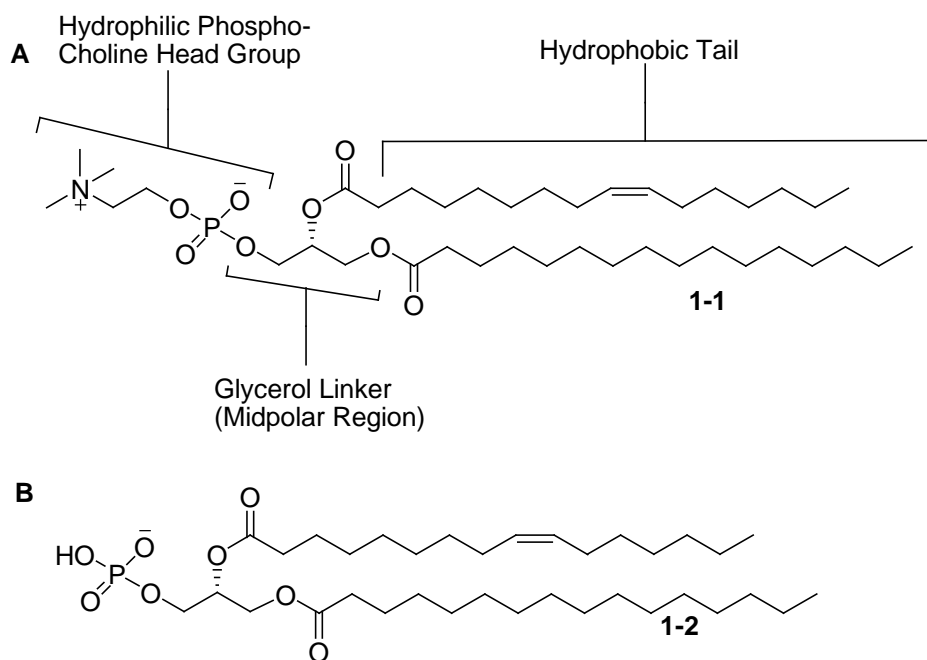


Figure 1.1: Common phospholipids. A: A phosphatidyl choline with regions distinguished by polarity. B: A phosphatidic acid.

In an aqueous environment the hydrophobic region of each lipid will aggregate, predominantly driven by entropy⁴. Entropy favors the creation of aggregates since a single hydrophobic tail exposed to an aqueous solution requires water to be highly ordered around that tail, which is entropically

unfavorable. Released water in the bulk solution then becomes disordered when hydrophobic tails interact with each other as aggregates form. Entropy is now increased. The shape that aggregates take is dependent on the critical packing parameter. The packing parameter (S) depends on hydrophobic chain length, l_c , chain volume, V , and area exposed to the aqueous environment, a_o , Figure 1.2A.

The aggregate that separates the internal cellular environment from the external has been termed the lipid bilayer, which inherently denotes structural symmetry. Bilayers are the same structures found in the cellular membranes of all domains of life and also in the membranes of eukaryotic organelles¹. The leaflets of a bilayer can be visualized in Figure 1.2B and consists of an inner and outer leaflet. When a bilayer forms a sphere, as a result of a particular packing parameter approximately equal to one, a vesicle is formed. The bilayer enables internal and external environments to operate away from equilibrium, a condition necessary for life¹.

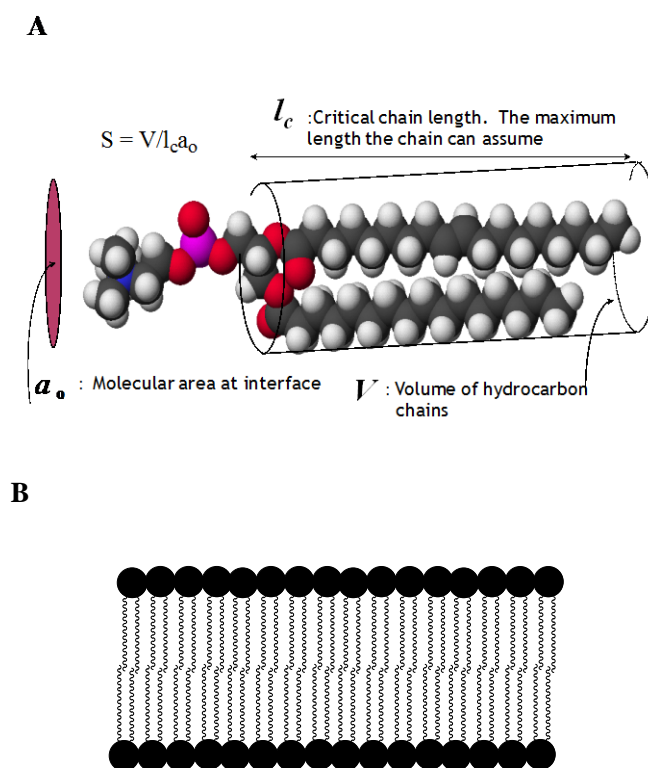
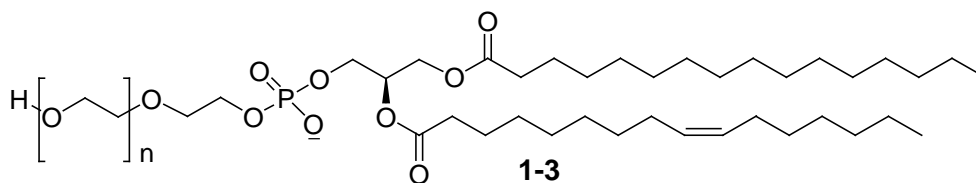


Figure 1.2: A: Packing parameter calculation for lipids. B: A vesicle bilayer formed when the packing parameter is $0.7 < S < 1$.

Having a hydrophobic chain region in the bilayer is the barrier that enables a vesicle to have dissimilar internal and external environments, creating a non-equilibrium state. The tight packing of the tails of the phospholipids creates an environment that is increasingly less permeable to large and charged molecules, and more permeable to smaller more hydrophobic compounds¹. The permeability of a bilayer is dependent on the lipid composition of the membrane^{1,5}. For example, when an extremely hydrophobic molecule such as cholesterol is introduced at the right concentration as part of the membrane, the packing of the tails is increased. This packing stiffens the upper regions of the hydrophobic tails, which results in decreased membrane permeability⁶. In the same way this stiffness makes the vesicle more mechanically stable to osmotic pressures. The increased stability of membranes however is extremely sensitive to the constituency of the lipids associated with the membrane. For lipids that are fully saturated, mono- or di-unsaturated, cholesterol increases stability and decreases permeability of a membrane, but for lipids with greater degrees of unsaturation stability drops off⁶. Another factor in vesicle stability is aggregation of multiple vesicles. During this aggregation, the stability of the vesicle is decreased and bilayer permeability goes up. One way that aggregation is avoided, in artificial vesicles, is the covalent addition of polyethylene glycol to phospholipid head groups such as **1-3**. The repeating ethylene glycol units create steric and electrostatic repulsion with other vesicles which results in decreasing the likelihood of vesicular aggregation, and therefore increasing stability⁷.

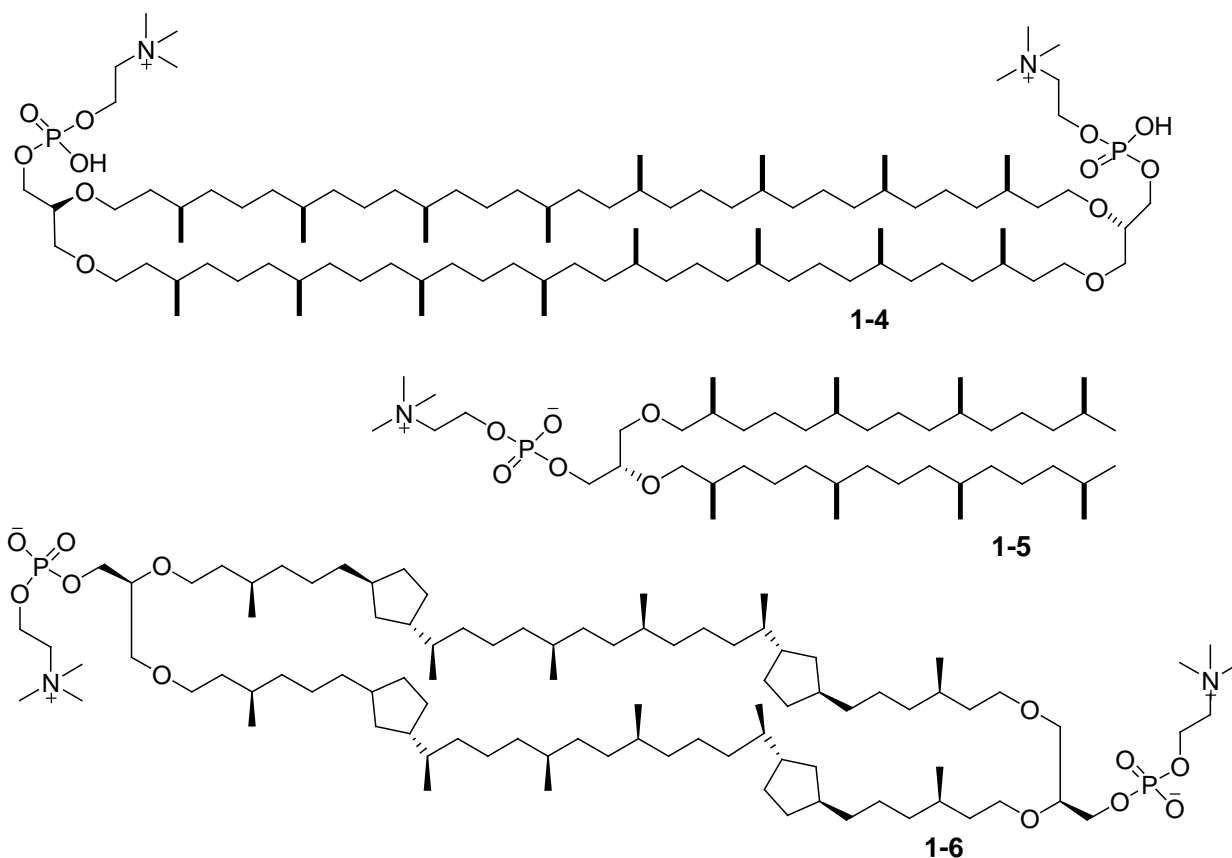


Stability of vesicles is extremely important for drug delivery in human systems⁵. Due to the amphiphilic nature of lipids, hydrophobic or hydrophilic drugs can be delivered by vesicles, by either self-inserting into the hydrophobic region, or in the vesicles aqueous interior. Ideal substrate transportation under physiological conditions requires a structure that will maximize the effective delivery of drugs to target sites. An efficiently transported drug reduces toxic side effects, and multiple dose requirements. However, vesicles assembled from conventional lipids are relatively unstable. Internal physiological conditions that destabilize vesicular structure include bile salts, serum proteins, and the action of phospholipases⁵. Phospholipases hydrolyze conventional lipids, serum proteins can remove lipids from a vesicle, and bile salts fluidize the membrane, all of these have the effect of making bilayer membranes less stable⁸. Inefficient delivery of drugs to target tissue results from this instability.

Improving upon vesicle stability, beyond an optimized cholesterol content or addition of polyethylene head groups, has led to research into lipids from the domain Archaea. Archaea are naturally

present in conditions that tend to the extremes of habitability, such as high and low pH, and salinity⁹. To be able to thrive in these environments these organisms must have membranes that have very low permeability to the life threatening concentrations of solutes present in the environment in which they live. The lipid composition found in Archaea distinguishes them as a unique domain separate from both Eukarya and Bacteria. It is also this lipid composition of their specialized bilayer membrane that enables Archaea to maintain an internal environment distinct from the harsh external environment in which they live; this presents Archaea lipids as ideal candidates for being able to increase vesicle stability. Vesicles that are composed with some portion of Archaea lipids have been termed archaeosomes. Research into activity and function of archaeosomes has shown that the stabilities issues existing in vesicles made from conventional lipids, such as aggregation or permeability, can be resolved with the use of Archaea lipids. Solving the issue of permeability of vesicles enables increased efficacy and reduced toxicity of the encapsulated drugs⁷.

Existing known archaic lipids are classified as archaeols or caldarchaeols. Archeols, such as **1-5**, are noncyclic lipids, with a single head group located on the inner or outer leaflet of a cell, whereas caldarchaeols, such as **1-4**, are macrocyclic, have two head groups, and are present on both leaflets of the bilayer making them membrane-spanning. In addition, archaea, in response to environmental pressures, can synthesize caldarchaeols like **1-6**, with cyclopentane rings in their hydrophobic chains. The distinguishing features that hold archaea membrane lipids apart from Eukarya and Bacteria found in both archaeols and caldarchaeols is the 1,5 branching phytanyl chains, ether linkages to head group moieties, and are identified with stereospecific numbering *sn*-2,3 stereochemistry for attachment of alkyl chains to the head groups, Figure 1.3⁵.



Bridging the gap of using Archaea lipids in the formation of drug delivery vesicles rather than conventional lipids has importance to creating more stable vesicles. However, this gap poses challenges. Archaea can be cultured and the polar lipids extracted to then be used in vesicle stability research, but at present this is expensive, labour intensive, and gives mixed lipid products such as varying concentrations of **1-4**, **1-5**, and **1-6**⁵. Movement away from cultured lipids requires the synthesis of artificial lipids. Artificial lipids present the opportunity for an expansion in the understanding of how a membrane-spanning lipid can influence bilayer stability.

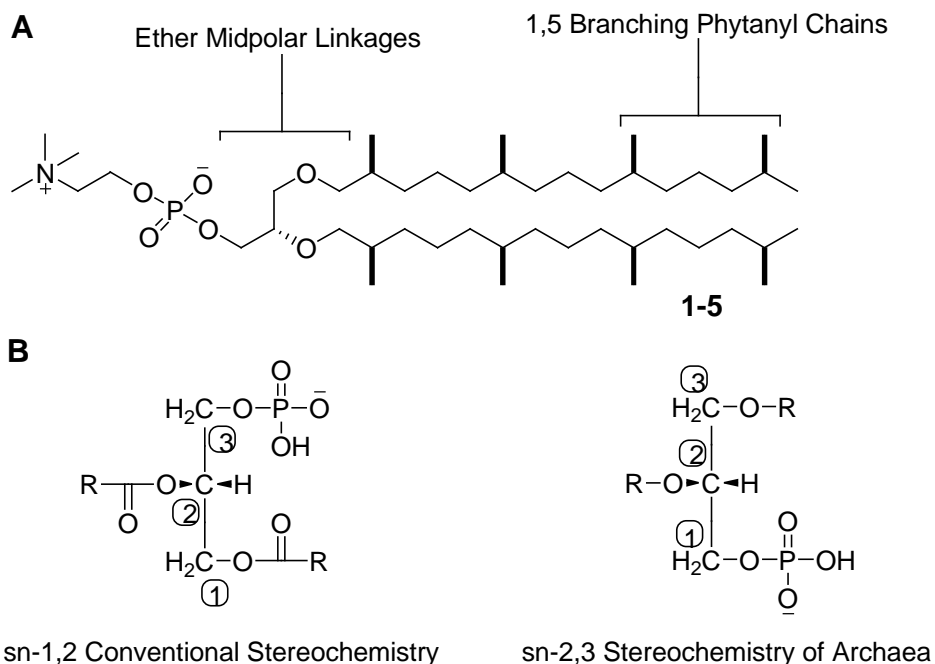
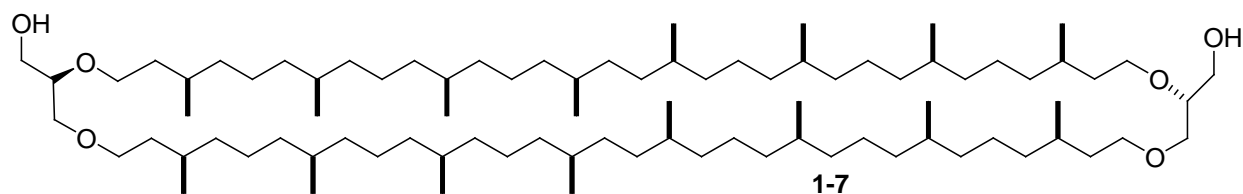


Figure 1.3: The differences between conventional lipids and archaea lipids. A: Differences in attachment and carbon chains. B: Stereochemical difference.

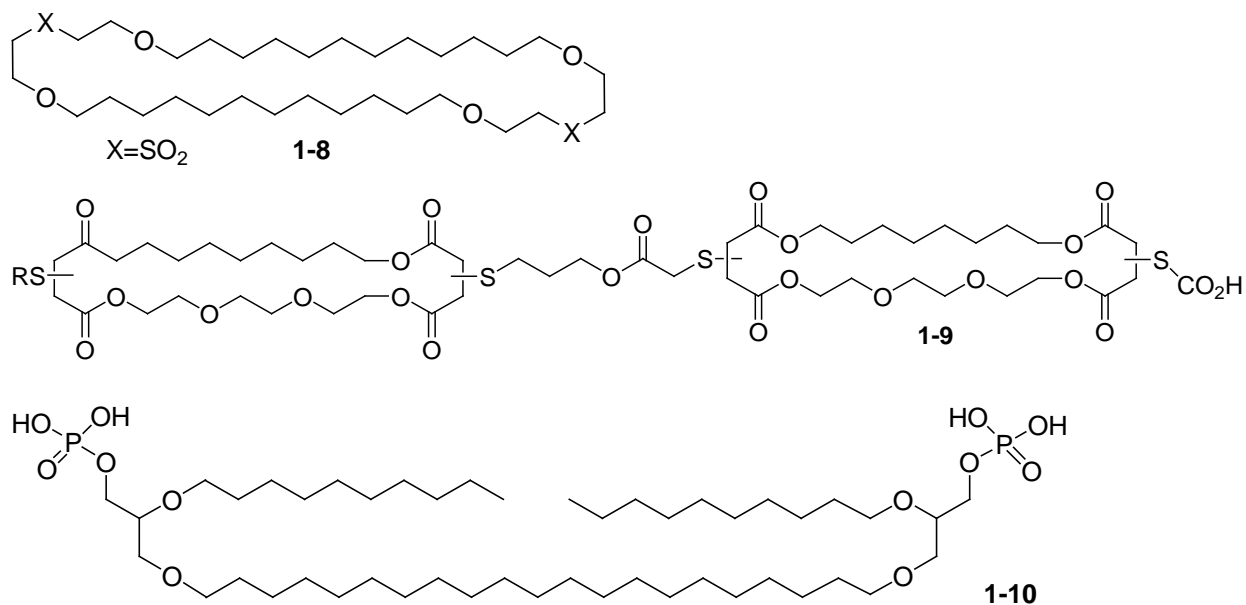
1.2: Synthetic Bolaamphiphiles

Synthetically replicating an Archaea membrane-spanning lipid is extremely challenging. One total synthesis of **1-7** has been done to replicate the caldarchaeol to a diol product, consisting of 20 steps and 1.9% total yield¹⁰. This demonstrates the complexity and labour required to replicate Archaea membrane-spanning lipids. From this challenge a new field of synthetic lipids was created to overcome the complexity of synthesizing caldarchaeols, while attempting to retain their function. These lipids were termed bolaamphiphiles¹¹. The bolaamphiphile has a two-headed structure that is amphiphilic, which means it contains both a hydrophobic and two hydrophilic regions in its structure. The orientations of these regions are similar to the South American bola, with two hydrophilic head groups attached by a hydrophobic core, creating the term bolaamphiphile.



Archaic lipids most likely increase stability and decrease permeability of a membrane because of their ability to span the bilayer; since the same increase in stability is not seen with archaeols⁵. Attempting

to replicate the stability performance of the caldarchaeol is the goal of many synthetic bolaamphiphiles. These natural mimics all vary in structure and chemical function; unfortunately, compounds already in this class are synthetically too simple to replicate the membrane stabilizing function of the archaic lipids. It is this macrocyclic moiety that makes it both a synthetic challenge and promises increased stability¹². Previously synthesized bolaamphiphiles either lack the hydrocarbon chain length to be membrane-spanning, **1-8**, form structures that destabilize the membrane, **1-9**, or, most importantly, have no cyclic moiety and therefore form structures that are U-shaped and not through membrane, **1-10**¹¹.



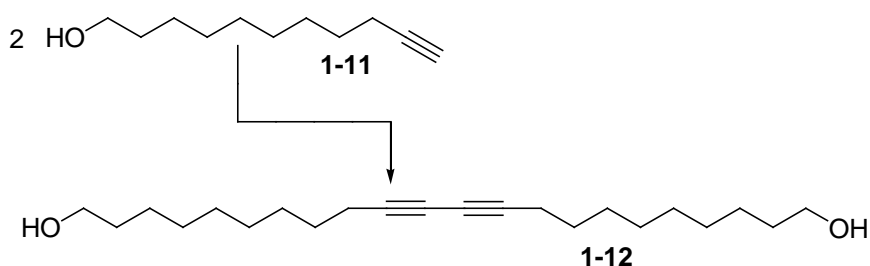
1.3: Design and Project Overview

A synthetically simple membrane-spanning bolaamphiphile would be a great step forward in providing stable vesicles for use in delivering a wide variety of bioactive chemicals within the human body⁵. Considering bolaamphiphiles that have already been synthesized and what features they lack in order to be membrane stabilizing, it is essential that a suitable target be designed. Key moieties in the target structure were; macrocyclic, a hydrophobic chain long enough to span a typical membrane (ca. 3.5 nm), two head groups on opposing ends of the hydrophobic core, and reduced flexibility in its hydrophobic core¹².

The structures required in the target bolaamphiphile are a challenging array of requirements and subsequently present a difficult synthesis. For this reason synthetic complexities to mimic the

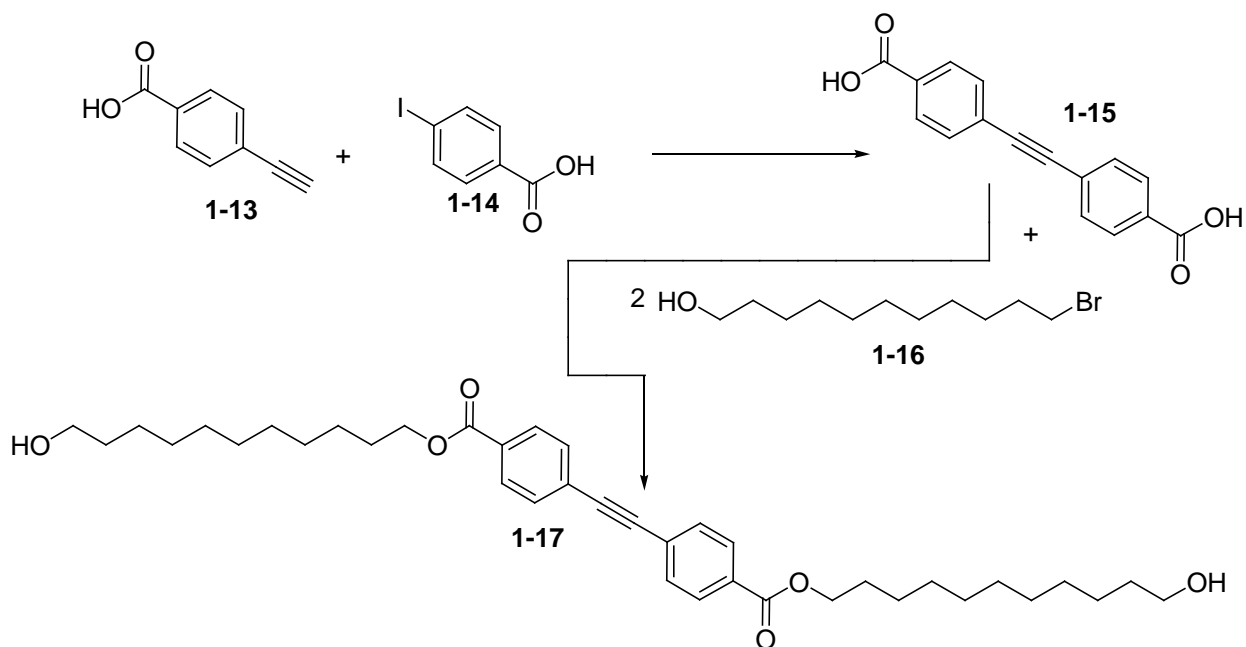
caldarchaeol such as 1,5 branching phytanyl chains, and proper stereochemistry of the midpolar linker were taken with lesser weight than efficiently reproducing a membrane-spanning lipid.

The initial challenge was to design a final structure that might be synthesized in as few steps as possible while retaining the essential outlined chemical properties. The first issue at hand with this was to devise a synthetic plan of the hydrophobic linking unit. It had to span a typical membrane, 35 Å, which is the equivalent of about a 32 methylene carbon chain, all in anti-conformation². Unfortunately; inexpensive, commercially available reagents, that are bifunctionalized for further synthesis steps are a maximum of eleven carbons in length. The reaction in Scheme 1.1 creates a linking unit of 22 carbons falling about 12 Å short of being capable of membrane-spanning.



Scheme 1.1: The coupling of two eleven carbon units to create a twenty-two carbon hydrophobic chain.

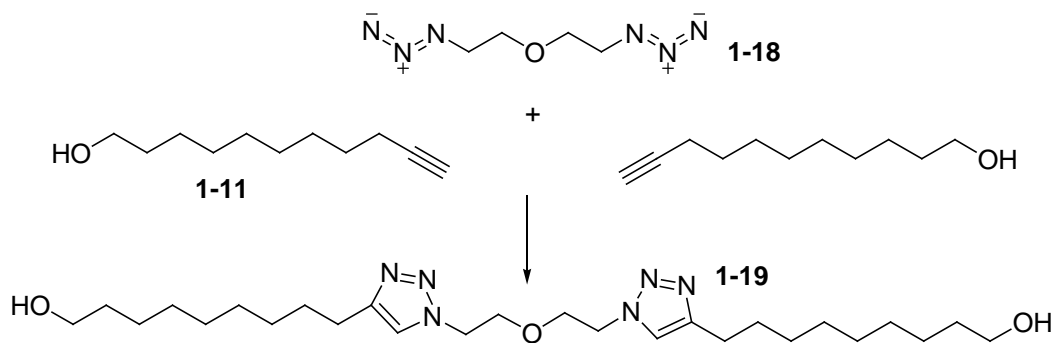
If a 12 Å chain could be synthesized linking the two bifunctionalized eleven carbon units then a hydrophobic chain long enough to span the membrane would be acquired. In addition, if this 12 Å linker was rigid, then the issue of hydrophobic chain rigidity could also be resolved. Reduced flexibility is achieved through the lipid having both a rigid chemical moiety in its hydrophobic core or the lipid being cyclic. Common forms of rigidity in organic molecules are acetylene, aromatic components, or ring structures. Using some of these structures solves the problem of creating a rigid hydrophobic chain, Scheme 1.2. The terminal functional groups on this hydrophobic chain are alcohols, so closing the macrocyclic ring would then be an esterification or an etherification reaction.



Scheme 1.2: A hydrophobic linker approximately 35 Å in length.

Unfortunately, macrocyclization is a competitive reaction with oligomerization. To overcome this roadblock many chemical reactions are diluted. Dilution increases the probability of macrocyclization by making the intramolecular reaction more probable than the intermolecular reaction. This technique may be successful for an etherification or esterification but it however has the drawback of producing a little product and a lot of solvent¹³. Another drawback to esterification and etherification is that these reactions are relatively slow; fast reactions are preferred for efficient macrocyclization¹⁴.

Solving the problem of needing a fast ring closing, along with alkyl chain rigidity, and 35 Å long hydrophobic core, was all possible by using “click” chemistry. Using “click” chemistry to form the hydrophobic core and close the macrocycle became a key part of the project. It enabled the fast formation of a link between two eleven carbon chains, Scheme 1.3.



Scheme 1.3: Demonstrative reaction that uses “click” chemistry as a way to create a hydrophobic core in a relatively fast reaction.

Copper catalyzed Azide-Alkyne Huisgen Cycloaddition (CuAAC) is a form of “click” chemistry that involves a reaction between an azide and a terminal alkyne resulting in a 1,2,3-triazole¹⁵. The linking unit used for creating the hydrophobic region was **1-18**. It was used because it had identical azide units on both its terminal ends, a bis-azide, giving it the ability to link two eleven carbon chains, creating a 35 Å hydrophobic core, Scheme 1.3. The resulting core would also have rigidity, provided through the triazoles of CuAAC. In addition, it was a promising way to close the macrocycle since it was a fast reaction and work has already been done that exemplifies macrocyclic ring closures in good yield and standard conditions using CuAAC¹⁶. The result was a rigid and hydrophobic chain approximately 35 Å in length.

Bolaamphiphiles have a hydrophobic core and a hydrophilic head. Designing a synthesis with these two properties would require being able to link them in some way. As seen in Figure 1.1A natural occurring lipids use a glycerol linking unit. However the glycerol linker posed challenges to incorporate into the structure of the lipid because it is difficult to functionalize compared to a linker that had ester groups in its structure. For these reasons the midpolar linker, **1-20** was chosen as the precursor. It was a strong choice because it offered the ability to become bifunctionalized through the two different types of ester chemistry offered by its anhydride moiety, both of which have been previously well worked out in the Fyles lab^{2, 17}. In addition, **1-20** was available as a protected material having the *tert*-butyl dimethylsilyloxy group already attached which could be later removed to provide the ability to attach a head group through the resulting alcohol, Figure 1.4.

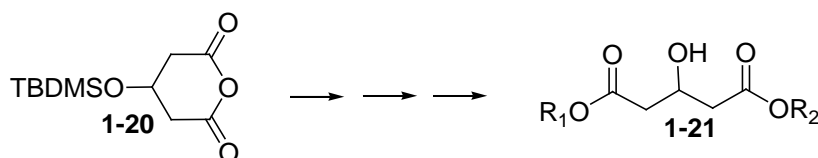


Figure 1.4: The versatility of the midpolar linking unit.

The orientation of the target compound in a bilayer membrane needed to be assessed, that is whether it was membrane-spanning or U-shaped. A lipid that has a single head group and is confined to the bilayer of a vesicle has its head group either facing inwards, endo-vesicular, or outwards, exo-vesicular. A bolaamphiphile in a U-shaped orientation would have both head groups associated with the same leaflet of the bilayer membrane, either both being endo- or exo-vesicular. The design for a membrane-spanning lipid must therefore have both an endo- and exo-vesicular head group.

To be able to determine if the head groups of a bolaamphiphile are on opposite sides of the bilayer membrane or not there needed to be some functional group that could produce a detectable signal showing where it was associated in the membrane. A unique head group, 4-nitrophenylphosphate, was used to determine this in an assay developed by Moss¹⁸. Although 4-nitrophenylphosphate is an unconventional head group when it is cleaved by a base it releases 4-nitrophenolate which absorbs in the visible electromagnetic spectrum. This is useful for determining where the head groups of the lipid are located, and thus how the lipid orients itself in the membrane.

The cleavage of p-nitrophenolate by a base occurs in an aqueous environment. Being able to have head group cleavage, and subsequent absorption, occur in aqueous conditions is an excellent set up to determine the concentrations of head groups located externally and internally. A bolaamphiphile lipid contained in the membrane bilayer of a vesicle having a head group that can identify its orientation through the concentration reading of absorbance could be shown to either have a greater concentration of head groups exposed to the internal aqueous environment, or the external aqueous environment. If a greater absorbance was visualized in an external absorbance reading than that of an internal one then more head groups would be located externally. A bolaamphiphile that favours to be membrane-spanning would logically have an equal number of head groups orientated externally and internally. On the other hand, a U-shaped configuration would have more head groups externally because of the increased surface area of the outer leaflet of the bilayer due to its greater radius.

A compound was designed that included a rigid 35 Å hydrophobic chain, a highly adaptable midpolar linker, and a hydrophilic head group. In addition the head group was specifically functionalized for a membrane-spanning assay. The synthesis of the designed macrocyclic bolaamphiphile was then carried to completion. Along with the macrocyclic bolaamphiphile, controls similar to conventional lipids and acyclic bolaamphiphiles needed to be synthesized to ensure that the assay developed properly, Figure 1.5.

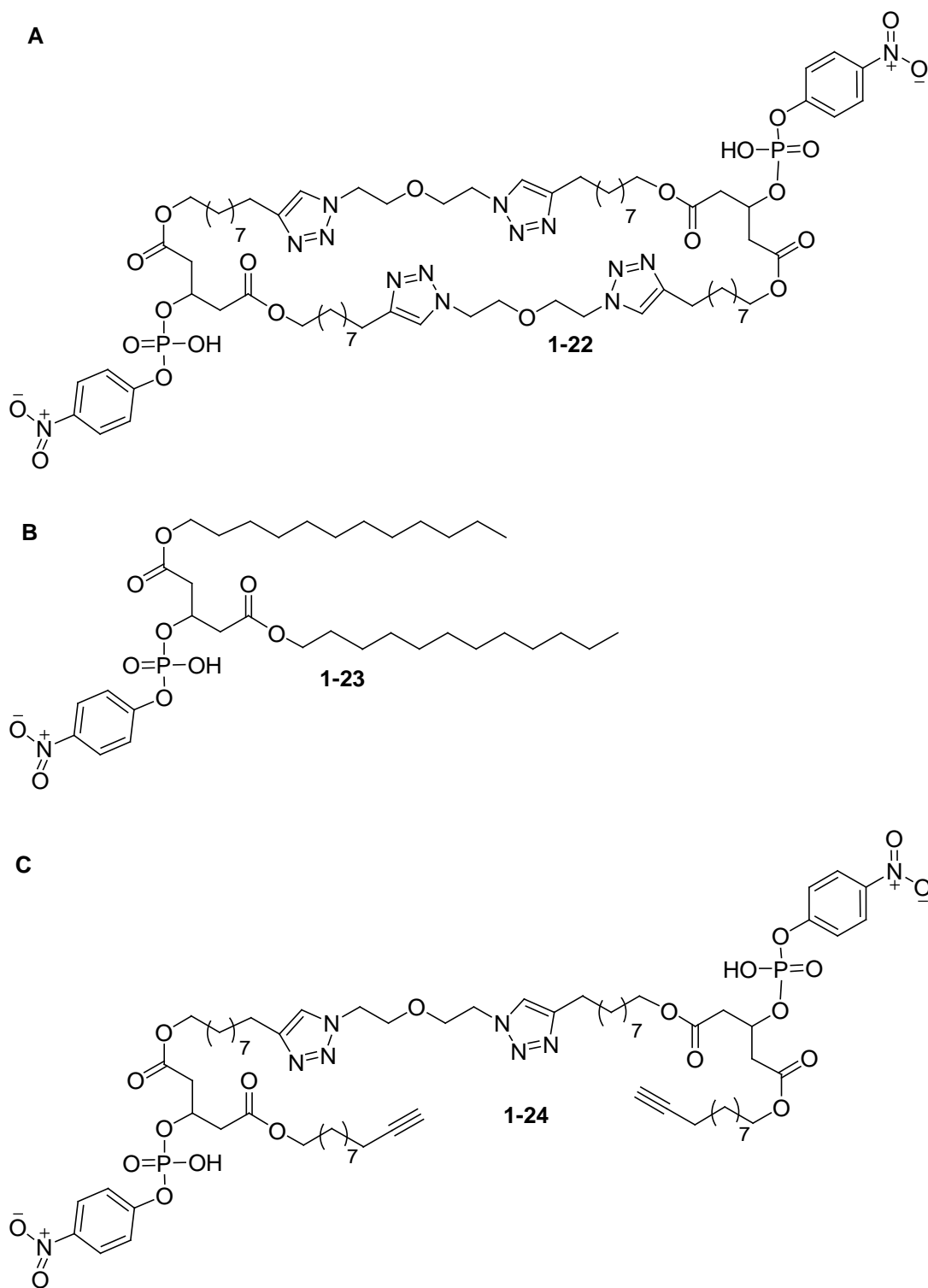
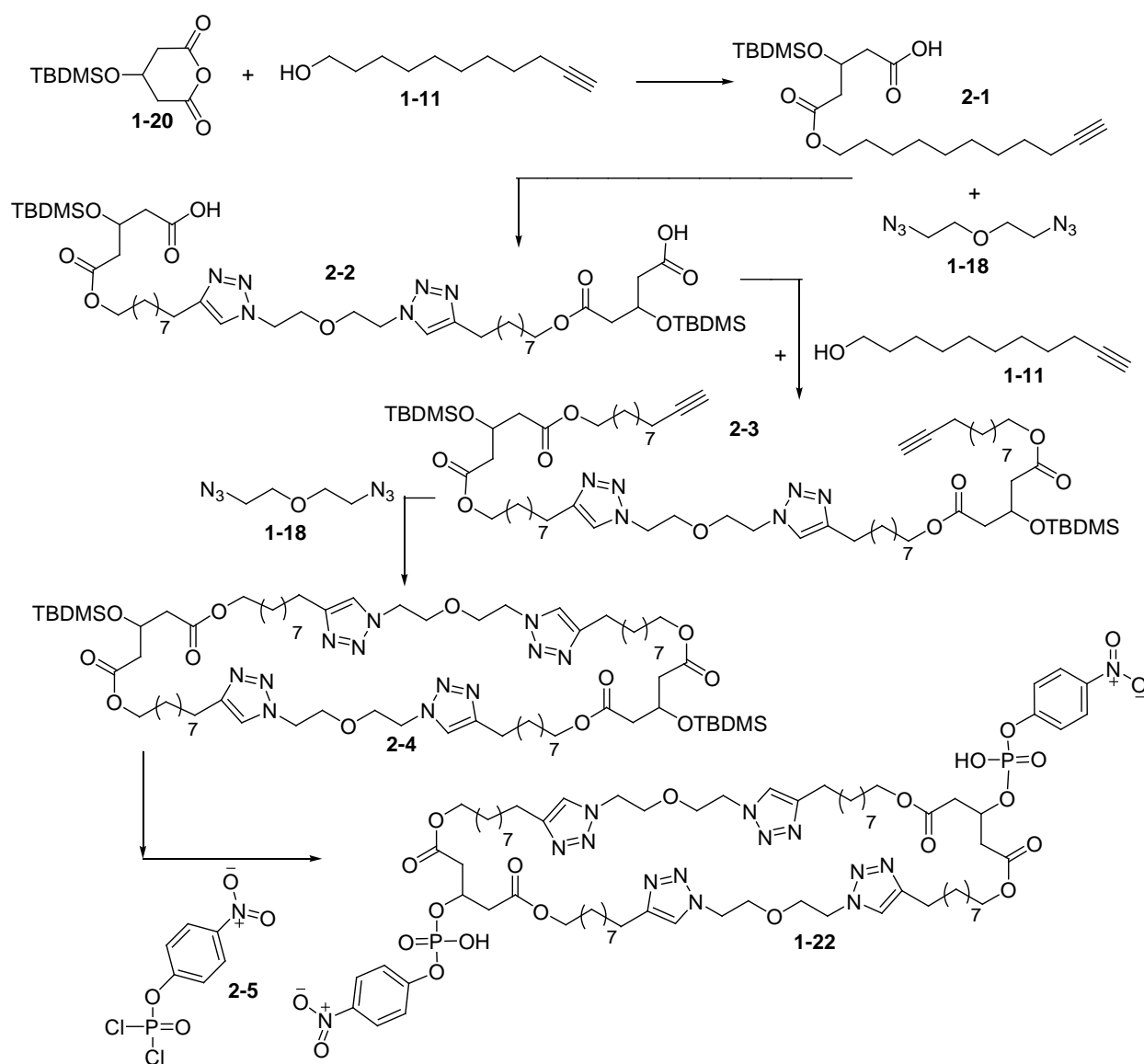


Figure 1.5: The macrocyclic bolaamphiphile target compound and amphiphiles for control against target compound. A: Conventional style lipid with a single 4-nitrophenylphosphate head group. B: Acyclic bolaamphiphile with two 4-nitrophenylphosphate head groups. C: Macrocyclic bolaamphiphile.

Chapter 2: Synthesis of Amphiphiles

2.1: Synthesis

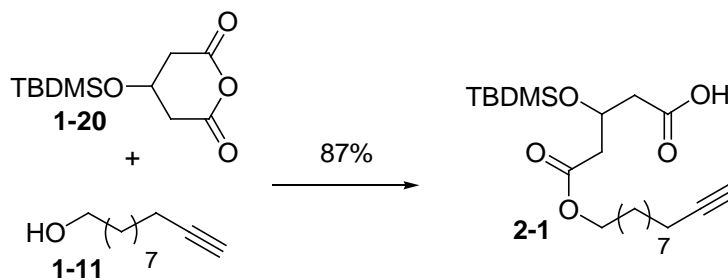
In order to study membrane orientation of the macrocyclic bolaamphiphile it and two other lipids were created and their synthesis will be detailed here. Full experimental detail can be found in Appendix 1, and NMR spectra can be found in Appendix 2. An overview of the synthesis of the macrocyclic bolaamphiphile can be found in Scheme 2.1, and the detailed synthesis of the macrocycle can be found in Scheme 2.8. The total synthesis of all three compounds was made up of five unique synthetic conditions.



Scheme 2.1: Overview of synthetic route taken to the macrocyclic bolaamphiphile.

2.2: Synthesis of Glutarate Monoester with 10-undecyn-1-ol

The first step in the synthesis of the macrocyclic bolaamphiphile was reacting the midpolar precursor, **1-20**, with the eleven carbon alcohol/alkyne bifunctionalized **1-11**. This involved dissolving 3-(*tert*-butyl dimethylsilyloxy) glutaric anhydride in toluene adding 10-undecyn-1-ol and bringing to reflux overnight, a reaction that has been seen in many other cases¹⁷. The reaction product was the monoester **2-1**.



Scheme 2.2: 3-(*tert*-butyl dimethylsilyloxy) glutaric anhydride reacting with 10-undecyn-1-ol to form the glutarate monoester **2-1**.

Unfortunately, a wet sample of **1-20** was used for the first few iterations of the starting reaction. In addition, this reaction produces an acid as a product so the solution becomes more acidic as the reaction proceeds. If water is present in the acidic solution then the product or starting material can easily hydrolyze to undesired diacid side products. To avoid this new 3-(*tert*-butyl dimethylsilyloxy) glutaric anhydride was purchased that had a reduced moisture content. In addition, a drying tube was placed on the condenser to reduce the atmospheric moisture in the reaction.

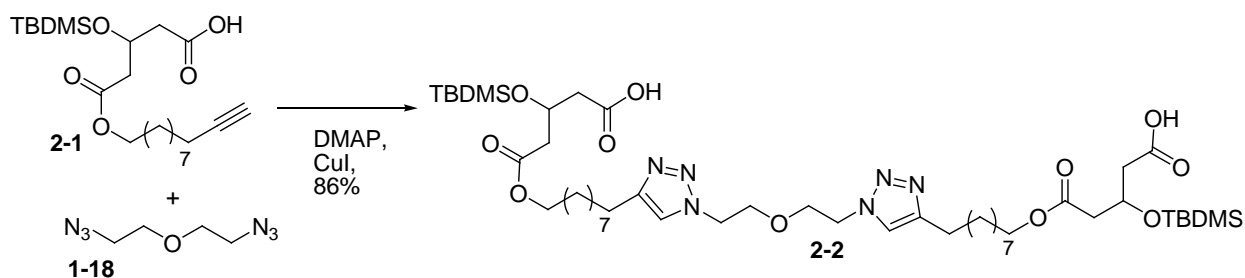
It was important to have 3-(*tert*-butyl dimethylsilyloxy) glutaric anhydride in excess for this reaction. This was because for work up excess alcohol is very hard to separate from the monoester product, but excess anhydride was easily crystallized out. The crystallization involved dissolving the crude product being dissolved in pentane and cooled in a dry ice/ethanol bath. Crystallation was repeated until all excess **1-20** was removed.

The purified product showed an expected ¹H-NMR. It had a glutarate-methine proton quintet at 4.55 ppm (1H), the triplet of the protons by the ester at 4.1 ppm (2H) and the inequivalent glutarate-methylene protons formed a multiplet at 2.6 ppm (4H). The methylene protons next to the terminal alkyne at 2.2 ppm (2H) formed a doublet of triplets due to long distance coupling with the methine proton of the terminal alkyne which was at 1.95 ppm (1H). The terminal alkyne-methine formed a triplet due to long distance coupling with the methylene protons of the alkyne. In addition, the hydrocarbon region of the

NMR spanned from (1.2-1.7) ppm (14H). Finally the methyl groups on the protecting group *tert*-butyl dimethylsilyloxy were at 0.95 ppm for the nine *tert*-butyl protons and at 0.5 ppm for the two methyl units bound directly to the silicon. ESI-MS in negative mode confirmed the structure giving M-1H at 411.20 m/z, a hydrogen-bonded dimer at 823.13 m/z, and a Na⁺ bridged dimer at 845.67 m/z.

2.3: Dimerization of Glutarate Monoester via CuAAC

Copper (I) Catalyzed Azide-Alkyne Cycloaddition (CuAAC), or Azide-Alkyne Huisgen Cycloaddition was the second step of the synthesis. The chemistry of CuAAC falls under the umbrella of the recently exploding area known as “click” chemistry¹⁵. This reaction requires a terminal alkyne and an azide. In this case the alkyne used was that of the product from the first reaction **2-1** with another alkyne on a different **2-1** molecule and the azide was 1,5-diazido-3-oxapentane. This commercially available bis-azide enabled two units of the terminal alkyne product, **2-1**, from the first reaction to be joined creating one chain of the hydrophobic core with a midpolar linker attached on either end.



Scheme 2.3: The CuAAC dimerization of the glutarate monoester **2-1** with the bis-azide **1-18**.

Frequently mentioned in the highly hyped area of “click” chemistry is the diversity of reaction conditions. This however presents the problem of finding the correct set of conditions for the designated material. The reaction requires a solvent, a copper catalyst, often a base, varying lengths of time, and varying temperatures, all of which can be exchanged for other bases, solvents, catalysts, times, and temperatures creating a diverse library of possible reaction conditions. Depending on what catalogue of conditions were attempted there were many outcomes to this reaction including, deprotection of the alcohol protecting group, incomplete reactions, no reaction, and cleavage of either of the ester groups. Loss of a protecting group could be determined by a shift of the methine proton peak from 4.55 ppm, incomplete reactions or no reactivity were seen from a resulting crude product having alkyne protons at 1.95 ppm and 2.2 ppm. Cleavage of the esters could be identified by the reduced integration at 4.1 ppm.

However, there eventually was successful optimization based on previous cases¹⁹. The product from the first reaction, **2-1**, was dissolved in DMF, DMAP, was added along with the bis-azide, **1-18**,

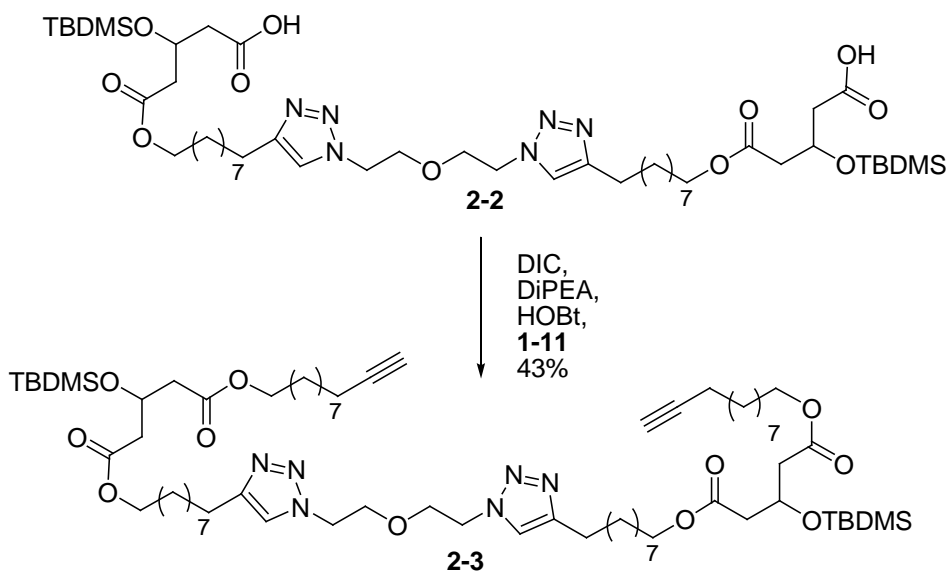
then finally CuI was added, and stirred for 21.5 hours at 12^oC. The key for this reaction was the base, DMAP, and adding an extremely precise 2:1 ratio of (**2-1**):(**1-18**) alkyne:bis-azide. These two keys provided a high yielding and pure product, an imperative outcome because triazoles tend to “streak” during column chromatography with silica gel, making them extremely difficult to purify. Another working problem was that the copper iodide was easily oxidized to an unreactive Cu(II), but this was avoided with a reaction done under nitrogen^{19b}. The resulting product was very sticky and trapped solvent well so extreme care had to be taken when removing solvent on the high vacuum. Compound **2-2** was seen to degrade in protic solvents so was stored in aprotic solvents or without solvent.

The pure product **2-2** ¹H-NMR spectrum included the expected glutarate-methine protons (2H), the ester-methylene protons (4H), the hydrocarbon region (28H), the protecting group *tert*-butyl (18H), and dimethyl (12H) that were similar to **2-1**. There was a broadening to the methylene protons of the glutarate at 2.6 ppm (8H) which was most likely due to decreased mobility around the carbons of the midpolar linker. The methylene protons of the starting material alkyne had coalesced into a single triplet instead of a double of triplets due to the coupling across the alkyne being extinguished, also shifting downfield to 2.7 ppm (4H). The terminal alkyne protons had disappeared and the methine of the triazole had sprouted as a singlet at 7.2 ppm (2H), in addition two triplets formed at 4.45 ppm (2H) and 3.8 ppm (2H) corresponding to the methylene protons on the diethylenoxy linking unit. Confirmation of the product structure was ESI-MS in negative mode with the M1-H ion at 979.73 m/z and the M-2H+Na⁺ ion at 1001.73 m/z.

2.4: Esterification of Dimerized Glutarate

Probably the most utilized reaction in the Fyles lab is esterification of an acid and alcohol with DIC/DiPEA and HOBt catalyst². This was the main reason for the choice behind this reaction because it was almost guaranteed to produce results. After struggling with the previous, difficult to optimize steps, this reaction was successful with the first attempt. The yield however, was poor.

Tetrahydrofuran was added to the diacid, **2-2**; DIC, HOBt, 10-undecyn-1-ol, DiPEA were then all added in that order and stirred overnight. In this reaction increasing the amount of DiPEA had some optimizing effect. The work up before purification of the final product was important because it removed all side products other than alcohol. If these side products are present on the column it can make separation range from hard to impossible, reducing purity and yield.



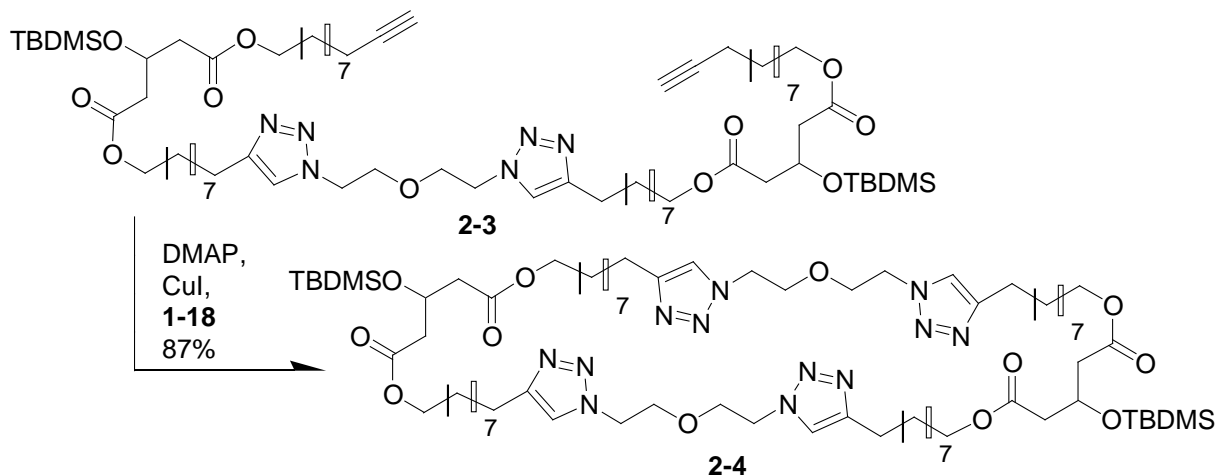
Scheme 2.4: The esterification of the diacid **2-2** with 10-undecyn-1-ol to form the bis-alkyne **2-3**.

The protons of the end product **2-3** that were expected to be similar and were similar to **2-2** were the glutarate-methine proton (2H), the protons of the diethylenoxy linking unit (8H), the hydrocarbon region (56H), the protecting group *tert*-butyl (18H), and dimethyl (12H). The glutarate-methylene protons at 2.5 ppm (8H) were now fully resolved into a doublet after an increase in mobility around the midpolar linker. Identical alkyne-methylene protons and alkyne-methine proton to compound **2-1** were again observed at 2.1 ppm (4H) and 1.95 ppm (2H), respectively. The methylene protons associated with the ester had increased in multiplicity to a doublet of triplets most likely due to chemical influence from the protecting group, but the chemical shift still remained at 4.1 ppm (8H). Confirmation of the structure came with a 1303.80 m/z peak for ESI-MS positive mode that corresponds to M+Na⁺.

2.5: Macrocyclization of Bis-alkyne

Repeating the “click” reaction was the most important step of the synthesis. It required that the two terminal alkynes of **2-3** (a bis-alkyne) react with the same molecule of 1,5-diazido-3-oxapentane(bis-azide) which was not guaranteed. The same conditions were used as for the reaction between **2-1** and **1-18** except with a 1:1 ratio of bis-alkyne:bis-azide. The product from the esterification reaction, **2-3**, was dissolved in DMF, DMAP, and added along with the bis-azide, **1-18**. Finally CuI was added, and stirred for 21.5 hours at 12°C, adapted from previous cases¹⁹. The stoichiometry of 1:1 ratio of bis-alkyne:bis-azide was essential as in the previous dimerization case of **2-2**. However, here stoichiometry was even more important, due to the product not just being difficult, but impossible to purify. Too much or too little of 1,5-diazido-3-oxapentane lead to the formation of a gel during the reaction resulting in impurities that

could not be removed. The concentration of this reaction was also very important. Too much or too little bis-azide or a too highly concentrated reaction could also lead to the formation of a gel and a low concentration would lead to incomplete products.



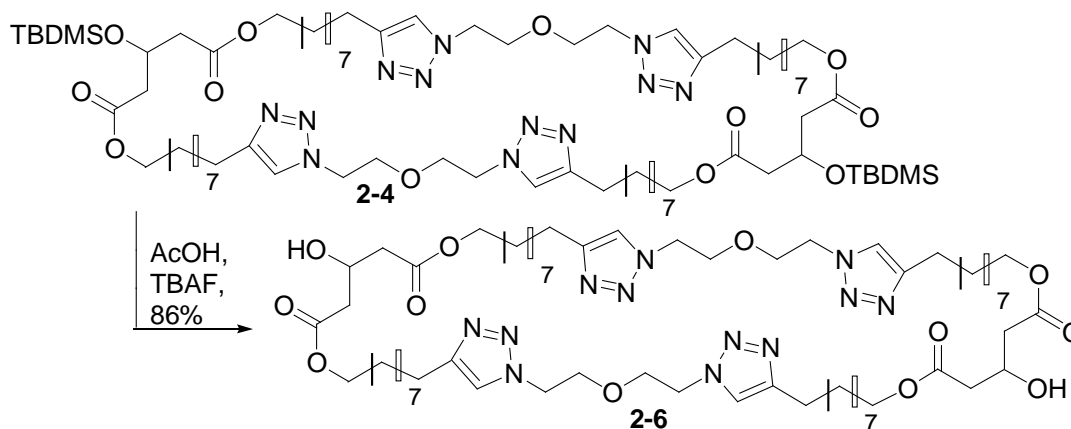
Scheme 2.5: The macrocyclization of the bis-alkyne **2-3** with the bis-azide **1-18**.

The outlined regiment of conditions produced a product that was a macrocyclic monomer with no hint that oligomers had formed. There was no broadening to the peaks in the $^1\text{H-NMR}$ and the product was fully soluble in chloroform.

The desired end product had expected $^1\text{H-NMR}$ signals due to glutarate-methine proton, the hydrocarbon region, the protecting group *tert*-butyl, and dimethyl being similar to **2-3**. In addition, two triplets doubled in integration at 4.45 ppm (8H) and 3.8 ppm (8H) corresponding to the diethylenoxy protons of the linking unit. The triplet corresponding to what were previously the alkyne-methylene protons at 2.7 ppm (8H) also doubled in intensity as the terminal alkynes reacted to form triazoles. The methine protons of the triazoles showed as two singlets at 7.15 ppm and 7.2 ppm, which was most likely due to coordination copper complexes that were too strongly bound to be removed with work up using disodium EDTA^{19b}. The resulting copper coordination complex would change the electron density around the triazoles-methine proton and therefore shift the proton peak. Copper can coordinate to the nitrogens of triazoles and to the acetylene units of the unreacted terminal alkyne while at the same time acting as a catalyst for the reaction²⁰. This template could explain both why there are multiple triazole peaks and why this reaction worked so well, as it gave up to an 87% yield. Since a copper ion would preferentially template a triazole and acetylene unit together in an intramolecular fashion, simply due to the proximity of the two moieties, then this would greatly increase the probability of macrocyclization over oligomerization.

2.6: Deprotection of Macrocyclic Bolaamphiphile

Removing the protecting groups on the alcohols was the most straightforward step of the synthesis. The protected precursor **2-4** was dissolved in THF and equivalents of AcOH and TBAF were added and stirred for just thirty minutes²¹. The cleaved protecting groups were easily removed due to the fact that the triazoles were extremely hard to move on silica gel and the cleaved groups were very greasy. However, it was noted that dry and relatively new TBAF was required to avoid hydrolysis of the ester groups.



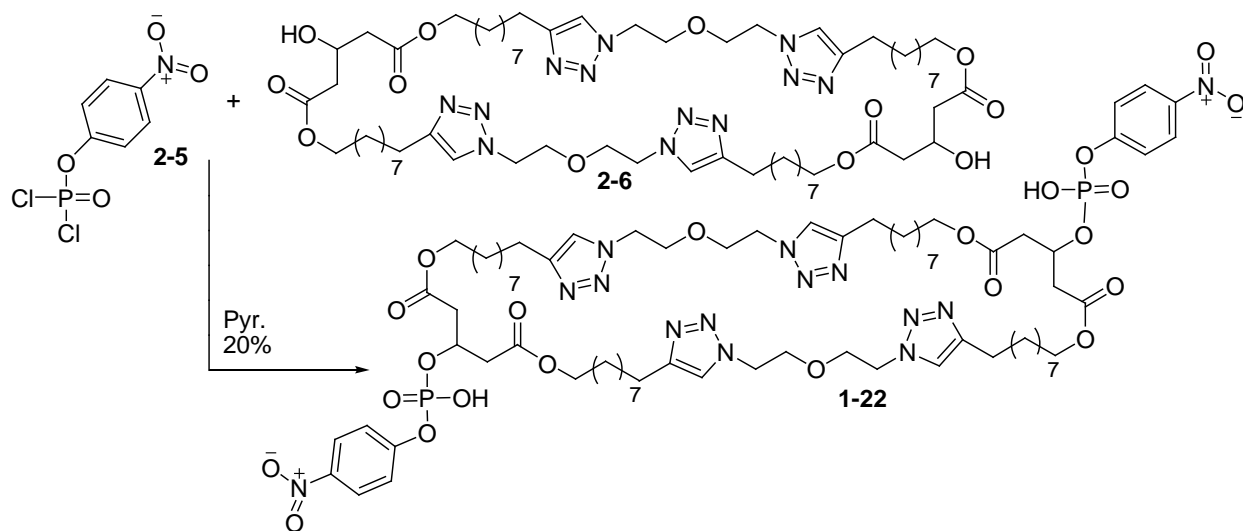
Scheme 2.6: The removal of the protecting groups on **2-4**, forming the diol **2-6**.

The mass spectrum analysis of incomplete reactions from this stage of the bolaamphiphile synthesis provided further evidence that in the earlier macrocyclization stage a macrocycle was formed and not competing oligomers. The sample only exhibited mass/charge peaks that were indicative of compounds that were fully deprotected [$M+Na^+$ (1231.797 m/z)], half deprotected [$M+Na^+$ (1346.862)] and still fully protected [$M+Na^+$ (1459.950)]. This could only be the case if there was just macrocycle present. If other fractions of masses were present other than just 0/2, 1/2, 2/2, it would indicate oligomeric molecules were present that had various ratios other than the predicted ones. The desired end product had an expected 1H -NMR spectrum. The hydrocarbon region, at (1.2-1.7) ppm (56H) was typical. In addition, two triplets were present at 4.45 ppm (8H) and 3.8 ppm (8H) corresponding to the diethylenoxy protons of the linking unit. The triplet corresponding to what were previously the alkyne-methylene protons at 2.7 ppm (8H) was present. Removal of the protecting group shifted the methine protons (2H) of the glutarate to be underneath the 4.45 ppm triplet of diethylenoxy linking unit and was only observable because of a corresponding integral change in that region (8H to 10H). Also after the protecting group removal the *tert*-butyl protons at 0.95 ppm and dimethyl protons at 0.5 ppm disappeared completely. In addition the broad -OH peak appears at 3.55 ppm (2H). The methine of the triazole was two singlets at 7.15 ppm and

7.2 ppm, which was most likely due to molecules that had copper coordinated to the triazole nitrogens which changed the electron density around the triazole protons.

2.7: Macrocylic Bolaamphiphile Head Group Addition

Finalizing the synthesis to the target molecule was the installation of the head groups on both of the deprotected alcohols of **2-6**. The precursor **2-6** was dissolved in DCM and a solution of pyridine and 4-nitrophenyl phosphorodichloridate were added and stirred at reflux for three hours and then cooled down and the remaining chloro- groups were hydrolyzed with ice water¹⁸. The end product was virtually insoluble and extremely difficult to deal with because it had both hydrophobic and charged regions in addition to having four triazoles. For every iteration of this reaction the product seemed to behave differently. This made it very difficult to handle. Removal the excess aqueous soluble 4-nitrophenylphosphate groups and pyridine consisted of adding a small quantity of DCM. The DCM was then warmed up in the flask containing the crude material and when at the reflux point of DCM a ~5% dose of MeOH was added. This sequence was able to dissolve the crude material. Water had to be added and then stirred which precipitated more pure product and left aqueous soluble material behind. With delicacy this procedure was repeated until a pure product was obtained. If it was absolutely necessary to increase purity a short column of silica gel could be used but this dramatically reduced yield because the product adhered to the silica.



Scheme 2.7: Head group addition to the diol **2-6**, forming the macrocyclic bolaamphiphile **1-22**.

The final compound was insoluble in many solvents and the ¹H-NMR spectrum was broad. Complications in the ¹H-NMR spectrum were most likely due to the final compound doing what it was designed to and forming large structures in solution. Depending on which solvent was used to take the

NMR the proton peaks would experience changes in integration and chemical shift. The multiplicity of the NMR was impossible to see because all the peaks appeared broadened. A $^1\text{H-NMR}$ in DMSO-d_6 showed more definition of the proton peaks and better integration than other solvents did so it was the most convincing argument for the presence of the final product. The methine proton of the midpolar linker had shifted, due to the phosphate anion deshielding, to 4.75 ppm (2H), the methylene protons of the esters were shifted only slightly to 3.85 ppm (8H), the aromatic proton peaks had appeared at 8.1 ppm (4H), and 7.3 ppm (4H), the triazole peaks had shifted to 7.6 ppm (4H) due to probable H-bonding with the anionic phosphate, the diethylenoxy protons of the linking unit were at a typical 4.45 ppm (4H) and 3.8 ppm (4H), the glutarate-methylene protons (8H) and the methylene protons that were previously alkyne-methylene protons (8H) had amalgamated with the DMSO-d_6 residual solvent peaks but were still present and identifiable. In addition the hydrocarbon-methylene protons (56H) were also present.

Confirmation of the structure of the macrocyclic bolaamphiphile was more difficult using solely a $^1\text{H-NMR}$ because the spectrum had broad peaks. The molecule also did not appear on ESI-MS most likely due to the number of triazoles in the product, since as the number of triazoles per molecule increased throughout the synthesis the sensitivity to ESI-MS went down. In addition, this molecule readily formed aggregates making it even less sensitive to mass spectra techniques. This is confirmed by broad peaks in the $^1\text{H-NMR}$ spectrum and both 2M-4H, and 3M-6H aggregates in the accurate mass results, Figure 2.1. The broad peaks made 2-dimensional NMR impossible. However, the product was sufficiently characterized with accurate mass results showing evidence of monomer, dimer, and trimer ions. Three isotopes of the M-2H ion are labeled in purple having zero, one, and two neutrons present. Four isotopes of the 2M-4H dimer are labeled in green having zero, one, two, three, and four neutrons. Six isotopes of the 3M-6H are labeled in yellow having zero, one, two, three, four, five and six neutrons, Figure 2.1. In addition, the charge finding algorithm is incorrect due to the presence of aggregates being interpreted as an isotope pattern.

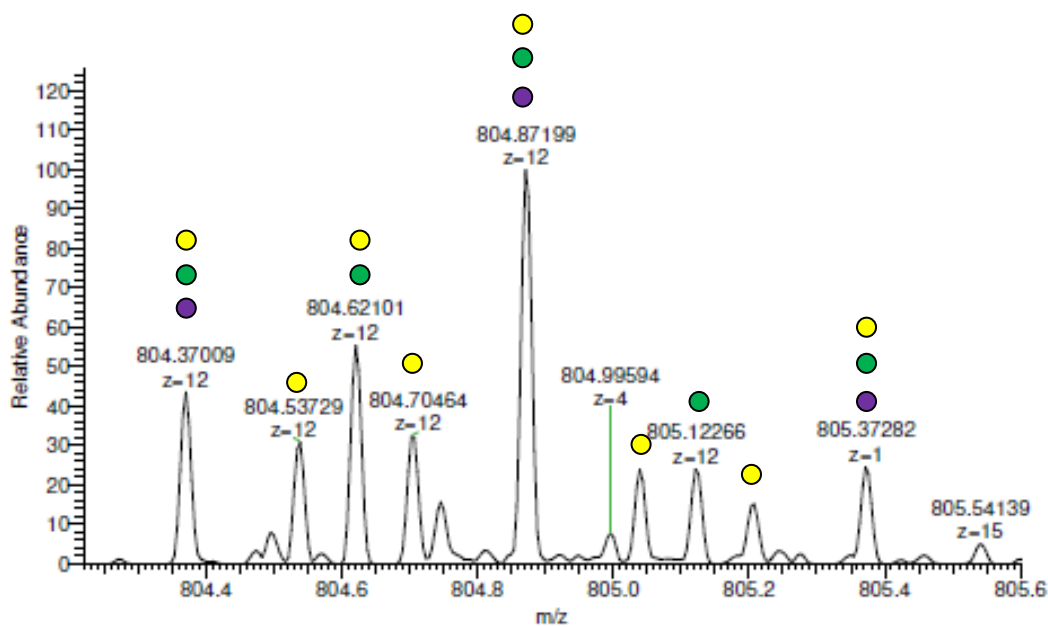
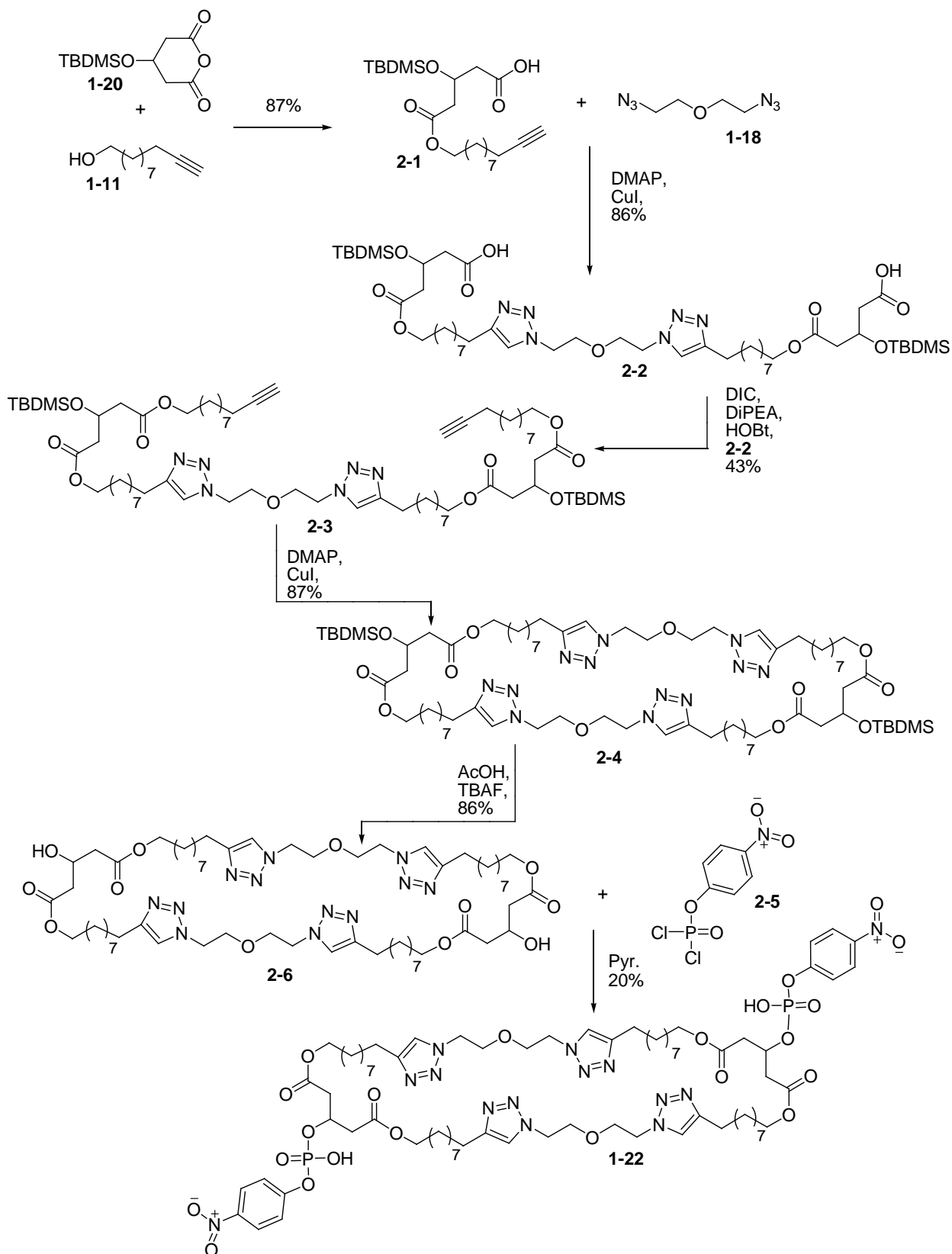


Figure 2.1: Accurate mass indicating the presence of the macrocyclic bolaamphiphile. Purple dots indicate masses obtained from the isotopes of M-2H ions, green dots indicate masses obtained from 2M-4H ions, and yellow dots indicate masses obtained from 3M-6H ions. The charge(z) finding algorithm of the Orbitrap incorrectly interprets the aggregates as an isotope pattern and therefore associates the wrong charge with the mass peaks.

The completed synthesis is given in Scheme 2.8. Starting with commercially available reagents and producing a macrocyclic bolaamphiphile with only six steps of chemical synthesis is not done easily. Although there were only a few types of chemical synthesis done here there was a lot of optimization. Optimization was critical to the synthesis of the final target since many of the resulting compounds could not be purified. It was only with great perseverance that the “click” chemistry even resulted in a workable method.

In addition to optimization challenges, the materials that were synthesized were often difficult to physically work with. Often, while optimizing the ring closure, seemingly the same reaction conditions would produce different materials. It would only take forgetting to do multiple washes of glassware when transferring the reagent to the reaction vessel, or a few degree changes in temperature of reaction to go from; a pure and soluble material macrocycle, to a solution with irremovable impurities, to a solid gel forming part of the way through the reaction. The perseverance paid off however and resulted in being able to close a 72-ring macrocycle in 87% yield. These results were not only of a extremely large macrocycle but also one synthesized in excellent yield. The reaction scheme for making the cyclic bolaamphiphile was a compilation of esterification, deprotection, and “click” chemistry. Four of six of the steps optimized here had over an 85% yield with the total overall yield being 4.8%.

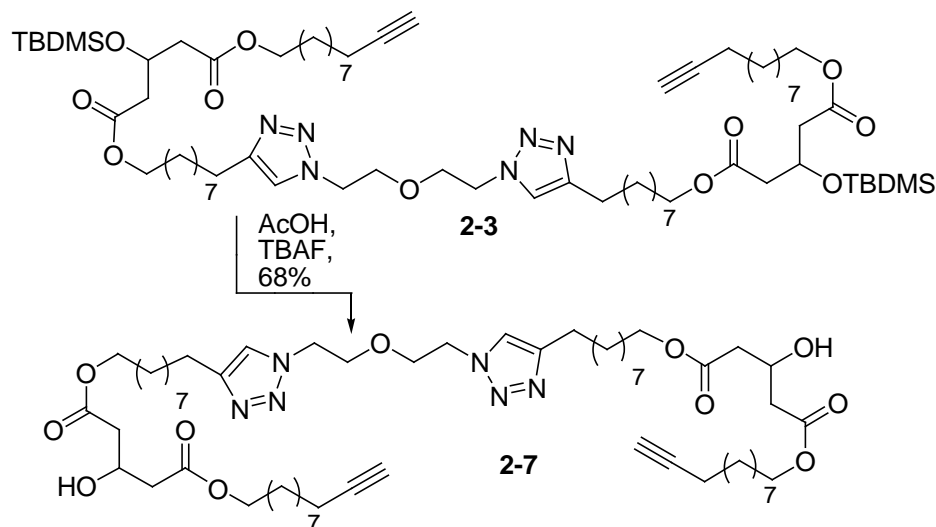


Scheme 2.8: Synthesis of the macrocyclic bolaamphiphile. Synthetic details in Appendix 1, NMR in Appendix 2.

2.8: Deprotection of Linear Bolaamphiphile

Synthesizing the second lipid, **1-24**, was a branching synthesis from the main compound synthesis at **2-3**. Removing the protecting group and installing the head groups were done identically to the last two synthesis steps of the macrocyclic bolaamphiphile.

Removing the protecting groups on the alcohols was done identically to the deprotection of the macrocyclic bolaamphiphile. The protected precursor, **2-3**, was dissolved in THF and equivalents of AcOH and TBAF were added and stirred for just thirty minutes²¹. The cleaved protecting groups were removed easily since the triazoles elute slowly on silica gel and the cleaved groups are hydrophobic and column quickly. However, it was noted that new TBAF with a moisture content of ~2.3% was required to avoid hydrolysis of the esters of **2-3**.



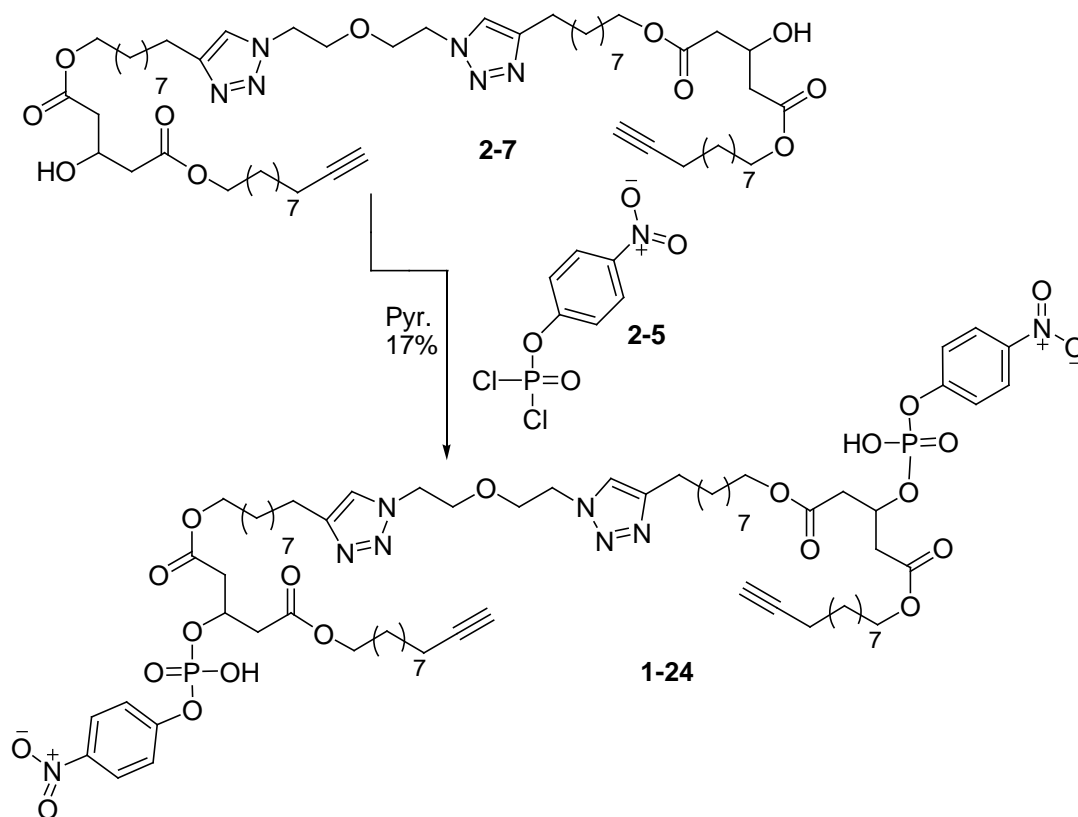
Scheme 2.9: The protecting group removal of TBDMS- to form the linear diol **2-7**.

The ¹H-NMR spectrum of the deprotected linear bolaamphiphile, **2-7**, was what was expected. The triazole singlets of the methine protons were visible at 7.2 ppm (2H), the set of two triplets for the diethylenoxy-methylene protons peaks of the linking unit were present at 3.75 ppm (4H) and 4.4 ppm (4H). In addition, the ester-methylene protons were visible at a typical 4.05 ppm (8H), the broad singlet of the -OH proton was present at 3.55 ppm (2H), the midpolar linker methylene protons were visible as a doublet at 2.5 ppm (8H), beside those was the triplet of the methylene protons which were previously the methylene protons next to the terminal alkyne before the “click” was performed, at 2.65 ppm (4H), the alkyne-methylene protons were present as a doublet of triplets at 2.1 ppm (4H) along with the triplet of the alkyne-methine protons at 1.9 ppm (2H). Finally the methine protons that are a part of the midpolar

linker and now present at 4.4 ppm (2H) were only detectable because of the integral change from the spectrum of **2-3** to the spectrum of **2-7** (4H-6H).

2.9: Linear Bolaamphiphile Head Group Addition

Finalizing the synthesis to the linear bolaamphiphile molecule was the installation of the head groups on both of the deprotected alcohols of **2-7**. The precursor **2-7** was dissolved in DCM and a solution of pyridine and 4-nitrophenyl phosphorodichloridate were added stirred at reflux for three hours and then cooled down and the remaining chloro- groups were hydrolyzed with ice water¹⁸. If it was absolutely necessary to increase purity after work up a short column on silica gel could be done but this dramatically reduced yields because the product adhered to the silica.

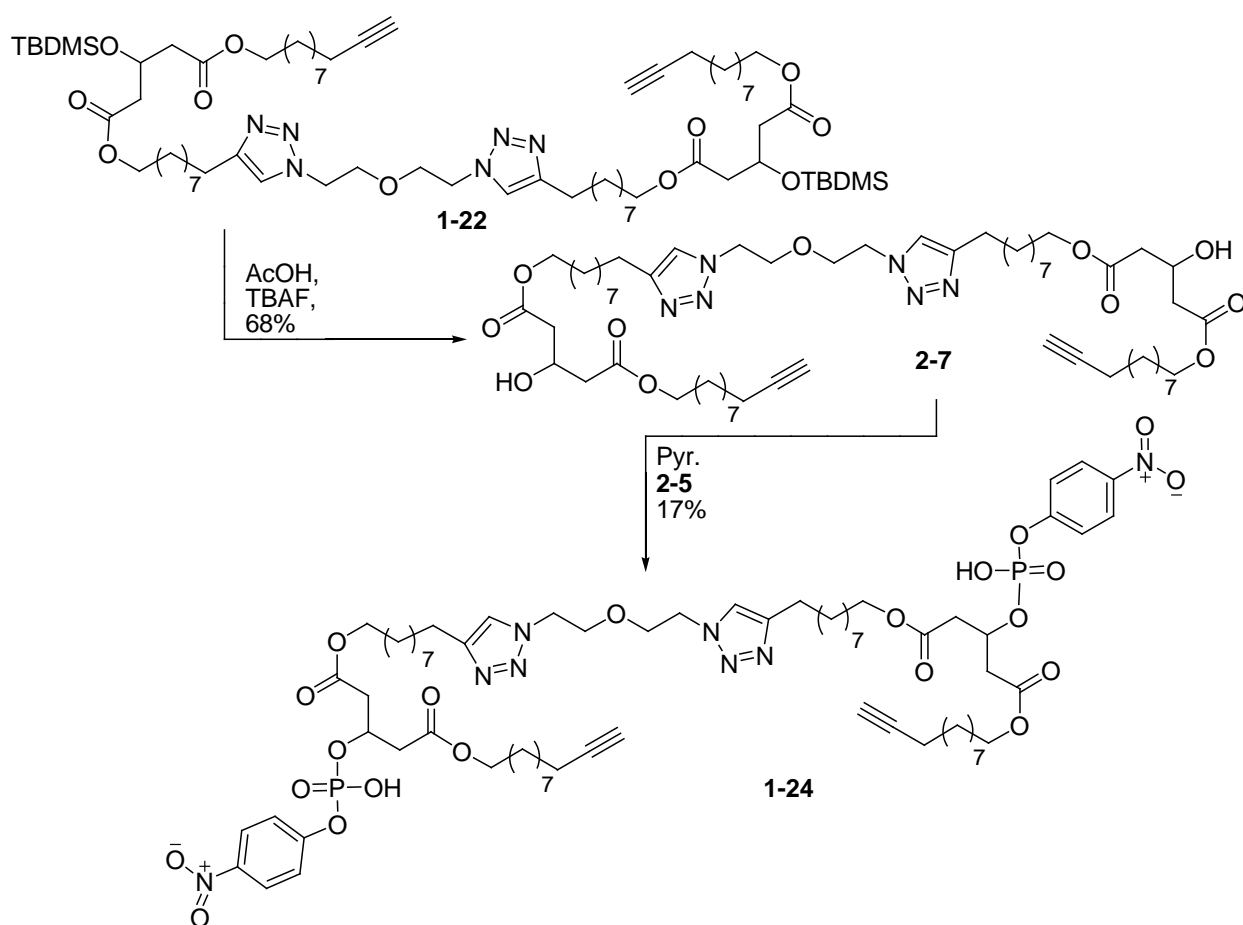


Scheme 2.10: The head group addition to the linear diol to form the linear bolaamphiphile **1-24**.

The resulting ¹H-NMR spectrum of **1-24** was the expected spectrum. The peaks in the NMR were broadened most likely because the molecule aggregated in solution, reducing its ability to freely rotate. The diethylenoxy-methylene protons peaks of the linking unit were present at 3.8 ppm (4H) and 4.5 ppm (4H) the former being amalgamated with the ester-methylene protons (8H) shifting up-field due to the change of the head group. It was confirmed that these peaks were correct because of the integration

for the set of two methylene groups was accurate (12H). Downfield of this however it was observed that a small mound was present which grew slowly over time and excessive handling which has the correct shift for ester-methylene with no head group present meaning that the head group was falling off. The aromatic-methine protons of the head group were present at 8.0 ppm (4H) and 7.3 ppm (4H) right next to the methine protons of the triazoles at 7.2 ppm (4H). The methine protons of the midpolar linker were shifted downfield to 5.15 ppm (2H) and presented as a broad singlet instead of a quintet, and the alkyne protons were present at 2.2 ppm (4H) and 1.95 ppm (2H). In addition, another amalgamation of peaks from 2.4-2.8 ppm (12H) were present which corresponded to the methylene protons previously associated with terminal alkyne and the methylene protons of the midpolar linker. ESI-MS in negative mode showed a M-2H peak at 726.80 m/z, and a M-1H peak at 1454.07 m/z.

Scheme 2.11 shows the completed synthesis of the linear bolaamphiphile. The final product is accessible in 4% yield from the starting alkyne-ol.

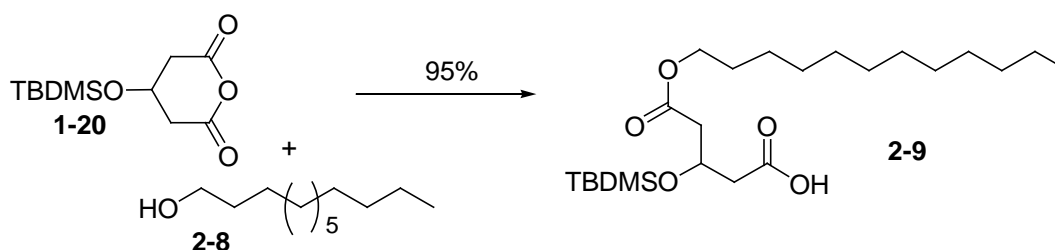


Scheme 2.11: Synthesis of the linear bolaamphiphile. Full synthetic details in Appendix 1, NMR in Appendix 2.

2.10: Synthesis of Glutarate Monoester with 1-dodecanol

A very similar synthesis was carried out to create the linear amphiphile. The linear amphiphile enabled control testing to be done when looking at head group orientation in bilayer membranes. It was created slightly differently by using the fully saturated hydrocarbon 1-dodecanol instead of 10-undecyn-1-ol that was used in the previous syntheses of the bolaamphiphiles. Since no “click” chemistry was needed in the synthesis of the linear amphiphile the terminal alkyne of 10-undecyn-1-ol was not needed.

The first step in the synthesis of the acyclic single head group amphiphile was reacting the midpolar precursor, **1-20**, with the twelve carbon alcohol, **2-8**. This proceeded by dissolving 3-(*tert*-butyl dimethylsilyloxy) glutaric anhydride in toluene adding 1-dodecanol and bringing to reflux overnight, a reaction that has been seen in many other cases¹⁷. The reaction product was the monoester **2-9**.



Scheme 2.12: 3-(*tert*-butyl dimethylsilyloxy) glutaric anhydride reacting with 1-dodecanol to form the glutarate monoester **2-9**.

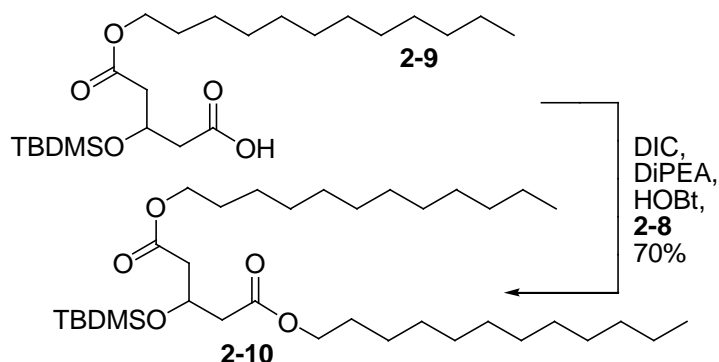
To simplify purification 3-(*tert*-butyl dimethylsilyloxy) glutaric anhydride was used in excess. If 10-undecyn-1-ol was in excess column chromatography on silica gel was needed. On the other hand, excess anhydride could be easily crystallized out. The crystallization involved dissolving the crude product in pentane, cooling with a dry ice/ethanol bath, then vacuum filtering the resulting heterogeneous solution, and keeping the filtrate for further crystallization.

The purified product showed an expected ¹H-NMR spectrum. It had the glutarate-methine proton quintet at 4.55 ppm (1H), the triplet of the protons by the ester at 4.1 ppm (2H) and the inequivalent glutarate-methylene protons formed a multiplet at 2.6 ppm (4H).

2.11: Synthesis of Glutarate Diester

This esterification of a carboxylic acid with an alcohol, uses DIC/DiPEA and a HOBt catalyst². This reaction was a reliable due to previous optimization in the Fyles lab and was successful in the first attempt. The yield however, was low.

The reaction described here is identical to the reaction in section 2.4 with the exception of changed molar ratios of reactants. Dry tetrahydrofuran was added to the monoacid, **2-9**. In succession DIC, HOBt, 1-dodecanol, DiPEA were then all added and stirred overnight. Increasing the amount of DiPEA optimized the amount of product obtained, while work up before purification was necessary to simplify purification. Removing excess alcohol for the purification of the product was simply washing the crude product in MeOH which dissolved the excess 1-dodecanol and left more pure **2-10**.

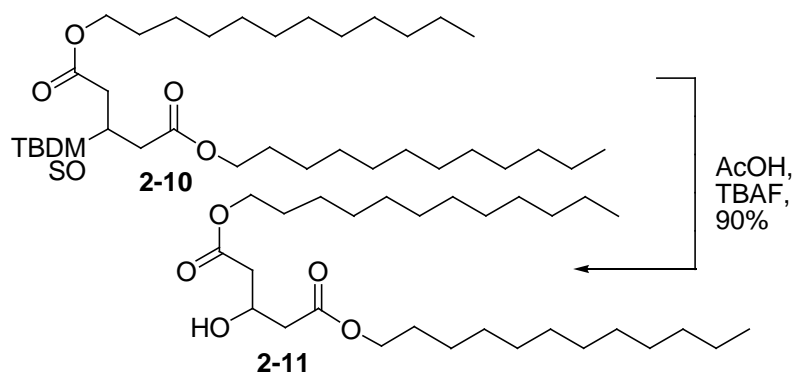


Scheme 2.13: The esterification of glutarate monoester with 1-dodecanol to form the glutarate diester **2-10**.

The desired end product had the expected $^1\text{H-NMR}$ spectrum. The glutarate-methine proton, the hydrocarbon region, the protecting group *tert*-butyl, and dimethyl were similar to **2-9**. The glutarate-methylene protons at 2.5 ppm (4H) were fully resolved into a doublet after an increase in mobility around the midpolar linker. The methylene protons associated with the ester had increased in multiplicity most likely due to the protecting group influencing ester-methylene protons creating a doublet of triplets, but remained at 4.1 ppm (4H).

2.12: Deprotection of Linear Amphiphile

To deprotect the linear amphiphile involved repeating the chemical procedures of **2.6** and **2.8** with a reduction in the molar equivalents of TBAF and AcOH. The protected precursor **2-10** was dissolved in THF and equivalents of AcOH and TBAF were added and stirred for just thirty minutes²¹. The cleaved protecting groups were removed by dissolving the crude product in pentane and crystallizing the pure product in a dry ice and ethanol bath. New TBAF with minimized moisture content is necessary for this reaction to proceed without de-esterification.

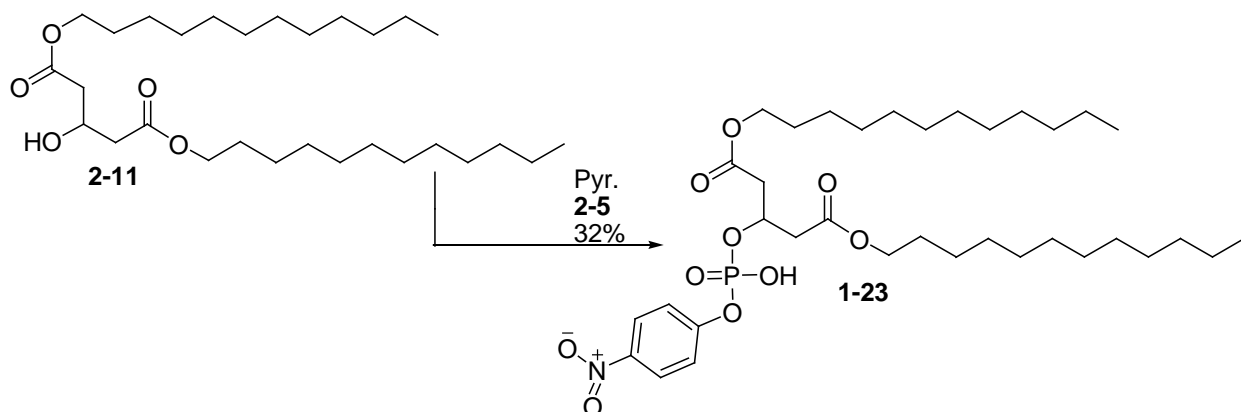


Scheme 2.14: The protecting group removal of TBDMS- to form a glutarate diester with an alcohol.

The glutarate-methine proton had shifted from **2-10** upfield to 4.45 ppm (1H), and the hydrocarbon region was at (1.2-1.7) ppm (40H). The glutarate-methylene protons formed a doublet at 2.5 ppm (4H), and were now fully resolved. The methylene protons associated with the ester had decreased in multiplicity due to the protecting group no longer influencing ester-methylene protons creating a triplet, and remained at 4.1 ppm (4H). These chemical shifts and integrations provided the expected $^1\text{H-NMR}$ spectrum.

2.13: Linear Amphiphile Head Group Addition

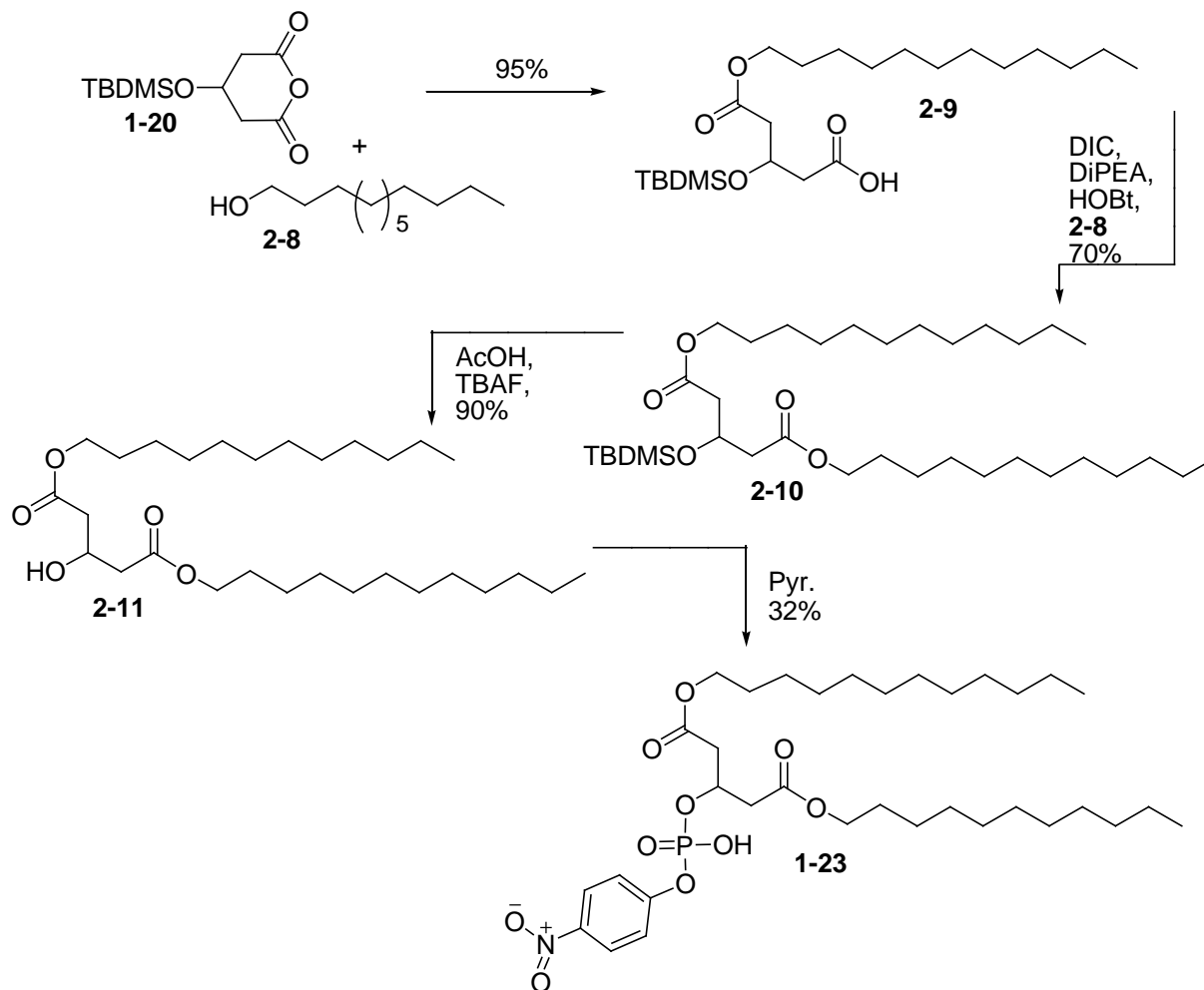
Finalizing the synthesis of the acyclic single head group amphiphile molecule was the installation of the head group on the deprotected alcohol. The procedure followed that of section **2.7** and **2.9** with the alteration of molar ratios of the reactants. The precursor **2-11** was dissolved in DCM and a solution of pyridine and 4-nitrophenyl phosphorodichloridate were added stirred at reflux for three hours. The reaction was then cooled down to zero degrees Celsius and the remaining chloro- groups were hydrolyzed with ice water¹⁸.



Scheme 2.15: The head group addition of **2-5** to the glutarate diester **2-11**.

The desired end product had what was an expected $^1\text{H-NMR}$ spectrum although the proton peaks were broadened due to macrostructures forming in solution. The glutarate-methine proton had shifted from **2-11** downfield to 5.15 ppm (1H), and the hydrocarbon region was at (1.2-1.7) ppm. The glutarate-methylene protons formed a multiplet at 2.7 ppm (4H) most likely due to the head group chemically influencing the protons. The methylene protons associated with the ester had decreased in multiplicity to a broad single, and were at 4.0 ppm (4H). The aromatic-methine protons were present at 8.15 ppm (2H) and 7.35 ppm (2H) both forming resolved doublets. Confirmation of the structure came with a 684.60 m/z peak for ESI-MS negative mode that corresponds to M-1H and a 2M-1H dimer at 1369.67 m/z.

The completed synthesis is given in Scheme 2.16. The amphiphile is available in 19% yield over four steps.



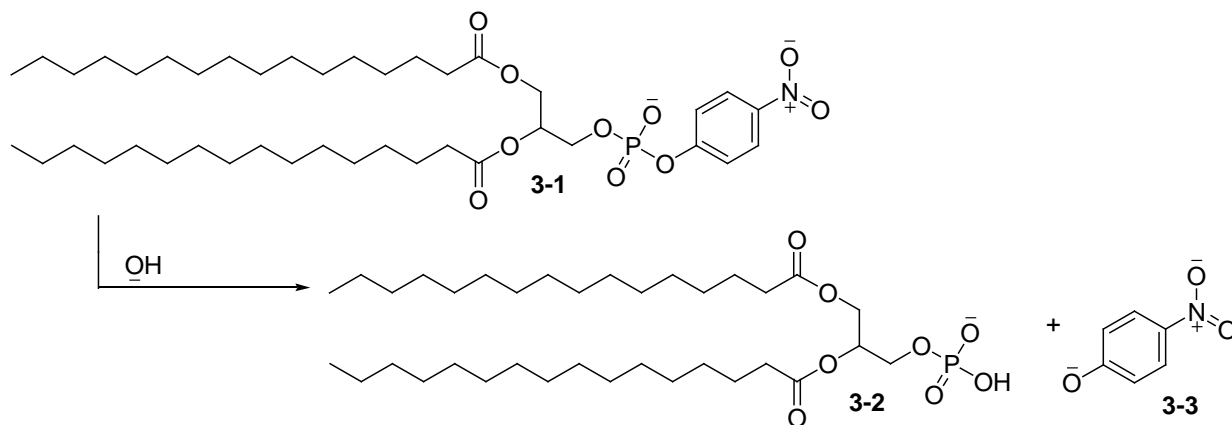
Scheme 2.16: Synthesis of amphiphilic lipid. Synthetic detail in Appendix 1, NMR in Appendix 2.

Chapter 3: Membrane-spanning Assay and Conclusions

It is asserted that a stable archaeal cell is due to the cardarchaeol spanning the organism's membrane. It was therefore of utmost importance to establish the synthesized cardarchaeol mimic **1-22** was membrane-spanning in the bilayer membrane of a vesicle. To do this, vesicles had to be made composed of a certain percentage of the macrocyclic bolaamphiphile. The vesicles could then be exposed to a base shock which would cleave the head groups of **1-22**, illuminating where the head groups of the macrocycle were physically situated. From the location of the head group it can be determined if the bolaamphiphile was predominantly in a U-shaped or through membrane conformation. To exemplify the procedure the results of the Moss assay can be examined.

3.1: Moss Assay

In previous work done by Moss vesicles were made with acyclic single head group lipids as constituents¹⁸. The idea behind the work was to have vesicles made with **3-1** which has a p-nitrophenylphosphate (p-NPP) head group and varying amounts of cetyltrimethylammonium chloride (CTACl), an emulsifier.



Scheme 3.1: The reaction of a nitrophenylphosphate lipid with a base to a phosphatidic acid and nitrophenolate chromophore.

The vesicles were made in an acidic buffer at a pH of 5.5 which were conditions that would create vesicles while leaving the head group of the lipid intact. Once vesicles had formed it was possible to have different internal and external conditions of the vesicle so while the internal condition remained at pH 5.5 the external condition of the solution was changed to pH 11.8. The basic solution associated with pH 11.8 cleaved the p-nitrophenolate chromophore, **3-3**, that was exposed to the external environment creating an absorbance over a period of time at 400 nm, Figure 3.1, and Scheme 3.1. If the vesicles were

then lysed the remaining head groups would be cleaved producing a similar absorbance to before if the vesicle had remained intact and no OH^- ions had leaked through the bilayer. The Moss group then showed that increasing the amount of CTACL pre-associated with the membrane increased leakage of OH^- ions into the vesicle. This resulted in an increased pH within the vesicle. More p-nitrophenolate chromophores were cleaved before vesicle lysis as a result. Therefore with an increasing concentration of CTACL there was an increasing absorbance before lysing the cell than after.

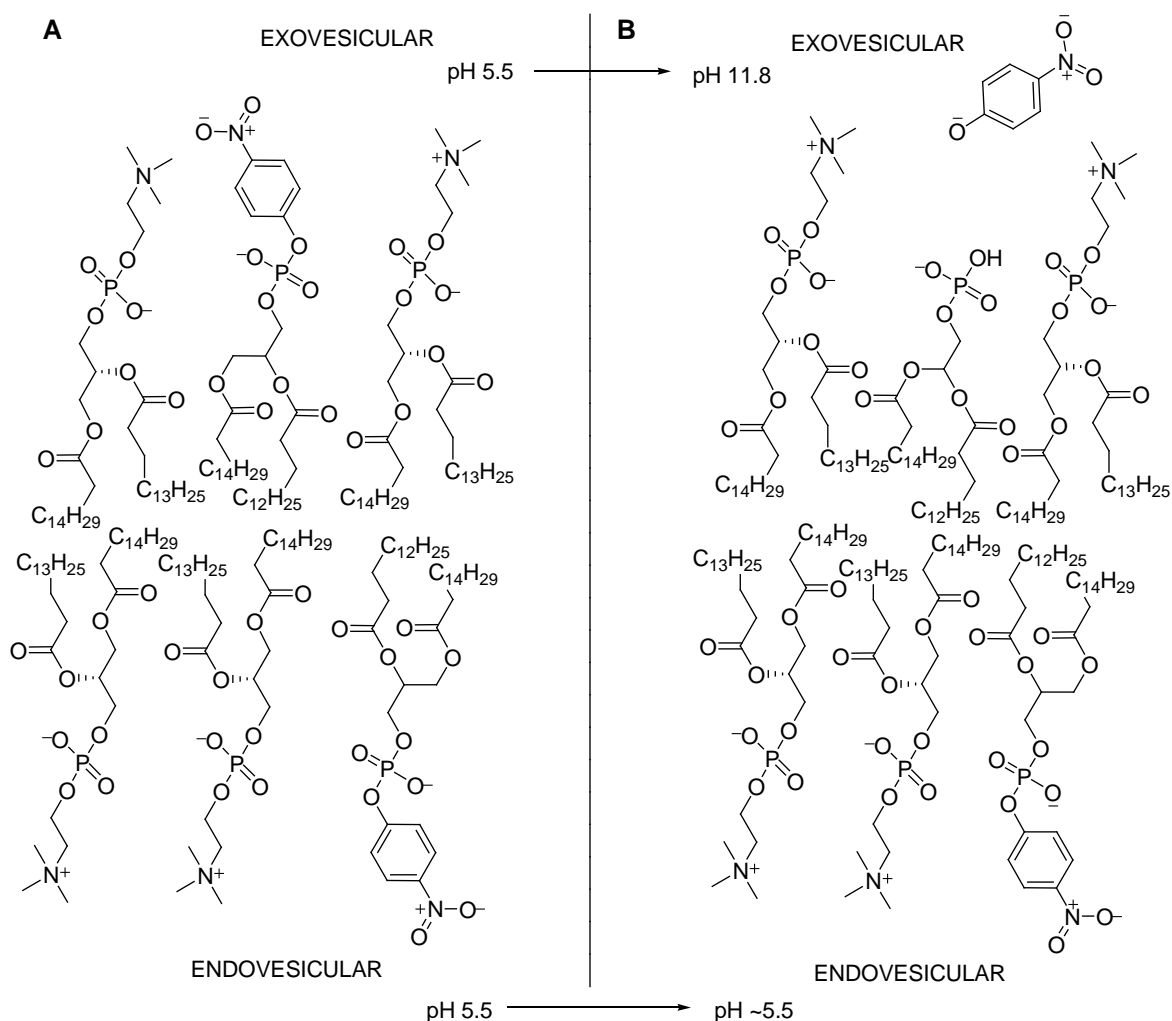


Figure 3.1: The idea behind the absorbance assay developed by Moss. A: A cross section of a lipid bilayer from a vesicle with p-nitrophenylphosphate lipids associated at an initial pH of 5.5. B: A cross section of a lipid bilayer from a vesicle showing how a change in pH cleaves p-nitrophenolate ions from a phospholipid head group.

3.2: Membrane-spanning Assay

This could then be adapted to the task of discovering whether more or fewer head groups for **1-22** were exposed to the internal or external environment of a vesicle. Elucidating the orientation of the head groups in this way tells whether or not the lipid was membrane-spanning or U-shaped. Looking

mathematically at the situation the outer leaflet of the membrane has a larger radius than the inner leaflet by about 4 nm and a typical vesicle has a radius of ~60 nm.

$$\text{Eqn 3.1: Surface Area of Outer Leaflet} = A_o = 4\pi r_o^2$$

$$\text{Eqn 3.2: Surface Area of Inner Leaflet} = A_i = 4\pi r_i^2$$

$$\text{Eqn 3.3: Ratio of Surface Areas} = A_o/A_i = r_o^2/r_i^2 = (64.5 \text{ nm})^2/(60.5 \text{ nm})^2 = 1.14$$

The difference in radius of the leaflets of the bilayer leads to a larger surface area of the external leaflet by, 14%, Equation 3.3. If the macrocyclic bolaamphiphile was membrane-spanning this difference in surface area would be irrelevant and an equal number of head groups would be located internally as externally. If the macrocyclic bolaamphiphile was U-shaped in the membrane and partitioned equally in both leaflets of the bilayer then the statistical difference of the surface area of the leaflets would give 57% of the head groups located externally and 43% located internally. However, if the partition favoured the bolaamphiphile being located externally then there would be greater than 57% of the head groups in the external leaflet and less than 43% of the head groups in the inner leaflet. On the other hand, if the bolaamphiphile favoured an internal U-shaped orientation, then less than 57% of the head groups would be located externally and greater than 43% would be located internally. This result could be ambiguous with a membrane-spanning orientation but since the U-shape is quite bulky it is unlikely it would favour a partition in the internal leaflet.

The assay then developed in a way that when the vesicles were exposed to a base shock of NaOH to obtain pH 11.8 outside the vesicle the external head groups would release p-nitrophenolate. The assay would result in 50% absorbance from external head groups in a through membrane lipid orientation and ~57% in a U-shaped orientation, Figure 3.2.

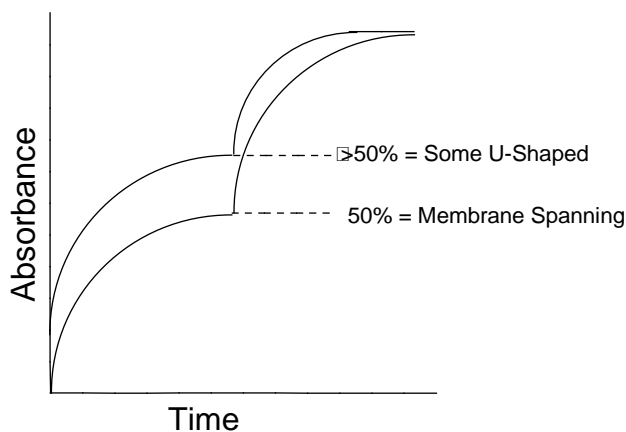


Figure 3.2: An idealized absorbance versus time graph displaying the difference between U-shaped and membrane-spanning absorbance readings.

The task was then set about to conclude whether compound **1-22** was membrane-spanning or U-shaped. Vesicles were made by sonication of L- α -Phosphatidylcholine and 5 mol% of **1-22** in a pH 6.45 buffer (10 mM Na₃PO₄, 100 mM NaCl) producing vesicles with effective diameter 125.6 nm, Appendix 3. The resulting vesicle solution had a concentration 2×10^{-4} M of p-nitrophenylphosphate lipid which if all the p-nitrophenolate was cleaved would produce a strong yellow color ($\lambda_{\text{max}} = 400 \text{ nm}$)¹⁸. However the resulting vesicles when exposed to a base shock, pH 11.8, while being recorded on a Cary 50 Bio UV-visible spectrometer there was no change in absorbance at 400 nm, Appendix 3. Logically this meant that one or several undesirable incidences occurred. **1-22** was not established in the membrane of the vesicles, **1-22** was established but experienced no cleavage of p-nitrophenolate, **1-22** was experiencing another reaction preferential to p-nitrophenolate cleavage, or **1-22** in particular was not reactive which might not necessarily be the case with **1-24**, or **1-23**. The latter possibility was eliminated when vesicle samples of **1-24** and **1-23** both did not produce an absorbance, Appendix 3. All three lipids failed the assay in a similar fashion.

Unfortunately, it was impossible to discover why the assay failed using compound **1-22**, since the ability to visualize **1-22** on ESI-MS and NMR was impossible. Inability to visualize with NMR was due to the vesicles having too little of **1-22** to be detected. In addition, inability for **1-22** to be easily detected by ESI-MS was due to the large number of triazoles in the compound and the compound aggregating with itself, both of these conditions reduce the ability for **1-22** to “fly” in ESI-MS. However, unlike **1-22** compound **1-24** and **1-23** were readily detectable with ESI-MS(-).

Vesicles were made in the same way with **1-23**, and **1-24** as they were with **1-22**. The vesicles were then lysed with Triton, diluted with MeOH, and submitted to ESI-MS. The resulting ESI-MS indicated that a mass over charge ratio of 1454.13 was present in the **1-24** sample and a 684.53 m/z peak was present in the **1-23** sample, Figure 3.3. This result confirmed that the lack of absorbance during the assays was not due to **1-22** being unable to associate with a bilayer membrane. The remaining possibilities that would cause no absorbance in the assay were, the phospholipids were not reacting, or a side reaction was taking place.

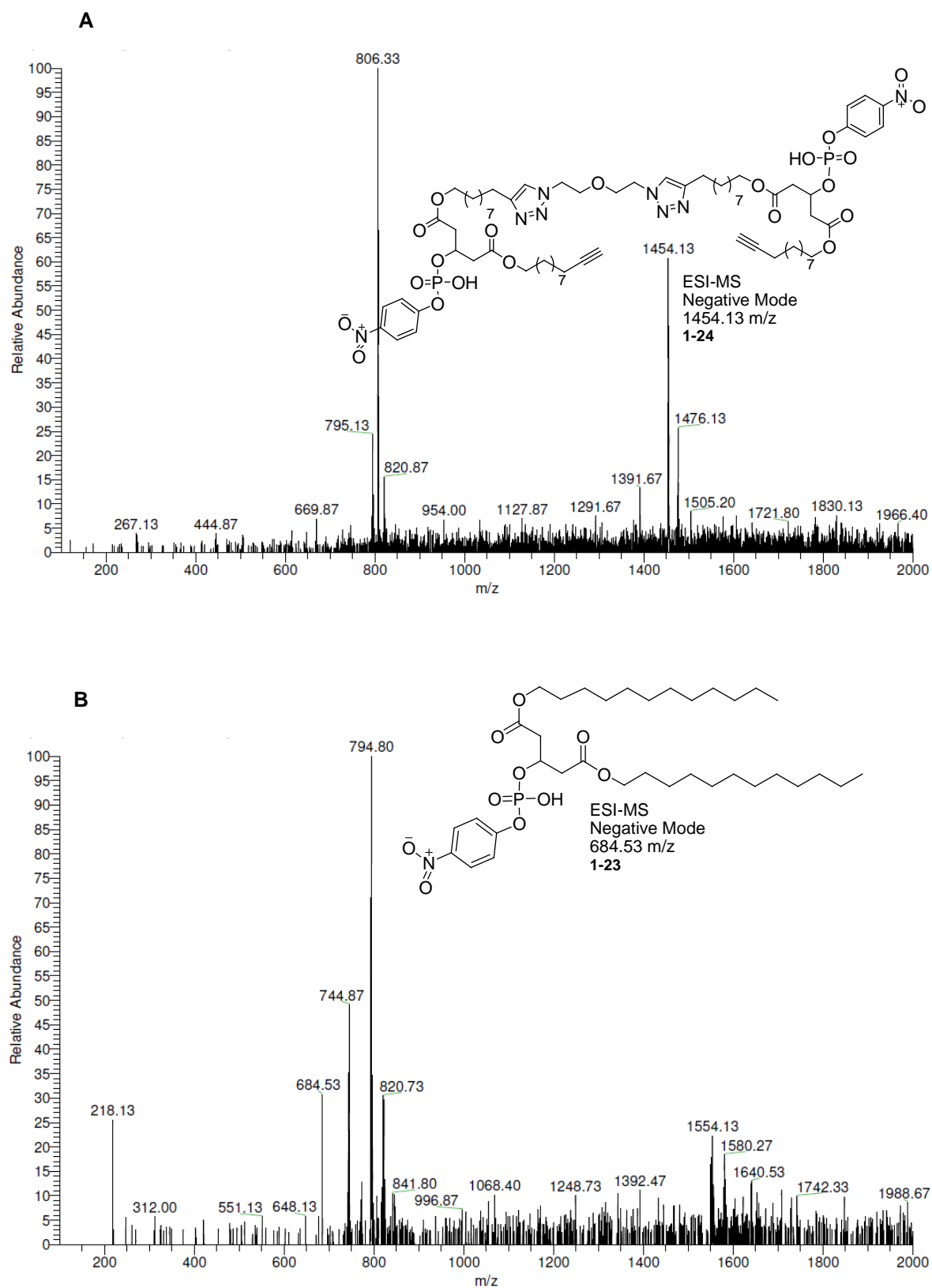
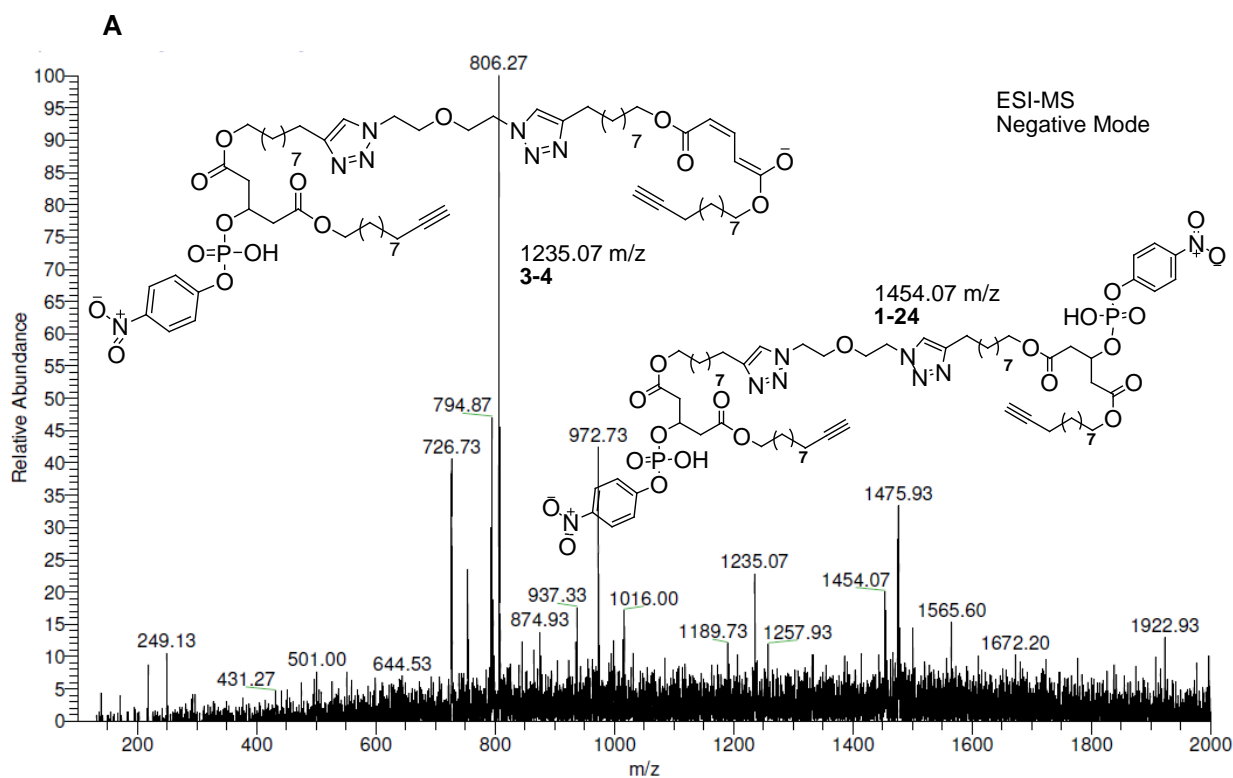


Figure 3.3: ESI-MS in negative mode. A: A mass spectrum confirming **1-24** was associated with the bilayer membrane of vesicles. B: A mass spectrum confirming **1-23** was associated with the bilayer membrane of vesicles.

It was left now to investigate whether there was: a side reaction occurring, or no reaction occurring at all after a base shock. The method of eliminating one or the other of these possibilities was simply to compare the ESI-MS before and after each of the vesicle samples were treated with base. If there was no product detectable by ESI-MS during the basic shock then the ESI-MS before and after would be comparable, and if there was a reaction taking place detectable by ESI-MS then there would be a noticeable and possibly similar change in each of the spectra. A set of vesicle samples from **1-24** and **1-23** was then subjected to 100 minutes of pH 11.8. The individual samples were then lysed using Triton and run on ESI-MS, Figure 3.4.

The spectra, from each of the two samples, after the treatment with a base showed masses from the original lipid 1454.07 m/z and 684.80 m/z which could have indicated that no reaction had occurred. However there was a strong indication that this was not the case. There were mass peaks in each of the spectra that were 219amu lighter than the starting lipid which was indication that a side reaction consistent with both compounds **3-4** and **3-5** had occurred, Figure 3.4.



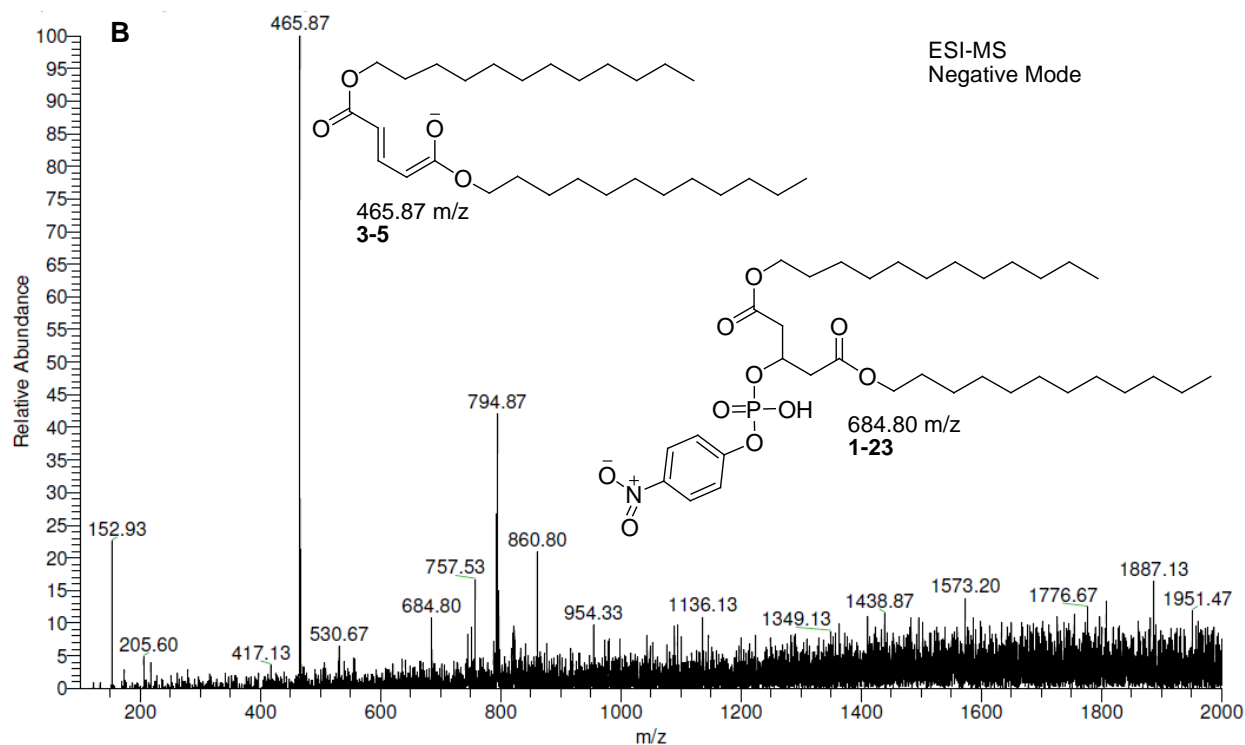
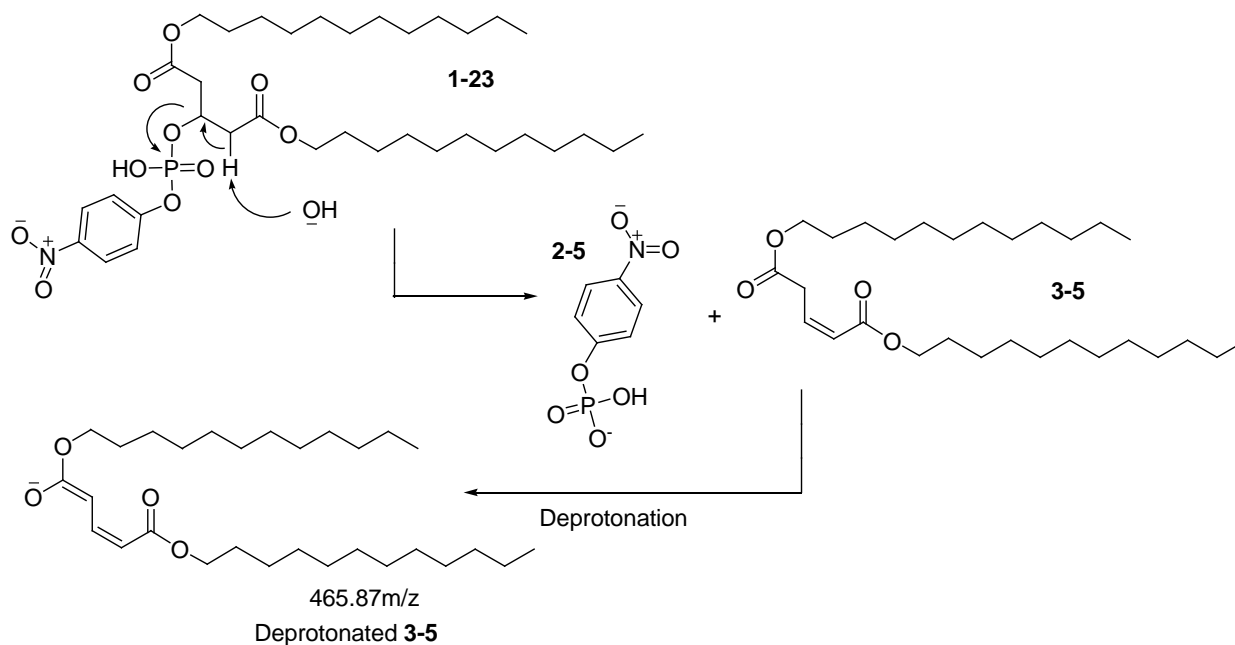


Figure 3.4: ESI-MS (-) mode spectra of vesicles, after treatment with a base. A: Vesicles initially containing **1-24**; the ion at 806.27 m/z is known to be a contaminant from a previous sample from another user. B: Vesicles initially containing **1-23**.

Both sets of vesicles one with bolaamphiphile **1-24** and the other with the single head group amphiphile **1-23** produced no detectable change in absorbance at 400 nm and were both fully associated with the bilayer membrane of their respective vesicle samples. On the other hand, there was a detectable change in their composition seen by ESI-MS. A possible reason for this was an elimination reaction of the phosphate head group by the OH^- ion, Scheme 3.2.



Scheme 3.2: Elimination of the p-nitrophenylphosphate head group from **1-23**, by a hydroxide ion, later undergoing the loss of a proton due to basic conditions which establishes the correct mass as detected by ESI-MS.

A mass being detected in both vesicles containing **1-23** and **1-24** that correlated with a mass loss of 219 amu was strong evidence for an elimination reaction of the entire p-nitrophenylphosphate head group. This coincided with the lack of absorbance at 400 nm during the assay, and was a competing reaction to the cleavage of p-nitrophenolate. Additional evidence was founded from the $^1\text{H-NMR}$ of **1-23** in a scaled up reaction that simulated the conditions found in the vesicle studies using the linear amphiphile. The NMR showed expected ester-methylene protons at 4.1 ppm (4H). Alkene-methine protons at 7 ppm (1H) and 6 ppm (1H) that had a coupling constant of 16 Hz, which is a distinct coupling constant to that of trans alkene protons. The chemical shifts of 7.0 ppm and 5.95 ppm were extremely close to the predictions from $^1\text{H-NMR}$ prediction software at 7.12 ppm and 5.97 ppm respectively. In addition the alkene proton with a 7.0 ppm chemical shift was coupled to the proton of 3.25 ppm (2H) with a coupling constant of 7 Hz. There was also long distance coupling of 2 Hz between the methine proton at 5.95 ppm and the methylene proton at 3.25 ppm, which is typical of an allylic coupling. Although the predicted shift for the methylene protons was different from observed chemical shift, the coupling to the alkene-methine protons, and the correct observed integrations for all four protons located between the two ester moieties, was confirmation that the assumed structure was indeed correct.

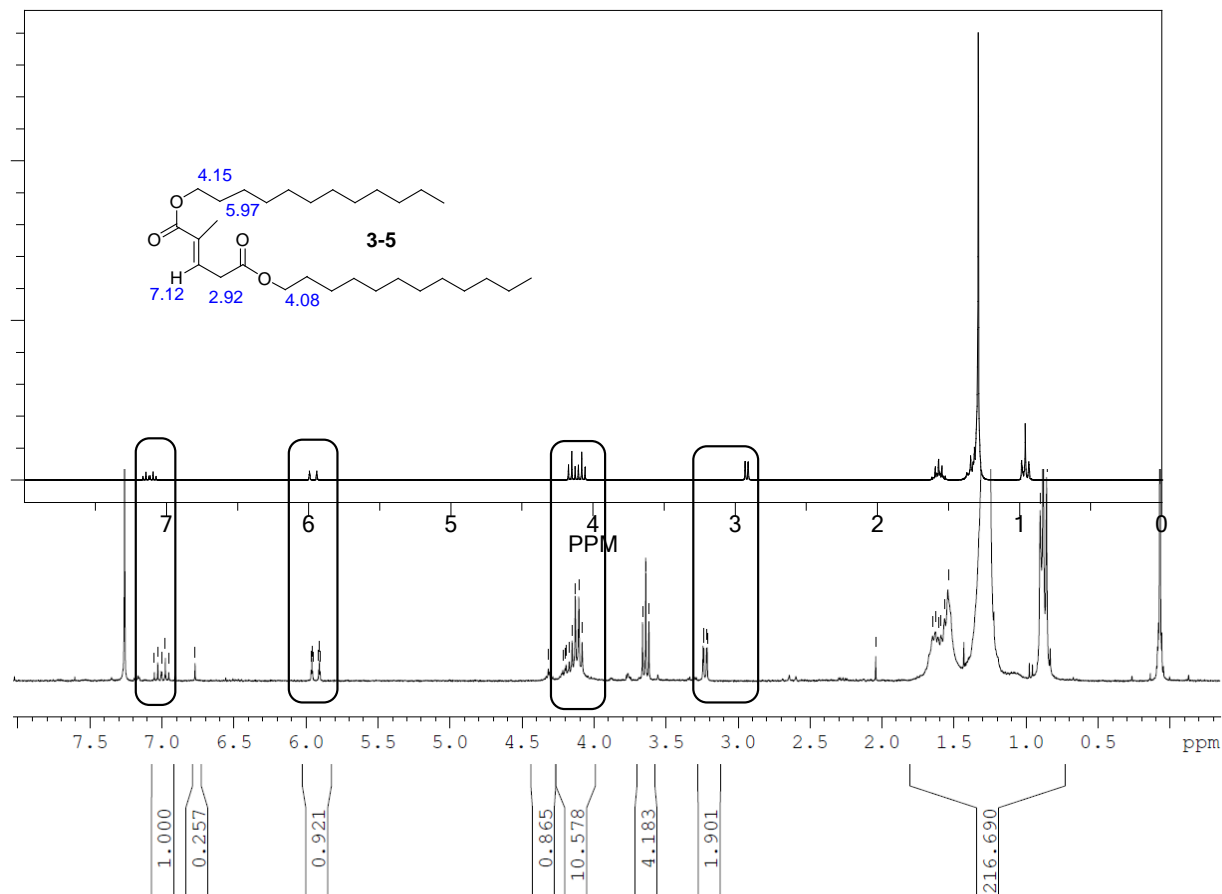


Figure 3.5: The observed NMR from the reaction that replicated conditions seen by vesicles in the membrane-spanning assay. The NMR is overlaid with a ¹H-NMR from prediction software and the chemical structure that was predicted.

Conclusive evidence that the membrane-spanning assay was flawed was found in both; ESI-MS results before, and after the membrane-spanning assay, and from predicted and observed ¹H-NMR. It was not because **1-22** had an atypical association with the membrane bilayer, or that it did not associate at all, or that it had an unreactive head group, but that an elimination reaction occurred instead of the cleavage of p-nitrophenolate. The difficulty to produce the p-nitrophenolate ion under basic conditions with the synthesized structures was due to the 1,3 stereochemistry of the head group. In conventional lipids the alkyl chains are stereospecifically numbered sn-1,2 and are the opposite stereochemistry on archaea lipids with sn-2,3 alkyl chains, Figure 3.6. In addition, the ester groups of **1-22** are in a reversed orientation than conventional lipids which gives an opportunity for the elimination reaction by providing either a protonated or deprotonated end product, Scheme 3.2.

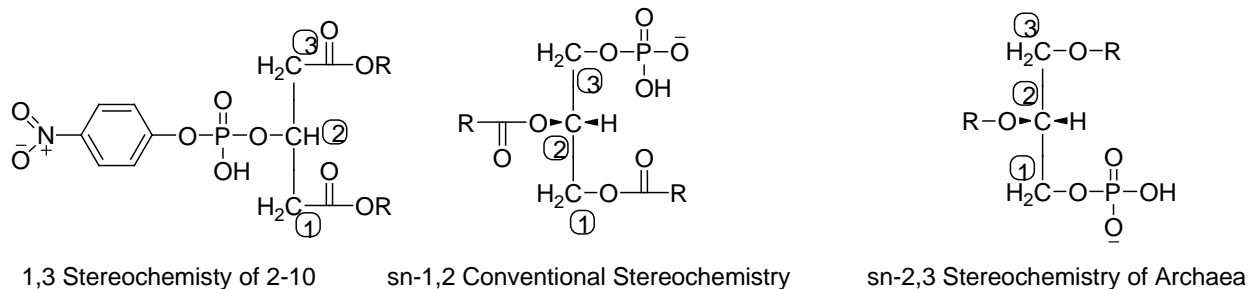


Figure 3.6: Illustrating the difference between naturally occurring midpolar linkers and the one chosen for the syntheses seen here.

3.3: Conclusions and Future Work

A macrocyclic bolaamphiphile, designed after membrane-spanning lipids found in Archaea was synthesized. The protected 3-(*tert*-butyl dimethylsilyloxy) glutaric anhydride was esterified with 10-undecyn-1-ol to a glutarate monoester. Two glutarate monoesters were then “clicked” using copper-mediated Azide-Alkyne Cycloaddition (CuAAC) and a bis-azide to obtain two carboxylic acid groups linked by a rigid hydrophobic chain ~ 35 Å long. The carboxylic acid groups were then esterified, each with an equivalent of 10-undecyn-1-ol resulting in a bis-alkyne. Through heavy optimization the bis-alkyne was again “clicked” creating a 72-membered macrocycle in an 87% yield. The resulting macrocycle was deprotected exposing a macrocyclic diol. Both alcohols were then reacted with 4-nitrophenyl phosphorodichloridate to produce a macrocyclic bolaamphiphile in six steps an overall yield of 5%.

To provide control structures which assisted in discovering the membrane orientation of the macrocyclic bolaamphiphile two other phospholipids were also synthesized. A linear amphiphile and linear bolaamphiphile were both synthesized in 4, and 5 synthetic steps with yields of 19, and 4% respectively. The macrocyclic bolaamphiphile was designed to be membrane-spanning and the *p*-nitrophenylphosphate head groups designed to be cleaved under basic conditions, elucidating the phospholipids membrane-spanning orientation.

A great deal has been worked out in terms of new chemistry and many of the steps in this synthesis, once worked out, are amazing in simplicity of workup and yield. Although “click” chemistry provided the synthesis with a reaction that was both able to rigidify the hydrophobic core and quickly close the macrocycle, the triazole moiety makes a compound synthetically more difficult to handle. The more triazoles in a compound made it increasingly less soluble in common solvents and much more difficult to purify using column chromatography. This challenges an organic chemist and revisions in ring closing should be looked at as a result.

In basic conditions the deprotonation of the methylene protons that were adjacent to the phosphate ester occurred instead of the anticipated p-nitrophenolate cleavage. This resulted in an elimination product which failed to provide evidence that the macrocyclic bolaamphiphile was membrane-spanning. It was however able to provide conclusive evidence that the synthesized amphiphilic lipids do associate with the bilayer membrane of vesicles.

The results of the membrane-spanning assay indicate that head group stereochemistry was key and has to be either sn-1,2 or sn-2,3, with the ester facing in the opposite direction. These two features of the midpolar linker used in the chemistry done here allow for a conjugated system to occur that stabilizes the final product. This allows for the elimination reaction to be preferred over p-nitrophenolate cleavage, Scheme 3.1. Stereochemistry of natural lipids lack protons on the adjacent carbon attaching the head group. Without these adjacent protons and the inability to form a product that has a conjugated system an elimination product would not occur. Instead under basic conditions p-nitrophenolate cleavage would be preferred.

For these reasons a similar synthesis would be recommended with a midpolar linker akin to a natural lipid. On the other hand, if more product was available from this chemical synthesis the technique of freeze-fracture could be used to establish the membrane orientation of a the macrocyclic bolaamphiphile²². This technique provides the ability to view membrane-spanning structures using an elaborate technique of vesicle visualization with a transmission electron microscope.

Bibliography

1. Alberts, B.; Johnson, A.; Lewis, J., *Molecular Biology of the Cell*. Garland Science: New York, 2002.
2. Moszynski, J., M. The synthesis and characterization of diphenylacetylene containing ion channels. Uvic, Victoria, British Columbia, Canada, 2011.
3. Yeagle, P., L., *Structure of Biological Membranes*. CRC Press: 2005.
4. Hadgiivanova, R. Aggregation of Amphiphilic Molecules in Solution: Thermodynamics, Metastability, and Kinetics. Tel Aviv University, 2009.
5. Patel, G., B.; Sprott, G., Dennis, Archaeobacterial Ether Lipid Liposomes (Archaeosomes) as Novel Vaccine and Drug Delivery Systems. *Critical Reviews in Biotechnology* **1999**, 317-357.
6. Needham, D.; Rashmi, S., Nunn, Elastic deformation and failure of lipid bilayer membranes containing cholesterol. *Biophysical Journal* **1990**, 997-1009.
7. Pippa, N.; Psarommati, F.; Pispas, S.; Demetzos, C., The Shape/Morphology Balance: A study of Stealth Liposomes via Fractal Analysis and Drug Encapsulation. *Pharmaceutical Research* **2013**, 2386-2395.
8. Hermetter, A.; Paltauf, F., Interaction between ether glycerophospholipid vesicles and serum proteins. *Biochimica et Biophysica Acta* **1983**, 444-450.
9. Canganella, F.; Wiegel, J., Extremophiles: from abyssal to terrestrial ecosystems and possibly beyond. *Naturwissenschaften* **2011**, 253-279.
10. Eguchi, T.; Ibaragi, K.; Kakinuma, K., Total synthesis of Archaeal 72-Membered Macrocyclic Tetraether Lipids. *Journal of Organic Chemistry* **1998**, 2689-2698.
11. Jurgen-Hinrich, F.; Tianyu, W., Bolaamphiphiles. *Chemical Reviews* **2004**, 2901-2937.
12. Bulacu, M.; Periole, X.; Marrink, S., J., In Silico Design of Robust Bolalipid Membranes. *Biomacromolecules* **2012**, 196-205.
13. Smit, W., A.; Bochkov, A., F.; Caple, R., *Organic Synthesis: The Science Behind the Art*. The Royal Society of Chemistry: 1998.
14. (a) Bedard, A.-C.; Collins, S., K., Microwave accelerated Glaser-Hay macrocyclizations at high concentrations. *Chemical Communications* **2012**, 6420-6422; (b) Gerardo, B.; Cohen-Ohana, M.; Raichman, D., Fast and Versatile Microwave-Assisted Intramolecular Heck Reaction in Peptide Macrocyclization Using Microwave Energy. In *Wiley Periodical*, Wiley: Ramat Gan, Isreal, 2005.
15. Liang, L.; Astruc, D., The copper(I)-catalyzed alkyne-azide cycloaddition (CuAAC) "click" reaction and its applications. An overview. *Coordination Chemistry Reviews* **2011**, 2933-2945.
16. Gagon, C.; Keith, J., CuAAC Macrocyclization: High Intramolecular Selectivity through the Use of Copper-Tris(triazole) Ligand Complexes. *Organic Letters* **2011**, 13 (10), 2754-2757.
17. Luong, H. Towards Voltage-Gated Ion Channels Synthesized by Solid-Phase Organic Synthesis. Uvic, Victoria, British Columbia, Canada, 2008.
18. Moss, R., A.; Swarup, S., Surface-Specific Phosphate Cleavage of a Substrate-Functionalized Vesicular Surfactant. *Journal of the American Chemical Society* **1986**, 5341-5342.
19. (a) Chui, J., K., W. A new paradigm for voltage-clamp studies of synthetic ion channels. Uvic, Victoria, British Columbia, Canada, 2011; (b) Kuang, G.-C.; Guha, P., M. ; Brotherton, W., S.; Simmons, J., Tyler; Stanke, L., A.; Nguyen, B., T.; Clark, R., J.; Zhu, L., Experimental Investigation on the Mechanism of Chelation-Assisted, Copper(II) Acetate-Accelerated Azide-Alkyne Cycloaddition. *Journal of the American Chemical Society* **2011**; (c) Liu, X.-M.; Thakur, A.; Wang, D., Efficient Synthesis of Linear Multifunctional

Poly(ethylene glycol) by Copper(I)-Catalyzed Huisgen 1,3-Dipolar Cycloaddition. *Biomacromolecules* **2007**, 2653-2658.

20. Hein, J., E.; Fokin, V., V., Copper-catalyzed azide-alkyne cycloaddition (CuAAC) and beyond: new reactivity of copper(I) acetylides. *Chemical Society Reviews* **2010**, 1302-1315.

21. Smith, A., B.; Ott, G., R., Total Synthesis of (-)-Macrolactin A. *Journal of the American Chemical Society* **1996**, 13095-13096.

22. Beveridge, T., J.; Choquet, C., G.; Patel, G., B.; Sprott, G., Dennis, Freeze-fracture planes of methanogen membranes correlate with the content of tetraether lipids. *Journal of Bacteriology* **1993**.

Appendix 1: Experimental Details

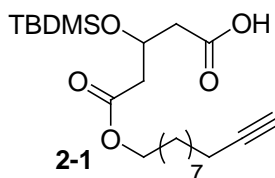
Synthetic Experimental Details

General Procedures:

Chemicals and solvents were used as received from known suppliers, except dry THF and dry DCM were obtained from a MBRAUN-SPS. NMR spectra were collected on a 300 MHz Bruker, or 500 MHz Bruker instruments. UV-vis spectra were run on a Cary 50 Bio UV-vis spectrometer in a 2 mm x 10 mm quartz cell. ESI Mass spectra were recorded on a LCQ-Classic instrument and exact mass was detected on a LC-MS/MS Thermo LTQ Orbitrap.

Synthetic Detail:

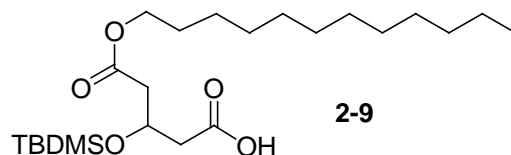
2-1: Glutarate Esterification:



In a 2 necked round bottom flask a stirred solution of toluene (19 mL) was prepared from 3-(*tert*-butyl dimethylsilyloxy) glutaric anhydride (2.182 g, 8.929 mmol, 1.15 equiv.) and 10-undecyn-1-ol (1.49 mL, 7.77 mmol, 1.00 equiv.). The reaction mixture was set to stir at reflux for 24 hours under a CaSO₄ drying tube. The reaction was monitored by TLC (silica gel, EtOAc/Hexanes as eluent, visualized by KMnO₄). Once complete, the reaction was cooled and toluene roto-evaporated. The crude product was then redissolved in pentane and cooled in a dry ice ethanol bath then vacuum filtered. Crystallization of excess anhydride was repeated using the filtrate until the excess crystals no longer formed. If alcohol impurities existed, visualized by NMR, the crude product was purified by column chromatography on silica gel, using EtOAc/Hexanes as eluent. A colourless oil was afforded in a 87% yield (2.78 g). ¹H-NMR (300 MHz, CDCl₃) δ: 4.54 (q, 1H, J=6.0 Hz), 4.06 (dt, 2H, J=6.9, 1.5 Hz), 2.7-2.54 (m, 4H), 2.19 (dt, 2H, J=2.7, 6.9 Hz), 1.93 (t, 1H, J=3.0 Hz), 1.25-1.66 (m, 14H), 0.86 (s, 9H), 0.09 (s, 3H), 0.08 (s, 3H). ¹³C-NMR (75 MHz, CDCl₃) δ: 177.0, 171.0, 84.6, 68.1, 66.1, 64.7, 42.4, 42.2, 30.3, 29.6,

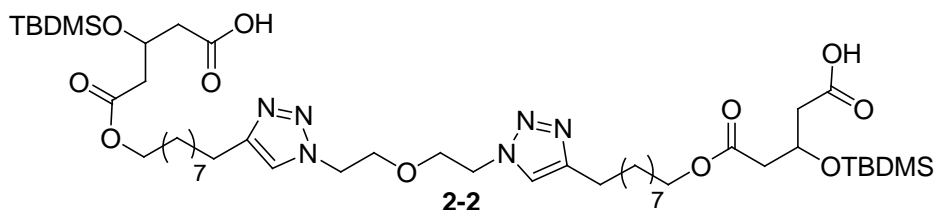
29.3, 29.1, 28.9, 28.6, 28.5, 28.4, 25.8, 25.6, 18.3, 17.8, -4.9, -5.0. MS (-ve Orbitrap; Exact mass): calc'd for $C_{22}H_{40}SiO_5$ = 411.2572 amu, obtained = 411.2570 amu.

2-9: Glutarate Esterification:



In a 2 necked round bottom flask a stirred solution of toluene (24 mL) was prepared from 3-(*tert*-butyl dimethylsilyloxy) glutaric anhydride (1.140 g, 4.665 mmol, 1.14 equiv.) and 10-undecyn-1-ol (0.780 mL, 4.07 mmol, 1.00 equiv.). The reaction mixture was set to stir at reflux for 10 hours under a $CaSO_4$ drying tube. The reaction was monitored by 1H -NMR. After 10 hours of reflux 3-(*tert*-butyl dimethylsilyloxy) glutaric anhydride (0.150 g, 0.150 equiv.) was added. Once complete, the reaction was cooled and toluene roto-evaporated. The crude product was then redissolved in pentane and cooled in a dry ice ethanol bath then vacuum filtered. Crystallization of excess anhydride was repeated using the filtrate until the excess crystals no longer formed. A colourless oil was afforded in a 95% yield (1.655 g). 1H -NMR (300 MHz, $CDCl_3$) δ : 4.54 (q, 1H, $J=6.0$ Hz), 4.06 (dt, 2H, $J=1.5, 6.9$ Hz), 2.70-2.55 (m, 4H), 1.64-1.26 (m, 20H), 0.90-0.87 (m, 12H), 0.10 (s, 3H), 0.09 (s, 3H). ^{13}C -NMR (75MHz, $CDCl_3$) δ : 177.0, 171.1, 67.9, 66.2, 64.8, 42.5, 42.4, 32.0, 29.7, 29.6, 29.5, 29.4, 29.3, 28.6, 26.0, 25.7, 22.7, 17.9, 14.1, -4.87, -4.92. MS (-ve Orbitrap; Exact mass): calc'd for $C_{23}H_{46}O_5Si$ = 429.304 amu, obtained = 429.306 amu.

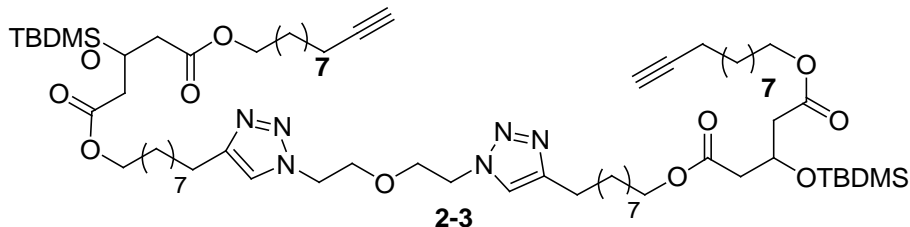
2-2: Dimer CuAAC:



In a round bottom flask a stirred solution of DMF (32 mL) was prepared from **2-1** (1.612 g, 3.920 mmol, 1.99 equiv.), and DMAP (0.039 g, 0.32 mmol, 0.16 equiv.). This was followed by 1,1'-oxybis(2-azidoethane)(0.308 g, 1.97 mmol, 1.00 equiv.). The solution was degassed for 20 minutes with N_2 , and then CuI (0.186 g, 0.977 mmol, 0.496 equiv.) was added. The flask was

evacuated with N₂ and then sealed to create a positive pressure of N₂. The reaction was set to stir for 21.5 hours at 12°C. When the reaction was complete, visualized by ¹H-NMR, the reaction solution was diluted in DCM, and washed with a saturated solution of disodium EDTA (50 mL) until the aqueous layer no longer remained blue. This was then followed two washes of H₂O (50 mL), and two washes of acidified H₂O (50 mL, 2 drops 1M HCl). In general no purification was necessary. If excess azide was present the half reacted product was removed by dissolving the crude product in EtOAc (2 mL) and then hexanes (25 mL). The insoluble material was removed and the solvent roto-evaporated. Washes were repeated until no impurities remained. The reaction afforded a colourless; extremely tacky solid that retained solvents extremely well, so the resulting oil needed to be concentrated well before being put on high vacuum. A colourless oil was afforded in a 86% yield (1.667 g). ¹H-NMR (300 MHz, CDCl₃) δ: 7.20 (s, 2H), 4.55 (q, 2H, J=6.0 Hz), 4.46 (t, 2H, J=4.8 Hz), 4.08 (t, 4H, J=6.0 Hz), 3.81 (t, 2H, J=4.8 Hz), 2.68 (t, 4H, J=8.4 Hz), 2.61-2.58 (m, 8H) 1.66-1.25 (m, 28H) 0.85 (s, 18H), 0.09 (s, 6H), 0.08 (s, 6H). ¹³C-NMR (125 MHz, CDCl₃) δ: 175.0, 171.2, 148.5, 121.9, 69.5, 66.4, 64.8, 50.2, 42.8, 42.5, 29.6, 29.4, 29.3, 29.2, 29.1, 28.6, 26.0, 25.5, 18.0, -4.7, -4.8. MS (-ve Orbitrap; Exact mass): calc'd for C₄₈H₈₈N₆Si₂O₁₁ = 981.6122 amu, obtained = 981.6121 amu.

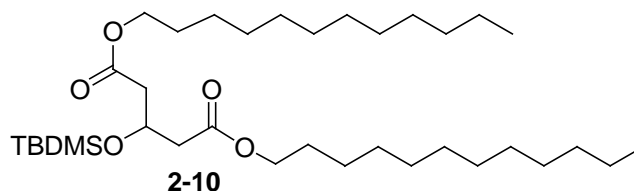
2-3: Diacid Esterification:



In a round bottom flask **2-2** (1.663 g, 1.694 mmol, 1.000 equiv.) was dissolved in dry THF (8.5 mL). While having a flow of N₂ DIC (0.640 mL, 4.09 mmol, 2.41 equiv.) was added and stirred for 5 minutes. HOBt (0.550 g, 4.07 mmol, 2.40 equiv.) was then added and stirred for 5 minutes, followed by 10-undecyn-1-ol (0.780 mL, 4.06 mmol, 2.40 equiv.) which was stirred for 5 minutes, followed by DiPEA (0.710 mL, 4.08 mmol, 2.41 equiv.). The reaction was left stirring at r.t. for 24 hours. The reaction was then vacuum filtered and the filtrate concentrated. The product was then dissolved in 50 mL DCM and extracted two times with Na₂H₂PO₄ buffer solution (50 mL, pH~3), two times with Na₂H₂PO₄ buffer solution (50 mL, pH~7), one time with H₂O (50

mL), two times with 10% brine solution (50 mL), and finally washed once with a saturated solution of NaCl (50 mL). The crude product was purified by column chromatography on silica gel, using EtOAc/hexanes as eluent affording a colourless oil in a 43% yield (0.930 g). ^1H -NMR (300 MHz, CDCl_3) δ : 7.18 (s, 2H), 4.50 (q, 2H, $J=6.3$ Hz), 4.42 (t, 2H, $J=5.1$ Hz), 4.04-3.98 (m, 8H) 3.78 (t, 2H, $J=4.8$ Hz), 2.65 (t, 4H, $J=7.8$ Hz), 2.51 (d, 8H, $J=6.3$ Hz), 2.14 (dt, 4H, $J=2.7$, 6.9 Hz), 1.90 (t, 2H, $J=2.7$ Hz) 1.64-1.22 (m, 56H), 0.80 (s, 18) 0.02 (s, 12H). ^{13}C -NMR (75 MHz, CDCl_3) δ : 171.2, 148.6, 121.4, 84.8, 69.6, 68.2, 64.7, 50.0, 42.7, 29.6, 29.5, 29.4, 29.3, 29.25, 29.1, 28.8, 28.7, 28.5, 26.0, 25.9, 25.8, 25.76, 18.5, 18.0, -4.8. MS (+ve Orbitrap; Exact mass): calc'd for $\text{C}_{70}\text{H}_{124}\text{N}_6\text{Si}_2\text{O}_{11}$ = 1281.893 amu, obtained = 1281.893 amu.

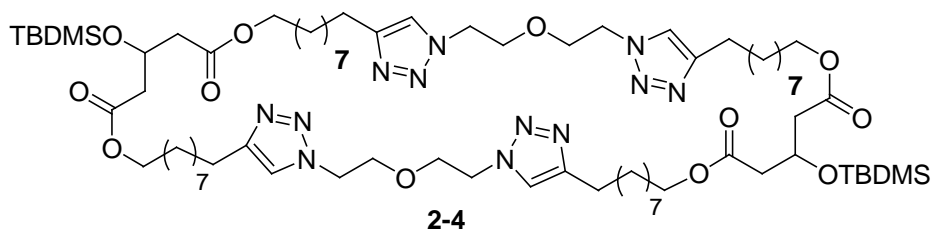
2-10: Monoacid Esterification:



In a round bottom flask **2-9** (1.270 g, 2.958 mmol, 1.000 equiv.) was dissolved in dry THF (15 mL). While having a flow of N_2 DIC (0.690 mL, 4.41 mmol, 1.49 equiv.) was added and stirred for 5 minutes. HOBt (0.598 g, 4.43 mmol, 1.50 equiv.) was then added and stirred for 5 minutes, followed by 1-dodecanol (0.990 mL, 4.41 mmol, 1.49 equiv.) which was stirred for 5 minutes, followed by DiPEA (1.540 mL, 8.842 mmol, 2.989 equiv.). The reaction was left stirring at r.t. for 3 hours. The reaction was then vacuum filtered and the filtrate concentrated. The product was then dissolved in 50 mL DCM and extracted two times with $\text{Na}_2\text{H}_2\text{PO}_4$ buffer solution (50 mL, pH~3), two times with $\text{Na}_2\text{H}_2\text{PO}_4$ buffer solution (50 mL, pH~7), one time with H_2O (50 mL), two times with 10% brine solution (50 mL), and finally washed once with a saturated solution of NaCl (50 mL). The crude product was washed with MeOH, the resulting solution was vacuum filtered and the remaining 'wet' oil was roto-evaporated. The MeOH wash was repeated as many times as necessary to increase purity. A colourless oil was afforded in a 70% yield (1.238 g). ^1H -NMR (300 MHz, CDCl_3) δ : 4.52 (q, 1H, $J=6.0$ Hz), 4.06-4.01 (m, 4H), 2.52 (d, 4H, $J=6.3$ Hz) 1.62-1.24 (m, 40H), 0.88-0.82 (m, 15H), 0.82 (s, 9H), 0.04 (s, 6H). ^{13}C -NMR (75 MHz, CDCl_3) δ : 171.2, 66.5, 64.8, 42.7, 32.0, 29.8, 29.7, 29.6, 29.5, 29.4, 28.7, 26.1, 25.8, 22.8, 18.0, 14.2, -

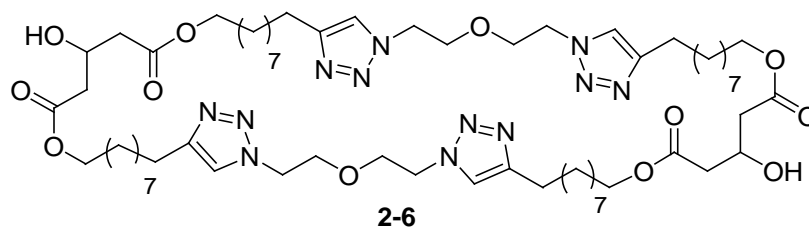
4.8. MS (+ve Orbitrap; Exact mass): calc'd for $C_{35}H_{70}O_5Si$ = 599.5065 amu, obtained = 599.5065 amu.

2-4: CuAAC Macrocyclization:



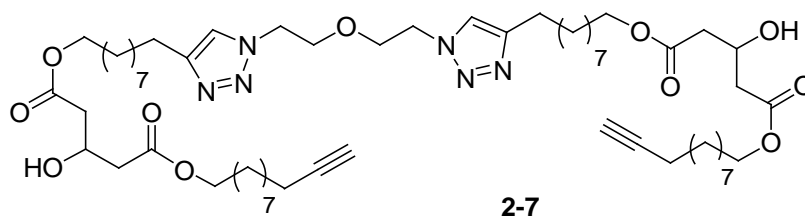
In a round bottom flask a stirred solution of DMF (2.550 mL) was prepared with **2-3** (0.371 g, 0.289 mmol, 1.00 equiv.), and DMAP (0.0025 g, 0.0020 mmol, 0.071 equiv.). This was followed by 1,1'-oxybis(2-azidoethane) (0.0452 g, 0.289 mmol, 1.00 equiv.). The solution was degassed for 20 minutes with N_2 , and then CuI (0.0227 g, 0.119 mmol, 0.412 equiv.) was added. The flask was evacuated with N_2 and then sealed to create a positive pressure of N_2 . Once the CuI was dissolved the reaction was set to stir for 21.5 hours at $12^\circ C$. When the reaction was complete, visualized by 1H -NMR, the reaction solution was diluted in DCM, and washed with a saturated solution of disodium EDTA (50 mL) until the aqueous layer no longer remained blue. This was then followed two washes of H_2O (50 mL), and two washes of acidified H_2O (50 mL, 2 drops 1M HCl). Purification was not necessary. A colourless solid was afforded in an 87% yield (0.307 g). 1H -NMR (300 MHz, $CDCl_3$) δ : 7.21-7.18 (m, 4H), 7.18 (s, 1H), 4.52 (q, 2H, $J=6.3$ Hz), 4.44 (t, 8H, $J=5.1$ Hz), 4.06-4.00 (m, 8H), 3.79 (t, 8H, $J=5.1$ Hz), 2.66 (t, 8H, $J=7.8$ Hz), 2.52 (d, 8H, 5.7 Hz), 1.66-1.23 (m, 56H), 0.82 (s, 18H), 0.04 (s, 12H). ^{13}C -NMR (125 MHz, $CDCl_3$) δ : 171.24, 171.19, 148.58, 148.54, 121.51, 121.48, 69.62, 69.58, 66.5, 64.78, 64.75, 50.0, 42.7, 29.8, 29.64, 29.55, 29.43, 29.35, 29.3, 28.7, 26.0, 25.8, 18.0, -4.8. MS (+ve Orbitrap; Exact mass): calc'd for $C_{74}H_{132}N_{12}Si_2O_{12}$ = 1459.951 amu, obtained = 1459.9542 amu.

2-6: Deprotection of Macrocyclic Bolaaphiphile Precursor:



The starting material **2-4** (93.2 mg, 0.0638 mmol, 1.00 equiv.) was placed in a round bottom flask. TBAF (0.645 mL, 0.65 mmol, 1.0×10^1 equiv. from a 1.0 M stock solution in THF), was added concurrently with AcOH (0.360 mL, 0.158 mmol, 2.48 equiv. from a 0.438 M stock solution in THF). The solution was stirred under N_2 for 30 minutes at r.t. while being monitored by NMR. When the reaction was complete it was quenched with a saturated $NH_4^+Cl^-$ solution and DCM (25 mL) was added. It was then washed with H_2O (25 mL), brine (25 mL), and finally H_2O (25 mL H_2O , 2 drops HCl). The solvent was then dried with Na_2SO_4 , vacuum filtered and removed under reduced pressure. The crude product was then dissolved in pentane (25 mL) and crystallized in an ethanol/dry ice bath. The crystallization was repeated until desired purity was obtained, affording a white solid in an 86% yield (77.2 mg). 1H - NMR (300 MHz, $CDCl_3$) δ : 7.21-7.17 (m, 4H), 4.43-4.46 (m, 10H), 4.08 (t, 8H, $J=6.9$ Hz), 3.80 (t, 8H, $J=5.1$ Hz), 3.54 (s, 2H), 2.67 (t, 8H, $J=8.1$ Hz), 2.53 (d, 8H, $J=6.3$ Hz), 1.13-1.63 (m, 56H). ^{13}C - NMR (75 MHz, $CDCl_3$) δ : 172.0, 148.6, 121.5, 69.6, 65.0, 64.9, 50.0, 40.9, 29.6, 29.5, 29.4, 29.3, 28.7, 26.0, 25.8. MS (+ve Orbitrap; Exact mass): calc'd for $C_{62}H_{104}N_{12}O_{12}$ = 1209.796 amu, obtained = 1209.795 amu.

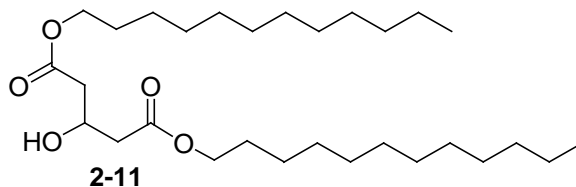
2-7: Deprotection of Bolaaphiphile Precursor:



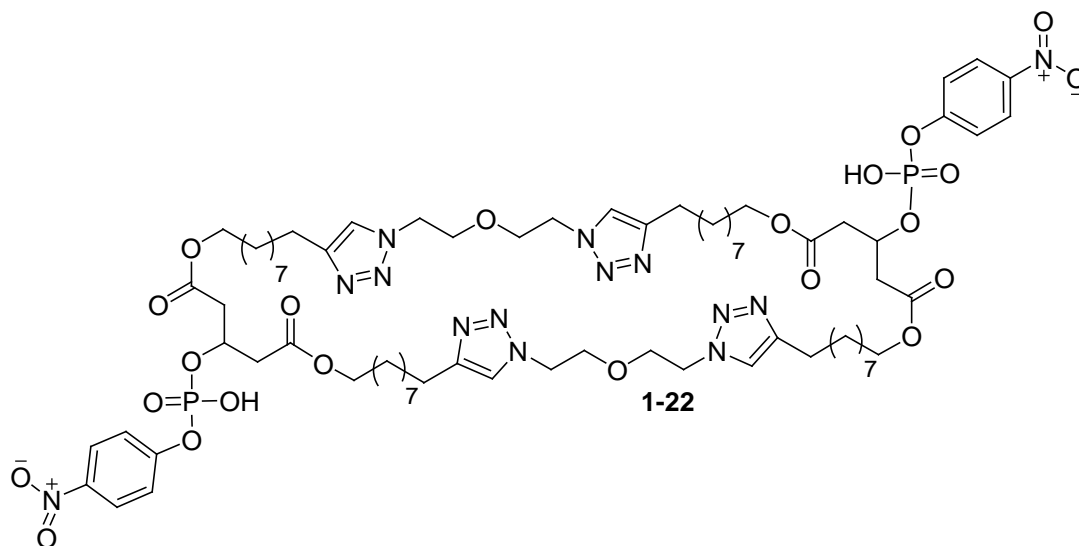
The starting material **2-3** (271 mg, 0.211 mmol, 1.00 equiv.) was placed in a round bottom flask. TBAF (2.155 mL, 2.2 mmol, 1.0×10^1 equiv. from a 1.0 M stock solution in THF), was added concurrently with AcOH (1.200 mL, 0.526 mmol, 2.49 equiv. from a 0.438 M stock solution in THF). The solution was stirred under N_2 for 30 minutes at r.t. while being monitored by NMR. When the reaction was complete it was quenched with a saturated $NH_4^+Cl^-$ solution and DCM (25 mL) was added. It was then washed with H_2O (25 mL), brine (25 mL), and finally H_2O (25 mL H_2O , 2 drops HCl). The solvent was then dried with Na_2SO_4 , vacuum filtered and removed under reduced pressure. The crude product was then dissolved in pentane (25 mL) and crystallized in an ethanol/dry ice bath. A short column was done with EtOAc in Hexanes to

remove impurities affording a white solid in a 68% yield (152 mg). ^1H -NMR (300 MHz, CDCl_3) δ : 7.16 (s, 2H), 4.40 (m, 6H), 4.03 (t, 8H, $J=6.8$ Hz), 3.75 (t, 4H, 5.1 Hz), 3.52 (s, 2H), 2.62 (t, 4H, 7.5 Hz), 2.49 (d, 8H, $J=6.3$ Hz), 2.11 (dt, 4H, $J=2.7, 6.9$ Hz), 1.88 (t, 2H, 2.7 Hz), 1.58-1.24 (m, 56H). ^{13}C -NMR (75 MHz, CDCl_3) δ : 171.8, 148.4, 121.4, 84.7, 69.5, 68.2, 64.9, 64.8, 49.9, 40.8, 29.5, 29.4, 29.3, 29.14, 29.13, 29.0, 28.7, 28.5, 25.8, 25.6, 22.7, 18.4. MS (+ve Orbitrap; Exact mass): calc'd for $\text{C}_{58}\text{H}_{96}\text{N}_6\text{O}_{11}$ = 1053.721 amu, obtained = 1053.720 amu.

2-11: Deprotection of Amphiphile Precursor:



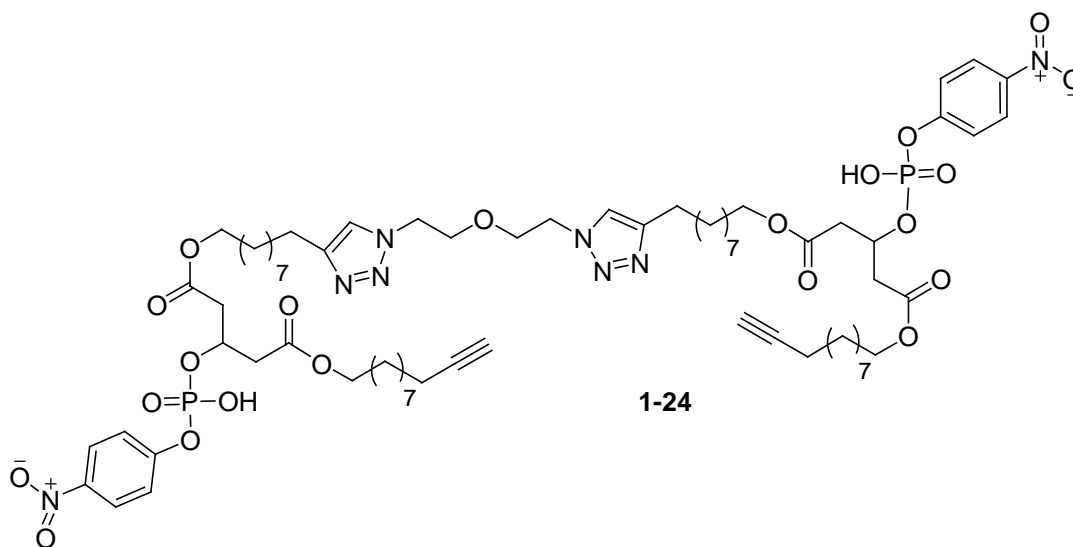
The starting material **2-10** (0.6900 g, 1.151 mmol, 1.000 equiv.) was placed in a round bottom flask. TBAF (5.80 mL, 5.8 mmol, 5.0 equiv. from a 1.0 M stock solution in THF), was added concurrently with AcOH (3.30 mL, 1.45 mmol, 1.26 equiv. from a 0.438 M stock solution in THF). The solution was stirred under N_2 for 30 minutes at r.t. while being monitored by NMR. When the reaction was complete it was quenched with a saturated NH_4^+Cl^- solution and DCM (25 mL) was added. It was then washed with H_2O (25 mL), brine (25 mL), and finally H_2O (25 mL H_2O , 2 drops HCl). The solvent was then dried with Na_2SO_4 , vacuum filtered and removed under reduced pressure. The crude product was then dissolved in pentane (25 mL) and crystallized in an ethanol/dry ice bath, affording a white solid in a 90% yield (502 mg). ^1H -NMR (300 MHz, CDCl_3) δ : 4.44 (q, 1H, $J=6.3$ Hz), 4.09 (t, 4H, $J=6.6$ Hz), 3.41 (s, 1H), 2.53 (d, 4H, $J=6.3$ Hz), 1.64-1.25 (m, 40H), 0.87 (t, 6H, $J=6.2$ Hz). ^{13}C -NMR (75 MHz, CDCl_3) δ : 172.0, 65.1, 64.9, 40.8, 32.0, 29.72, 29.67, 29.6, 29.4, 29.3, 28.7, 26.0, 22.8, 14.2. MS (+ve Orbitrap; Exact mass): ESI: calc'd for $\text{C}_{29}\text{H}_{56}\text{O}_5$ = 485.4200 amu, obtained = 485.4199 amu.

1-22: Macrocylic Bolaamphiphile:

An oven baked round bottom flask was cooled to r.t. and 4-Nitrophenyl phosphorodichloridate (157.5 mg, 0.6153 mmol, 6.03 equiv.) was added. The round bottom flask was capped and a flow of N₂ started, dry DCM (700 ul) was added along with pyridine (98 ul, 1.2 mmol, 12 equiv.). The mixture was then stirred for 30 minutes. Another oven baked round bottom flask was concurrently cooled with the first round bottom flask to r.t. and **2-6** (124 mg, 0.102 mmol, 1.00 equiv.) was then added to the second round bottom flask and an oven baked condenser was placed on top. A flow of N₂ was started. Dry DCM (100 ul) was then added to the second flask and stirred. Upon completion of thorough mixing 4-Nitrophenyl phosphorodichloridate and pyridine were added dropwise to the reaction flask and the new solution stirred at r.t. for 30 minutes. The temperature was then increased to reflux for 7.5 hours, monitored by NMR. The reaction was cooled to r.t. and Et₂O: H₂O (200 ul, 50:50) at 0°C was added to the reaction and set to stir vigorously overnight. In the morning the product was seen as a yellow/orange precipitate in the round bottom flask. The solvent mixture was poured out and the precipitate dissolved in DCM:MeOH (4 mL, 95:5). The mixture was then washed with H₂O (2 mL) in the round bottom flask followed by an acidified H₂O (2 mL H₂O, 1 drop HCl), and washed again H₂O (2 mL). If necessary the product was then adsorbed onto silica gel and a short column was done with

DCM:MeOH to remove crude material, affording a brown yellow solid in a 20% yield (33.0 mg). $^1\text{H-NMR}$ (300 MHz, DMSO-d_6) δ : 8.108-8.083 (m, 4H), 7.59 (s, 4H), 7.32 (s, 4H), 4.74 (s, 2H), 4.41 (s, 8H), 3.82 (s, 8H), 3.74 (s, 8H), 2.71 (s, 8H), 2.53 (s, 8H), 1.52-1.19 (m, 56H). $^{13}\text{C-NMR}$ (125 MHz, DMSO-d_6) δ : 170.0, 146.7, 124.9, 121.9, 119.9, 68.5, 63.8, 49.0, 29.0, 28.9, 28.71, 28.67, 28.6, 27.9, 25.3, 25.0. MS (-ve Orbitrap; Exact mass): calc'd for = $\text{C}_{74}\text{H}_{112}\text{N}_{14}\text{O}_{22}\text{P}_2$ 1608.740 amu, obtained 1608.740 = amu.

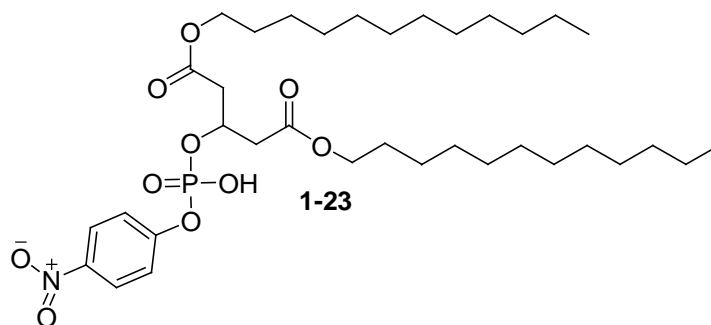
1-24: Linear Bolaaphiphile:



An oven baked round bottom flask was cooled to r.t. and 4-Nitrophenyl phosphorodichloridate (138 mg, 0.539 mmol, 5.92 equiv.) was added. The round bottom flask was capped and start a flow of N_2 was started, dry DCM (800 μl) was added along with pyridine (85 μl , 1.1 mmol, 12 equiv.). The mixture was then stirred for 30 minutes. Another oven baked round bottom flask was concurrently cooled with the first round bottom flask to r.t. and **2-7** (95.5 mg, 0.091 mmol, 1.00 equiv.) was then added to the second round bottom flask and an oven baked condenser was placed on top. A flow of N_2 was then started. Dry DCM (5.0 mL) was then added to the second flask and stirred. Upon completion of thorough mixing 4-Nitrophenyl phosphorodichloridate and pyridine were added dropwise to the reaction flask and the new solution stirred at r.t. for 30 minutes. The temperature was then increased to reflux for 7.5 hours, monitored by NMR. The reaction was cooled to r.t. and $\text{Et}_2\text{O}:\text{H}_2\text{O}$ (1.6 mL, 50:50) at 0°C was added to the reaction and set to stir vigorously overnight. The mixture diluted with DCM (10 mL) and added to a

separatory funnel, then washed with H₂O (10 mL), then with acidified H₂O (10 mL H₂O, 2 drop HCl), and again with H₂O (10 mL). If necessary the product was then adsorbed onto silica gel and a short column was done with DCM:MeOH affording a brown solid in a 17% yield (22.4 mg). ¹H-NMR (300 MHz, CDCl₃) δ: 7.99 (d, 4H, J=8.4 Hz), 7.17 (s, 4H), 5.13 (s, 2H), 4.84-4.45 (m, 4H) 4.11-4.04 (m, 12H), 2.68-2.54 (m, 12H), 2.16 (dt, 4H, J=2.7, 6.9 Hz), 1.92 (t, 2H, J=2.7 Hz) 1.64-1.22 (m, 56H). ¹³C-NMR (125 MHz, DMF-d₇): 171.6, 148.4, 142.8, 125.9, 123.0, 121.2, 85.4, 71.0, 70.1, 65.1, 50.5, 40.8, 26.7, 18.9. MS (-ve Orbitrap; Exact mass): calc'd for C₇₀H₁₀₄N₈O₂₁P₂ = 1452.664 amu, obtained 1452.660 = amu.

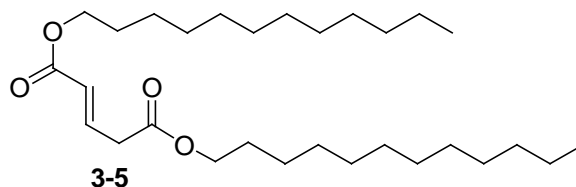
1-23: Linear Amphiphile:



An oven baked round bottom flask was cooled to r.t. and 4-Nitrophenylphosphoro dichloridate (79 mg, 0.31 mmol, 3.1 equiv.) was added. The round bottom flask was capped and a flow of N₂ was started, dry DCM (4.5 mL) was added along with pyridine (5.0x10¹ ul, 0.62 mmol, 6.2 equiv.). The mixture was then stirred for 30 minutes. Another oven baked round bottom flask was concurrently cooled with the first round bottom flask to r.t. and **2-11** (50 mg, 0.10 mmol, 1.0 equiv.) was then added to the second round bottom flask and an oven baked condenser was placed on top. A flow of N₂ was then started. Dry DCM (600 ul) was then added to the second flask and stirred. Upon completion of thorough mixing 4-Nitrophenyl phosphorodichloridate and pyridine were added dropwise to the reaction flask and the new solution stirred at r.t. for 30 minutes. The temperature was then increased to reflux for 7.5 hours, monitored by NMR. The reaction was cooled to r.t. and Et₂O: H₂O (1.2 mL, 50:50) at 0⁰C was added to the reaction and set to stir vigorously overnight. The mixture diluted with DCM (2 mL) and added to a separatory funnel, then washed with H₂O (2 mL), then with acidified H₂O (2 mL H₂O, 1 drop HCl), and again with H₂O (10 mL). If necessary the product was then adsorbed onto silica gel and a short

column was done with EtOAc in hexanes affording an off yellow solid in a 32% yield (22.6 mg). $^1\text{H-NMR}$ (300 MHz, CDCl_3) δ : 8.14 (d, 2H, $J=9$ Hz), 7.36 (d, 2H, 8.7 Hz), 5.16 (s, 1H), 3.98-3.95 (m, 4H), 2.82-2.66 (m, 4H), 1.51-1.22 (m, 40H), 0.87 (t, 3H, $J=6.3$ Hz). $^{13}\text{C-NMR}$ (125 MHz, CDCl_3): 170.9, 125.5, 120.7, 65.7, 39.9, 32.1, 29.82, 29.76, 29.7, 29.50, 29.45, 28.58, 26.0, 22.8, 14.2. MS (-ve Orbitrap; Exact mass): calc'd for $\text{C}_{35}\text{H}_{60}\text{NO}_{10}\text{P}$ = 684.3881 amu, obtained 684.3865 = amu.

3-5: Attempted preparative-scale synthesis of α , β -unsaturated Ester:



In a round bottom flask **1-23** (15 mg, 0.022 mmol, 1.0 equiv.) was added and dissolved in DCM (2.5 mL). THF (20 mL) was then added followed by 1 M NaOH (145 μL , 0.1 mmol, 7 equiv.) while the solution was stirring. The solution was then stirred at r.t. for 4 hours. The resulting reaction mixture was yellow and subsequently acidified to clear with 1 M HCl (6.0×10^1 μL , 0.06 mmol, 3 equiv.). The majority of the solvent (~90%) was roto-evaporated and diluted with DCM (5 mL), then washed with H_2O (5 mL), then with acidified H_2O (5 mL H_2O , 1 drop HCl), and again with H_2O (5 mL). The resulting product was columned on silica gel with hexane and EtOAc to get a crude product with a 29% yield (~3 mg). $^1\text{H-NMR}$ (300 MHz, CDCl_3) δ : 7.00 (dt, 1H, $J=7.2, 15.6$ Hz), 5.93 (dt, 1H, $J=1.5, 15.6$ Hz), 4.21-4.08 (m, 4H), 3.22 (dd, 2H, $J=1.5, 7.2$ Hz), 1.64-1.259(m, 40H), 0.87 (t, 3H, $J=6.3$ Hz).

ASSAY EXPERIMENTAL DETAILS

Membrane-spanning Assay

Vesicle Preparation: Vesicles were prepared as previously described². To a chloroform solution of L- α -phosphatidylcholine (2.00 mL ~25 mg/mL) and ~1.5 mg of either **1-23**, **1-24**, or **1-22** were added (3 wt%; 3.2, 1.5, 1.3 mol% amphiphile in lipid respectively). The lipid was transferred to a pear shaped flask and roto-evaporated and then left of the high vacuum line overnight. The resulting lipid film was hydrated

with 800 μl of a pH 6.4 buffer solution consisting of 1.00×10^{-2} M Na_3PO_4 , $\sim 1.00 \times 10^{-1}$ M NaCl in Millipore water with the pH adjusted using concentrated H_3PO_4 . The solution was then sonicated and vortexed until all of the lipid material was suspended in solution. The resulting mixture was quick frozen with liquid nitrogen for thirty seconds and then thawed with cool tap water for 10 minutes. The freeze-thaw procedure was repeated two more times. The mixture was then sonicated for 20 seconds at 1 second on 1 second off pulses of 3W using a probe sonicator. The solution was cooled with ice water and sonication repeated two more times. The vesicle suspension was then sized through a 0.1 μm Nucleopore membrane 19 times. The sized sample was gel filtered on a Sephadex G-25 column. The first 3 cloudy drops through the column were thrown away and the rest of the cloudy drops from the column were collected until the drops from the column became clear again. The cloudy fraction was diluted to 5.00 mL in a volumetric flask. Preparations of this stock solution created vesicles with a diameter of 125-150 nm and a polydispersity of 0.162-0.177 (as determined by dynamic light scattering on a Brookhaven Instruments, ZetaPALS particle sizing software), Table A1. The vesicle solution was stored at 5°C and used within 24 hours.

Vesicle Sample	1-22	1-24	1-23
Effective Vesicle Diameter	125.6 nm	148.3 nm	146.9 nm

Table A1: Effective diameter of vesicles containing all three synthesized phospholipids.

Typical Experiment: 500 μl of the sized and diluted vesicle solution was transferred to a 2 mm x 10 mm quartz cell. 10 μl of a 1M NaOH solution was added to the cell resulting in a solution with $\text{pH} \sim 11.8$. The cell was then transferred to a UV-vis spectrometer and absorbance readings were taken every 30 seconds for 100 minutes, Figure A1, Table A2.

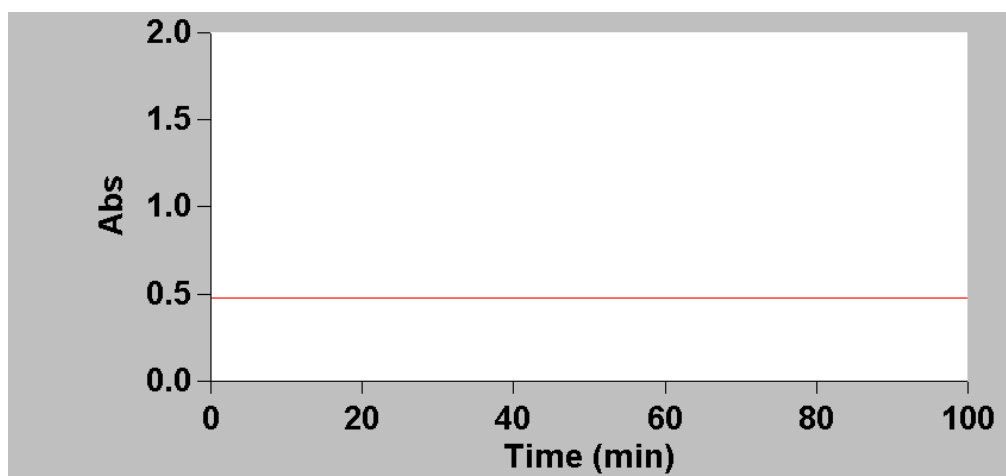
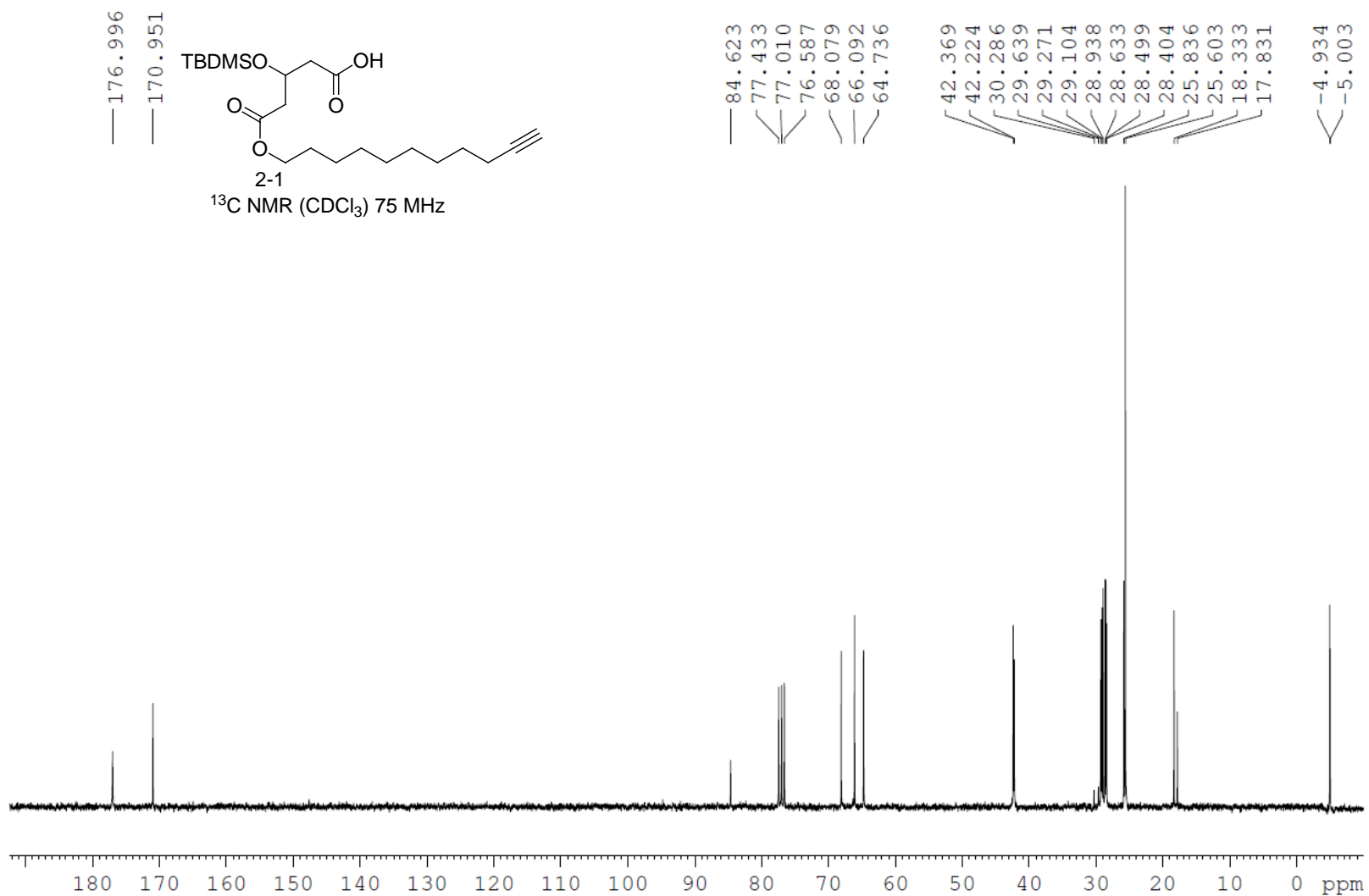


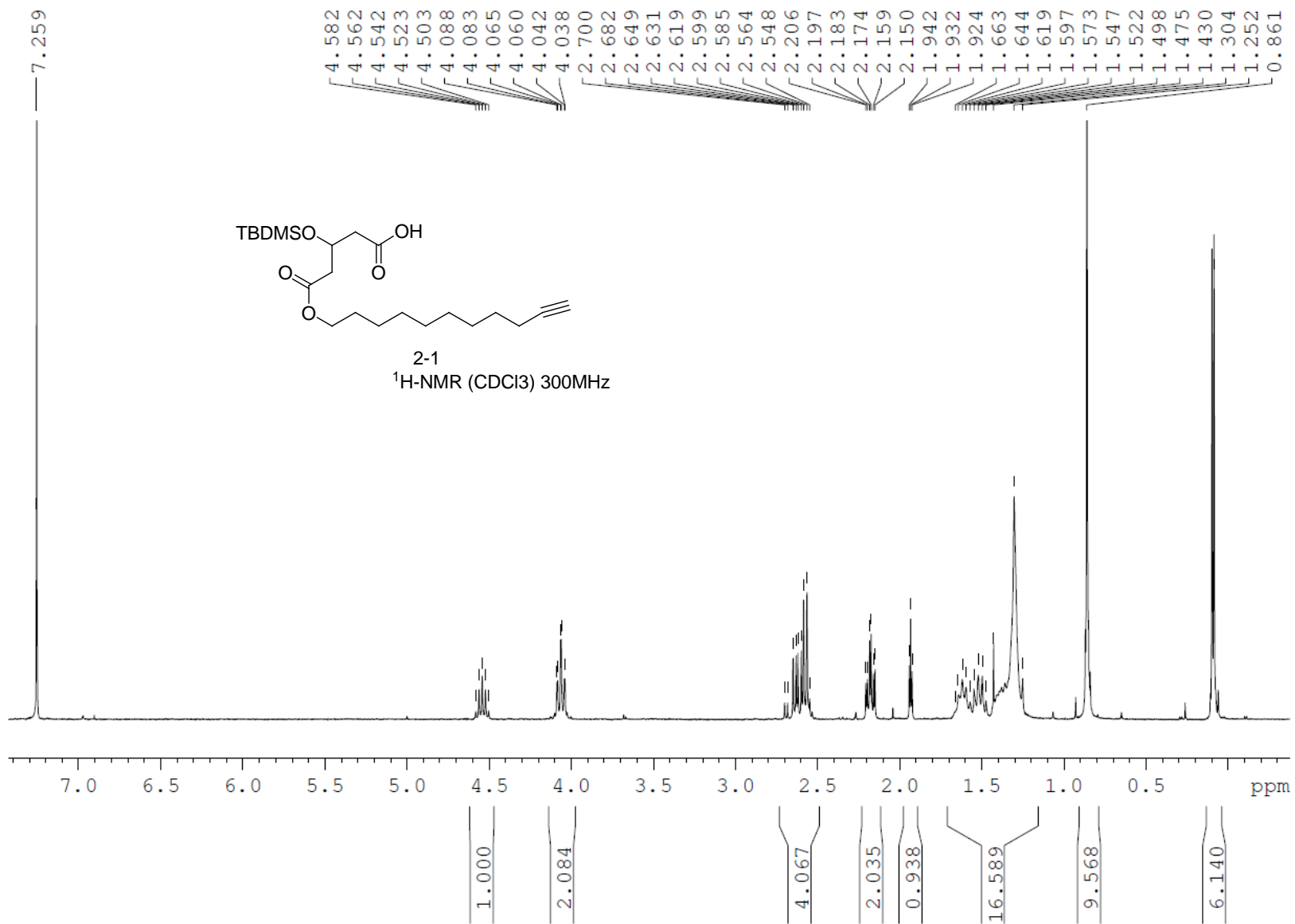
Figure A1: Absorbance as a function of time at 400 nm during the membrane-spanning assay. Vesicles prepared with 1-22 at a pH 6.4 following a base pulse to pH 11.8. Absorbance reading every 30 seconds for 100 minutes.

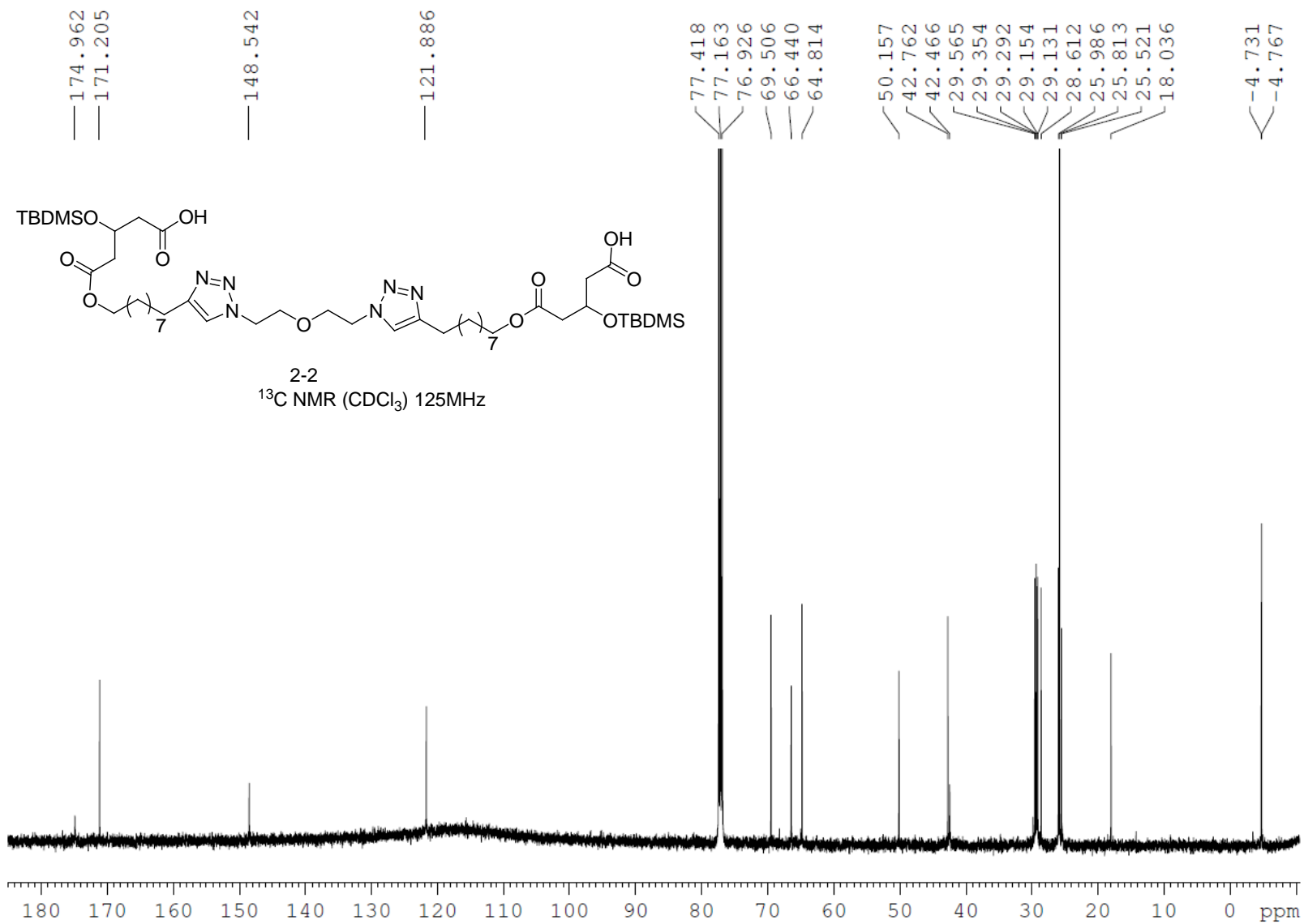
Compound	Start (min)	Stop (min)	Slope (Abs/min)	Abs Start	Abs Stop	S.D.
1-22	0.000	100.000	0.0001	0.4765	0.4778	0.0007
Compound	Start (min)	Stop (min)	Slope (Abs/min)	Abs Start	Abs Stop	S.D.
1-24	0.000	100.000	0.0001	0.1673	0.1689	0.0003
Compound	Start (min)	Stop (min)	Slope (Abs/min)	Abs Start	Abs Stop	S.D.
1-23	0.000	100.000	-0.0001	0.2021	0.2015	0.0004

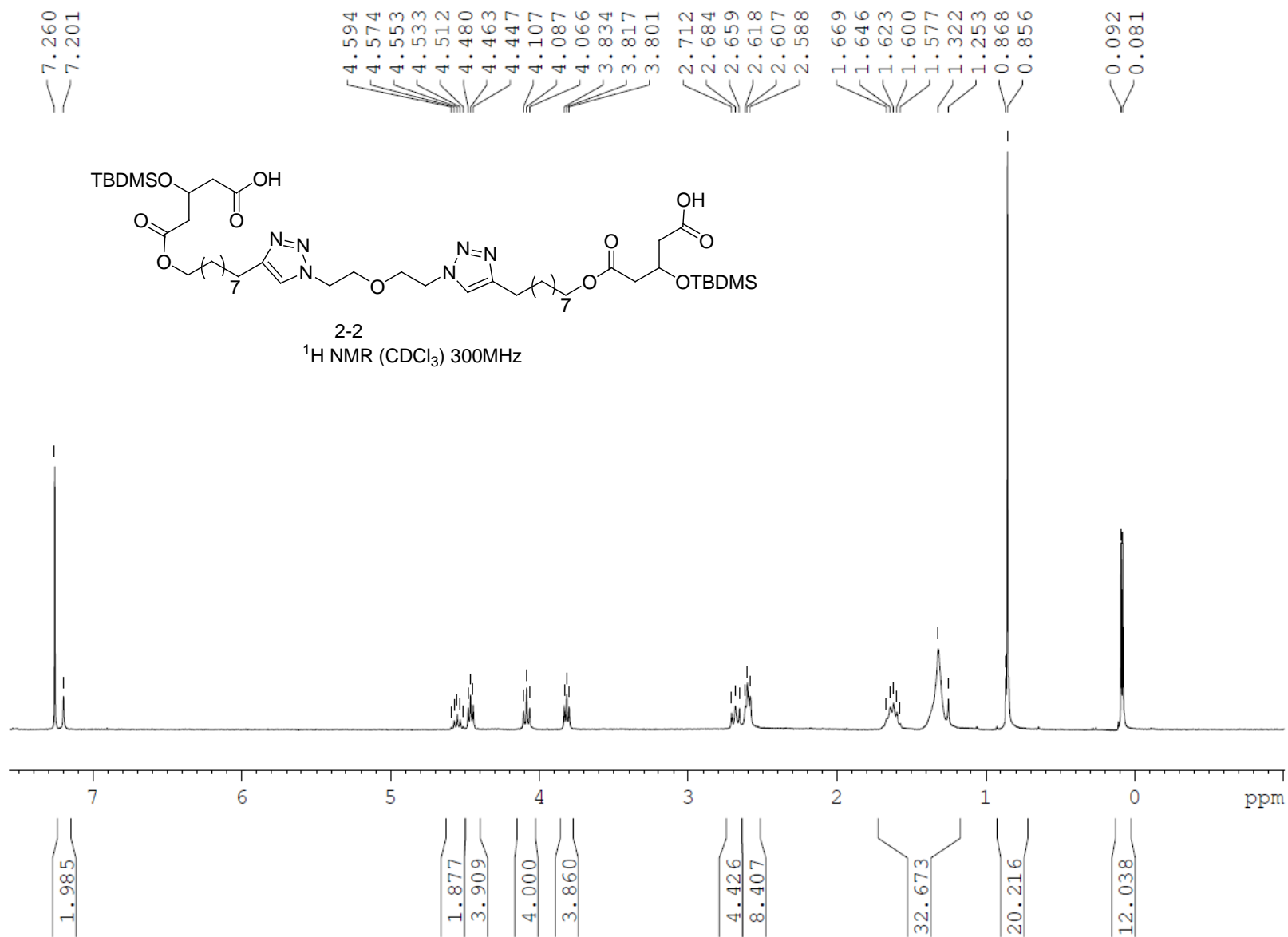
Table A2: Absorbance data from the membrane-spanning assay showing no change in absorbance over 100 minutes.

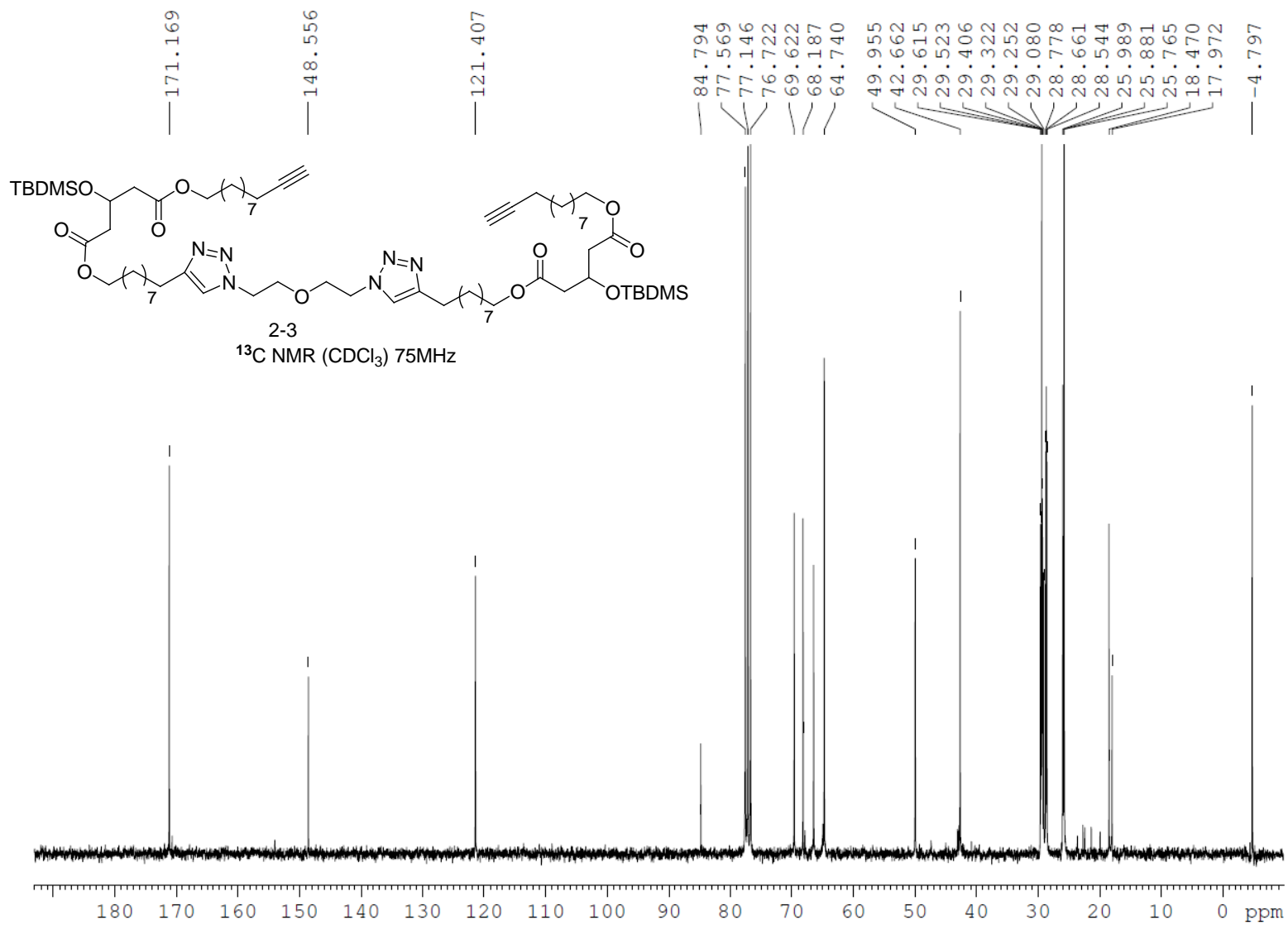
APPENDIX 2: SUPPORTING INFORMATION; SYNTHESIS

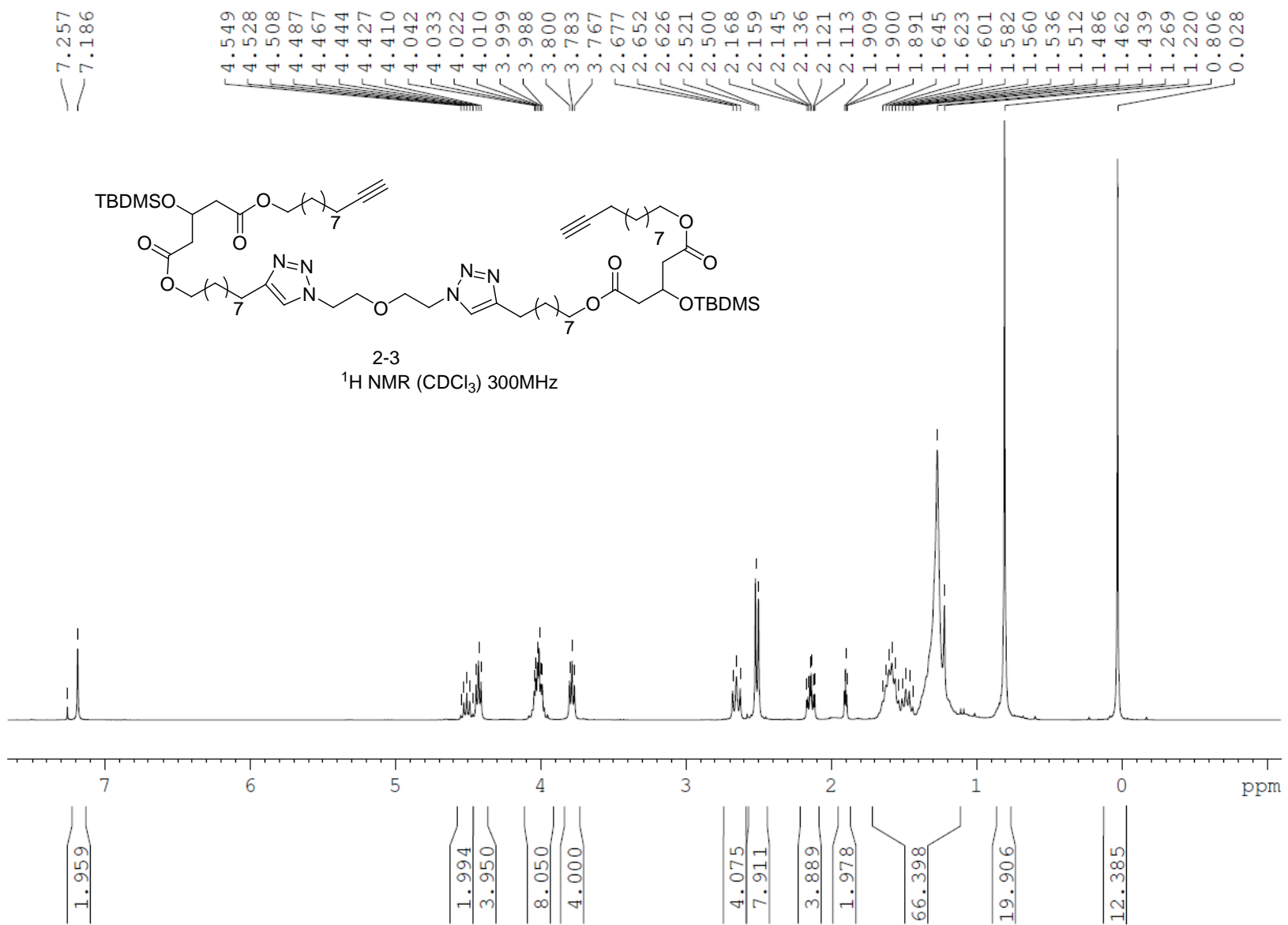


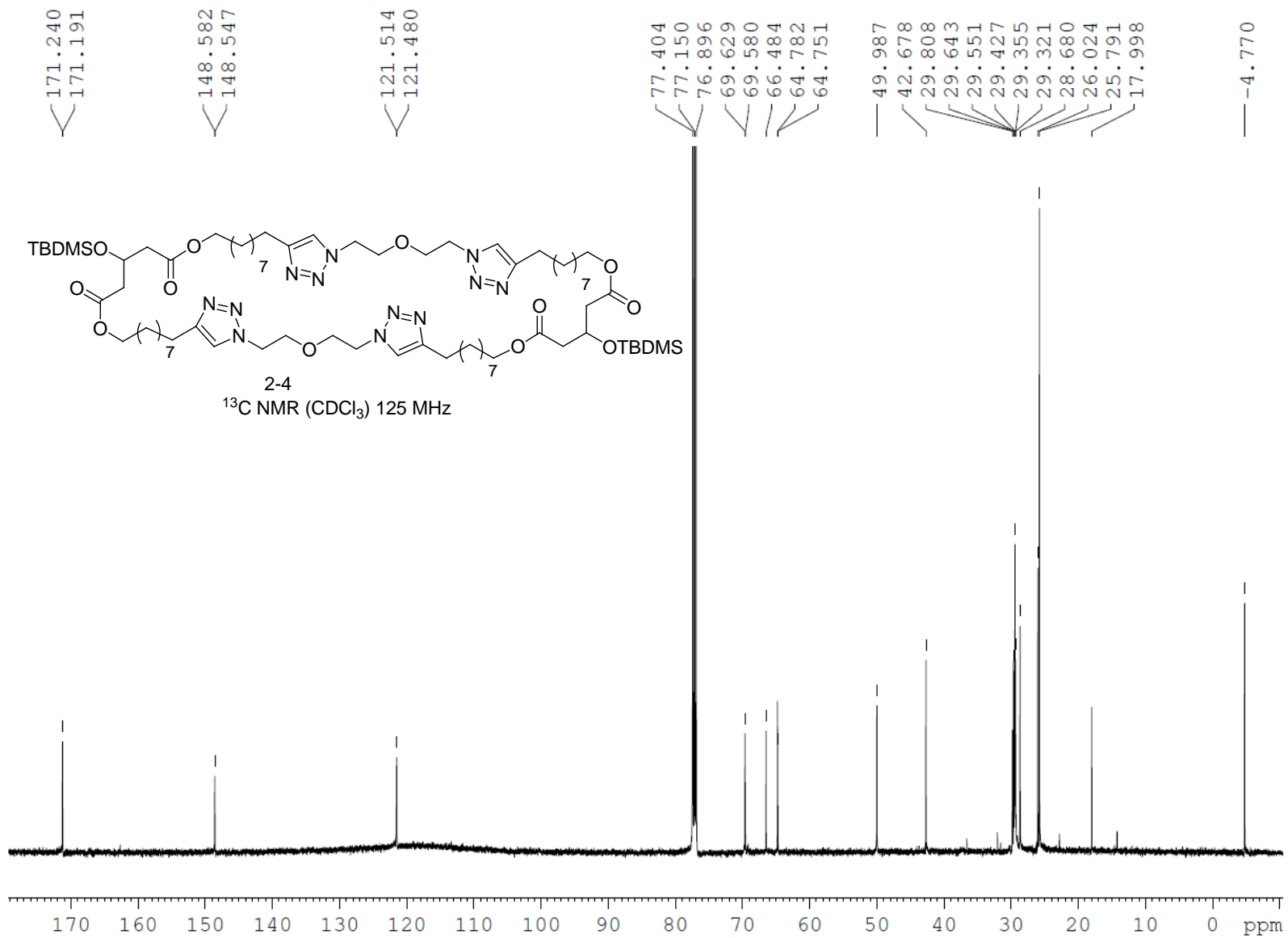












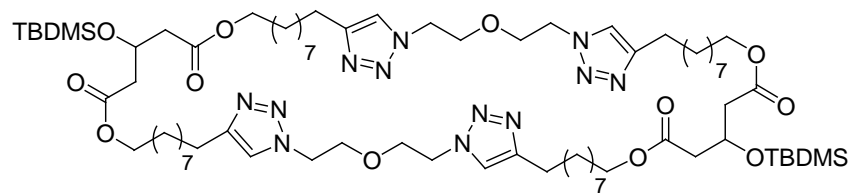
7.252
7.210
7.180

4.564
4.543
4.523
4.503
4.489
4.483
4.460
4.443
4.426
4.403
4.363
4.056
4.046
4.033
4.023
4.011
4.001
3.816
3.799
3.782
2.693
2.667
2.641
2.536
2.517

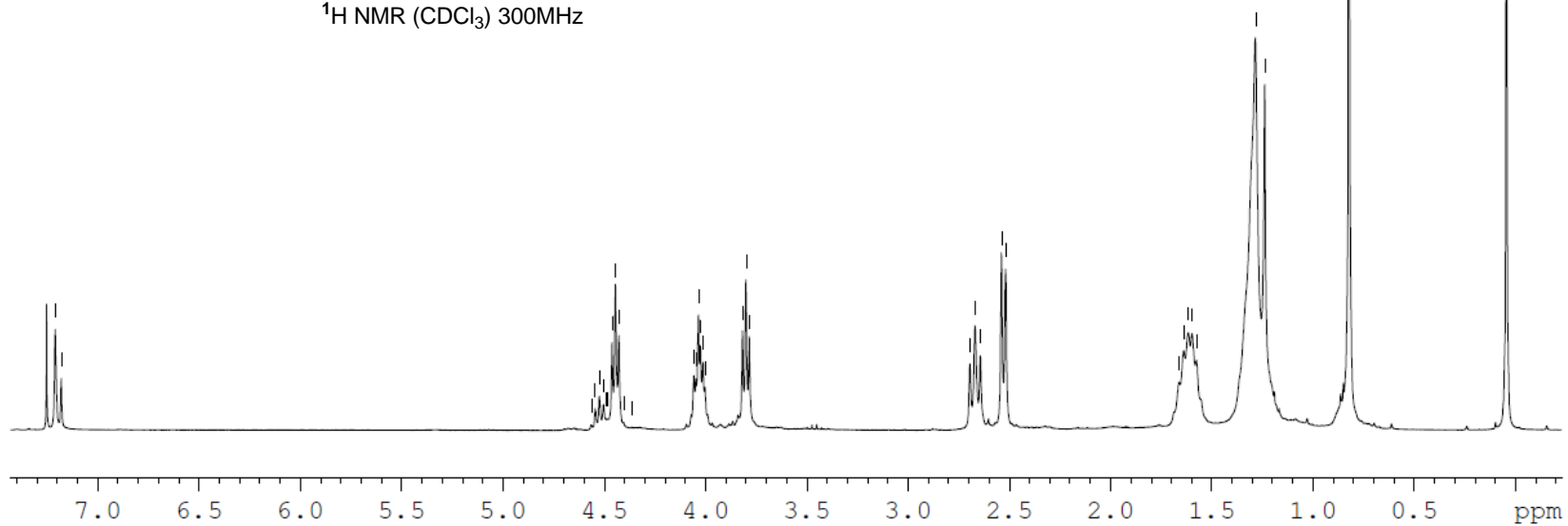
1.660
1.637
1.614
1.596
1.574
1.283
1.237

0.820

0.042



2-4
 $^1\text{H NMR}$ (CDCl_3) 300MHz



3.557

9.334

8.685

8.000

7.589

8.131

80.390

19.886

12.941

